Context Specific Signaling of TGF-β Receptor II

Dissertation zur Erlangung
des akademischen Grades des
Doktors der Naturwissenschaften
(Dr. rer. nat.)

eingereicht im Fachbereich Biologie, Chemie, Pharmazie
der Freien Universität Berlin

vorgelegt von

Daniel Walter Horbelt

aus Erlenbach am Main

2010

Diese Arbeit wurde von Oktober 2004 bis August 2010 in der Arbeitsgruppe von Prof. Petra Knaus am Institut für Chemie-Biochemie der Freien Universität Berlin angefertigt.

1. GUTACHTER: PROF. DR. PETRA KNAUS

2. GUTACHTER: PD DR. PETER N. ROBINSON

Disputation am 12.11.2010 .

Contents

List of Figures

List of Tables

Summary

Transforming growth factor β (TGF-β) is a modulator in developmental processes and a regulator in homeostasis. Dysregulation of TGF-β signaling is associated with human diseases such as cancer and cardiovascular disease. Hereditary defects predispose to metabolic, musculoskeletal, and cardiovascular malfunctions.

Even though the principal functions and pathways of TGF-β signaling have been elucidated in the past decades, increasing levels of complexity regarding its role *in vivo* and its signaling mechanisms have emerged, emphasizing the highly context specific nature of this pathway. In the present work two aspects of TGF-β signaling were subject to investigation.

In one study the biochemical and functional characteristics of hereditary mutations in the kinase domain of the TGF-β type II receptor (TβRII) which are associated with distinct diseases related to Marfan syndrome (MFS), namely type II MFS, Loeys-Dietz syndrome (LDS), and thoracic aortic aneurysms and dissections syndrome (TAAD) were characterized in biochemical and cell biological experiments. The consequences of these mutations were traced at various levels of the TGF-β signaling pathway and correlated with their effects on the protein structures.

Results from this study suggest that the balance of canonical TGF-β-Smad signaling and non-canonical ERK signaling is a determinant for the development of thoracic aortic aneurysms and dissections (TAAD) on one hand and additional manifestations including skeletal and craniofacial phenotypes on the other hand. These findings contribute important information to the unresolved issue of how distinct phenotypes arise from mutations in the same protein. Specifically, TβRII-R460C, which was regarded to disrupt TβRII kinase acitvity before, displayed residual kinase activity and Smad signaling capability.

Evaluation of clinical manifestations of TβRII mutations revealed that R460C tends to be associated with milder phenotypes restricted to the development of thoracic aortic aneurysms while additional manifestations were observed for other mutations. Based on these findings it could be concluded that residual Smad signaling by R460C prevents skeletal or craniofacial phenotypes but fails to suppress the development of aortic aneurysms.

In another project the signaling properties of an alternatively spliced isoform of TβRII, TβRII-B, were investigated. This isoform was shown before to exhibit unique binding specificities for the three known TGF-β isoforms, TGF-β1, -2, and -3. Monoclonal an-

tibodies were generated which specifically recognize TβRII-B. Moreover, one of those antibodies had a highly specific inhibitory effect on TβRII-B signaling as it interfered with binding of TGF-β2 but not of TGF-β1.

It could be shown in this study that the ligand binding specificities of TβRII-B are determined by an insert of 25 amino acids in the TβRII-B ligand binding domain. These findings provide significant insights regarding the mechanism by which different TGF-β isoforms are bound by TβRII-B to activate TGF-β signaling.

Zusammenfassung

Der Transformierende Wachstumsfakor beta (TGF-β) ist maßgeblich an der Steuerung von Entwicklungsprozessen beteiligt, ebenso wie an der Regulation der Homöostase im adulten Organismus. Eine Dysregulation des TGF-β Signalübetragungswegs steht im Zusammenhang mit Krebs und mit kardiovaskulären und fibrotischen Krankheiten. Erbliche Mutationen in Komponenten dieses Signalwegs bedingen unter anderem die Enstehung von Defekten des muskuloskeletalen und kardiovaskulären Systems. Durch die Erforschung des TGF-β Signalwegs in den letzten 20 Jahren konnten grundsätzliche Funktionen und Mechanismen seiner Signalübertragung aufgeklärt werden. Gleichzeitig wurde deutlich, daß gerade dem TGF-β Signalweg eine außergewöhnliche Komplexität und Kontextabhängigkeit innewohnt.

In dieser Arbeit wurden zwei verschiedene Aspekte des TGF-β Signalwegs untersucht. Zum einen wurden eine Reihe von neun erblichen Mutationen im TGF-β Typ II Rezeptor (TβRII) untersucht, die für die Entstehung von Krankheiten verantwortlich sind, welche dem Marfan Syndrom ähneln. Diese Mutationen wurden in biochemischen und zellbasierten Experimenten im Hinblick auf ihre Aktivität in verschiedenen TGF-β induzierten Signalwegen verglichen, sowie ihre Auswirkungen auf die Proteinstruktur nachvollzogen.

Die Ergebnisse dieser Studie legen nahe, daß die Balance zwischen dem klassischen TGF-β Signalweg, an dem die Smad Proteine beteiligt sind, und dem nicht-kanonischen Signalweg, der in der Aktivierung von MAP Kinasen resultiert, von Bedeutung ist. Die Aktivitäten beider Signalwege zusammen scheinen darüber zu entscheiden, ob sich isolierte Aneurysmen der Thoraxaorta bilden, und ob diese mit zusätzlichen Symptomen im Skelett- oder Gesichtsbereich einhergehen. Diese Erkenntnisse tragen zur Klärung der Frage bei, wie verschiedene Mutationen im selben Protein zu unterscheidbaren klinischen Manifestationen führen.

Es konnte gezeigt werden, daß die Mutation R460C nicht wie bislang angenommen die Kinaseaktivität des Rezeptors vollständig auslöscht, sondern eine reduzierte, aber signifikante Aktivität aufweist, die allerdings auf den Smad-Signalweg beschränkt ist. In der Tat scheinen sich die klinischen Symptome bei Patienten, die diese Mutation tragen, auf die Bildung von Aortenaneurysmen zu beschänken, während die übrigen untersuchten Mutationen mit zusätzlichen skelettalen und kraniofazialen Veränderungen einhergehen.

In einem weiteren Projekt wurde die Signalübertragung einer alternativ gespleißten Isoform des TβRII untersucht. Diese Variante des TβRII, TβRII-B, besitzt eine einzigartige Bindungsspezifität für die drei Isoformen von TGF-β, welche den TβRII-B vom TβRII abgrenzen. In dieser Studie wurde ein monoklonaler Antikörper hergestellt, der spezifisch den TβRII-B erkennt, und der darüber hinaus als ein hochspezifischer Inhibitor für die Bindung von TGF-β2 an TβRII-B fungiert, während die Bindung von TGF-β1 unbeeinflußt blieb. Es konnte gezeigt werden, daß eine zusätzliche Sequenz von 25 Aminosäuren in der Ligandenbindungsdomäne des TβRII-B seine Spezifität bestimmt. Auf diese Weise konnten wichtige Informationen im Hinblick auf die Frage gewonnen werden, wie TβRII-B seine Liganden bindet.

1 Introduction

1.1 The TGF-β superfamily

Transforming growth factor β (TGF-β) is the prototype member of the TGF-β superfamily of secreted polypeptide growth factors (Derynck and Miyazono, 2007). The TGF-β family comprises 33 structurally related proteins including TGF-βs, bone morphogenetic proteins (BMPs), growth and differentiation factors (GDFs), activins, inhibins, nodal, myostatin, and anti-Müllerian hormone (AMH, or Müllerian-inhibiting substance, MIS).

Cytokines of the TGF-β superfamily are essential regulators in developmental processes such as germ-layer specification and patterning in embryogenesis, and governors of homeostasis in physiological and disease processes by controlling cell growth, differentiation, migration, apoptosis and extracellular matrix (ECM) production (Gordon and Blobe, 2008; Wu and Hill, 2009). Dysregulation of TGF-β signaling pathways is associated with serious human diseases such as cancer, fibrosis, and cardiovascular disease, and hereditary defects predispose for metabolic and musculoskeletal as well as cardiovascular malfunctions, to name a few (Gordon and Blobe, 2008; Goumans et al., 2009; Padua and Massagué, 2009; Verrecchia and Mauviel, 2007).

Members of the TGF-β superfamily share a common principal pathway of signal transduction, however, findings in the past 20 years of research have uncovered increasing levels of diversity which provide a basis for the pleiotropic functionality of TGF-β superfamily ligands (Moustakas and Heldin, 2009). The canonical theme of TGF-β superfamily signaling involves binding of the ligands to cognate transmembrane receptor kinases, which induces transphosphorylation and activation of a type I receptor by a type II receptor in a multimeric complex consisting of ligand, type I and type II receptors (Fig. 1) (Shi and Massagué, 2003). Upon activation, type I receptors activate by phosphorylation their intracellular mediators of signal transduction, the receptor-activated (R-) Smads. In complex with the common-mediator (Co-) Smad, Smad4, activated R-Smads not only transmit the signal from the cell membrane into the nucleus but also directly regulate transcription in concert with transcriptional co-activators and co-repressors as well as additional transcription factors (Schmierer and Hill, 2007). Ligands of the TGF-β superfamily are traditionally grouped in the TGF-β/Activin/Nodal family which transduce their signal through R-Smads Smad2 and Smad3, and the BMP/GDF/AMH family in which Smads1, Smad5, and Smad8 execute transcriptional regulation. However,

it has become apparent in the recent years that there is significant promiscuity between both groups.

In addition to canonical Smad pathways, both TGF-βs and BMPs activate other signaling pathways without direct involvement of Smads (Moustakas and Heldin, 2005; Zhang, 2009). Among those non-Smad pathways are extracellular-signal regulated kinase (ERK), p38 mitogen-activated protein kinase (p38 MAPK), c-jun N-terminal kinase (JNK), Rho-like small GTPase pathways, and phosphatidylinositol-3-kinase (PI3K/AKT) pathways which originate from the receptor complex and in some cases involve adaptor proteins (Fig. 1). In turn, non-canonical roles of Smads have been identified beyond their function TGF-β signaling pathways (Hoover and Kubalak, 2008).

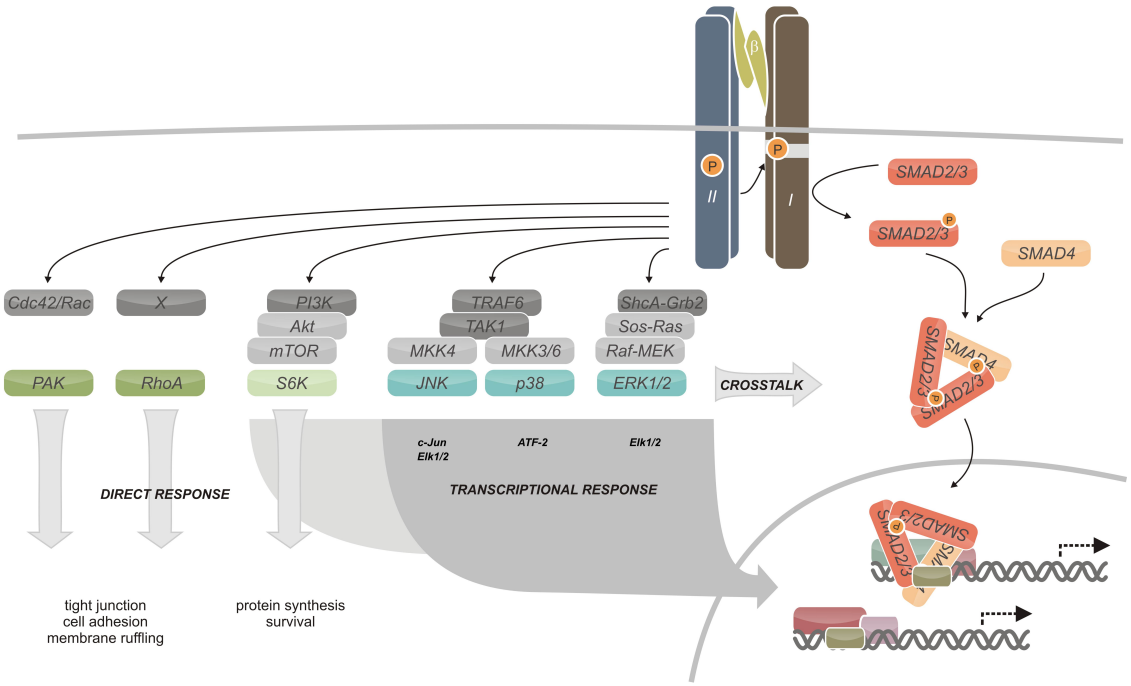

Fig. 1: Pathways in TGF-β signaling. TGF-β signals through the canonical Smad pathway and through non-Smad pathways. Smad signaling is initiated by binding of dimeric TGF-β (β) to TβRII (II). Subsequently, the type I receptor for TGF-β (TβRI, ALK5; (I)) is recruited into a heteromeric signaling complex and phosphorylated by the constitutively active kinase of TβRII in its GS domain to activate the TβRI kinase. Smad proteins Smad2 and Smad3 interact with active TβRI and become phosphorylated at their C-terminus. Phosphorylated Smads associate with the common mediator Smad4 and translocate to the nucleus to regulate transcription. TGF-β induced non-Smad signaling pathways that originate directly at the receptor complex involve interaction of adaptor or mediator proteins (dark grey) with the receptors and additional mediator proteins (light grey). TGF-β induced non-Smad response may be direct or at the transcriptional level, and non-Smad pathways crosstalk to TGF-β Smad signaling.

1.2 Mechanisms of TGF-β signaling

1.2.1 Secretion and activation of TGF-β

The TGF-β isoforms, TGF-β1, TGF-β2, and TGF-β3 are encoded by separate genes. TGF-β is synthesized as a pro-peptide that is proteolytically processed (ten Dijke and Arthur, 2007). During passage through rough endoplasmic reticulum, the N-terminal signal peptide of pre-pro-TGF-β is removed. Two TGF-β molecules subsequently form a disulfide-bond dimer, which represents the pro-form of TGF-β. In secretory vesicles or extracellularly, pro-TGF-β is cleaved into an N-terminal pro-peptide and the C-terminal mature TGF-β by furin convertase (Annes et al., 2003). The pro-peptide remains non-covalently associated to TGF-β thereby keeping TGF-β in an inactive state; the pro-peptide, or latency-associated peptide (LAP), together with TGF-β form the small latent complex (SLC). SLC in turn is bound to latent TGF-β binding protein (LTBP) through covalent binding of the pro-peptide/LAP to LTBP1 and LTBP3. The SLC-LTBP complex is termed large latent complex (LLC) (Saharinen et al., 1996).

Upon secretion, the LLC associates with the extracellular matrix by binding of N-terminal and C-terminal regions of LTBP to fibronectin and Fibrillin-1, respectively (1.3.1) (Nunes et al., 1997; Isogai et al., 2003). TGF-β becomes activated by liberation from the LLC. Thrombospondin-1 was shown to directly interact with LAP to disrupt its interactions with mature TGF-β (Crawford et al., 1998). A role for integrins has also been described. Integrins $\alpha_V\beta_6$ and $\alpha_V\beta_8$ were demonstrated to bind to arginine-glycine-aspartate- (RGD-) sequences in LAP and to mediate activation of TGF-β by mechanisms that involve matrix metalloproteinases (MMP) ($\alpha_V\beta_8$) or are independent from MMP activity ($\alpha_V\beta_6$), respectively (Sheppard, 2005). *In vitro*, latent TGF-β can be activated by low pH, high temperature, or proteases like plasmin, MMP2, and MMP9. In addition, reactive oxygen species were shown to promote activation of TGF-β both *in vivo* and *in vitro* (Annes et al., 2003).

TGF-β mobility, activation and bioavailability are thus linked to the cellular context and environmental changes. The TGF-β LLC may serve as a sensor that regulates TGF-β bioavailability in response to changes in extracellular matrix proteins, integrins, or protease activities which accompany processes like vascular remodeling (1.4), wound repair, or inflammation (Annes et al., 2003).

1.2.2 Ligand binding and receptor activation of TGF-β receptors

Crystal structures of the extracellular domain of TβRII alone or in complex with TGF-β3 have been determined (Boesen et al., 2002; Hart et al., 2002) as well as an NMR solution structure of the TβRII ECD (Deep et al., 2003). The ternary complexes of the TGF-β type I and type II receptors together with TGF-β1 and TGF-β3, respectively, have been resolved

recently (Radaev et al., 2010; Groppe et al., 2008), in which two type I and two type II receptors bind to one dimeric TGF-β molecule (Fig. 2).

The dimer of TGF-β consists of two identical monomers whose structures resemble slightly curved left hands with α-helix 1 and helix 3 representing the thumb and wrist, respectively, whereas the four fingers are formed by two antiparallel β-sheets. The monomer structure is dominated by an arrangement of six cysteines linked in a cysteine-knot conformation (Sun and Davies, 1995). Assembly of the dimer is stabilized by hydrophobic interactions and one intermolecular disulfide bond (Daopin et al., 1992). The TGF-β3 dimer was reported to exist in an additional, open conformation, with one monomer rotated by 100° relative to the other monomer, around an axis parallel to the β-strand fingers (Hart et al., 2002). The open conformation has not been observed in the ternary complex structures and is incompatible with binding to the type I TGF-β receptor (TβRI, ALK5) in the ternary complex (Groppe et al., 2008).

The cysteine rich ECDs of TβRI and TβRII adopt a three finger toxin fold which was first described for Activin type II receptors (ActRII) (Greenwald et al., 1999), with some deviations in finger 1 and finger 3. The topology of receptor binding as well as the assembly process of the signaling complex for TGF-β is significantly different from BMPs and GDFs. BMPs and GDFs bind to multiple type I and type II receptors in mixed order, through wrist and knuckle epitopes of the ligand dimer, respectively (Allendorph et al., 2006; Weber et al., 2007). In a sequential mode of binding, BMP2/4 first associate with their high affinity receptors, BMP-receptor Ia (BRIa) or BRIb. Type II receptors are subsequently recruited to form an active receptor signaling complex (BISC, BMP-induced signaling complex) (Nickel et al., 2009). Alternatively, fractions of BMP type I and type II receptors were shown to reside as pre-formed type I:type II receptor complexes (PFCs, pre-formed complex) which bind their ligands in a cooperative manner (Gilboa et al., 2000). Of note, the ECDs of BMP I and type II receptors do not contact each other in the ligand-bound complex (Allendorph et al., 2006).

The binding mode for TGF-β1 and TGF-β3, by contrast, is stepwise and cooperative (Wrana et al., 1992, 1994; Groppe et al., 2008). TGF-β1 and -3, exhibit a pronounced preference for the type II receptor whereas they have only low affinity for TβRI alone (Zúñiga et al., 2005). TβRII binds to the fingertips of one TGF-β monomer in a wedge-like fashion. The base of the TβRII-toxin fingers interacts with the TGF-β-fingers predominantly through polar interactions. Neither TβRII nor TGF-β undergo significant conformational changes during binding. Binding of TGF-β to TβRII creates a composite binding interface with reasonable affintiy for TβRI, and TβRI is subsequently recruited into the signaling complex (Groppe et al., 2008; Radaev et al., 2010). In this complex TβRI contacts the type two receptor as well as both monomers of TGF-β (Fig. 2).

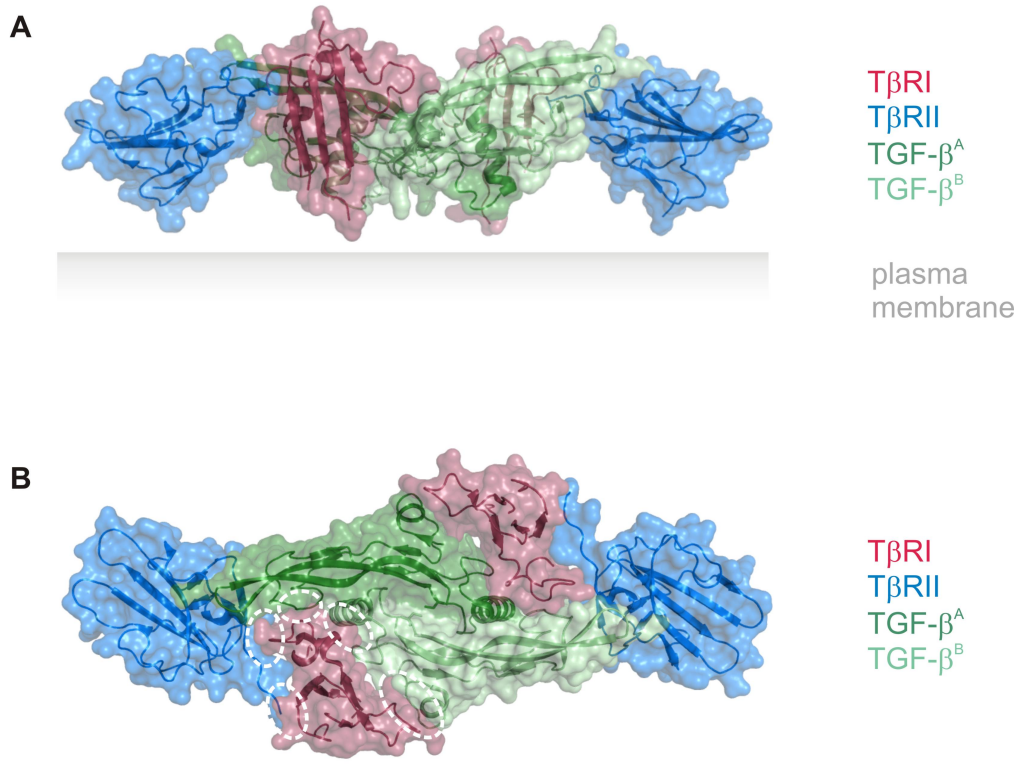

Fig. 2: Structure of the TGF-β receptor signaling complex. (A) Side view of the receptors. In a heterohexameric receptor signalling complex the butterfly-shaped TGF-β dimer - formed by monomers TGF-β^A and TGF-β^B - is bound by two type I and two type II receptors. (B) Top view. Each TβRII binds to the tips of one TGF-β monomer by mainly polar interactions. TβRII and both monomers of TGF-β together form a composite binding interface for TβRI, allowing it to interact with TβRII as well as with both monomers of TGF-β through hydrophobic contacts (indicated with dashed lines). Images were generated using PyMOL based on PDB 3KFD (Radaev et al., 2010).

The mode of binding of TGF-β2 differs from that of TGF-β1 and TGF-β3. The affinity of TGF-β2 for TβRII is 100- to 1000-fold lower as compared to the other isoforms, and does not suggest the same sequential binding (Groppe et al., 2008; Radaev et al., 2010; Zúñiga et al., 2005). Instead, TGF-β2 is bound by betaglycan, a TGF-β type III receptor, which serves as a co-receptor that binds TGF-β2 and presents it to TβRII (López-Casillas et al., 1993).

The differential affinities of the TGF-β isoforms are based on the substitution of three residues which are conserved in TGF-β1 and -3, R25, V92 and R94, by K25, I92, and K94 in TGF-β2, respectively (Crescenzo et al., 2006). These residues contribute to the TβRII-TGF-β1/3 binding interface (Fig. 3) (Hart et al., 2002; Radaev et al., 2010). Mutated TGF-β2 in which these three amino acids were replaced by the corresponding residues of TGF-β1 and -3 conferred TGF-β2 with a binding affinity for TβRII which was only slightly reduced as compared to TGF-β1 and -3. Moreover, mutated TGF-β2 was shown to induce a cellular TGF-β response in cells that did not respond to TGF-β2 due to the absence of TβRIII (Crescenzo et al., 2006).

An alternatively spliced isoform of TβRII, TβRII-B, could be shown to bind TGF-β2 in the absence of betaglycan (Rotzer et al., 2001). TβRII-B contains an insert of 26 amino acids replacing V9 of the mature recpetor which was suggested to create an additional binding site endowing the receptor with increased affintiy for TGF-β2 (1.2.4).

1.2.3 TGF-β isoform specificity

The three isoforms of TGF-β, TGF-β1, TGF-β2, and TGF-β3 are encoded by separate genes and are expressed in a developmentally regulated and tissue specific manner. The TGF-β isoforms share 70% to 81% sequence homology and significant structural similarity with backbone root mean square deviations $\leq$1.5Å (Daopin et al., 1992; Hinck et al., 1996; Mittl et al., 1996; Schlunegger and Grütter, 1992). Isoform-specific knockouts showed non-overlapping phenotypes.

Mice with disruption of the TGF-β1 gene (*TGFB1*) died around day 20 post-natum as a consequence of a general wasting syndrome which was accompanied by symptoms of a multifocal inflammatory cell response leading to organ failure. Developmental abnormalities were absent in *TGFB1* null mice (Kulkarni et al., 1993; Shull et al., 1992).

By contrast, targeted disruption of *TGFB2* resulted in severe developmental defects with cardiac, lung, craniofacial, skeletal, ocular and urogenital manifestations (Sanford et al., 1997). Two third of TGF-β2 deficient mice died perinatally, and the remainder were born cyanotic and died shortly after birth. The TGF-β2 knockout phenotype showed no overlapping features with knockouts for TGF-β1 or TGF-β3.

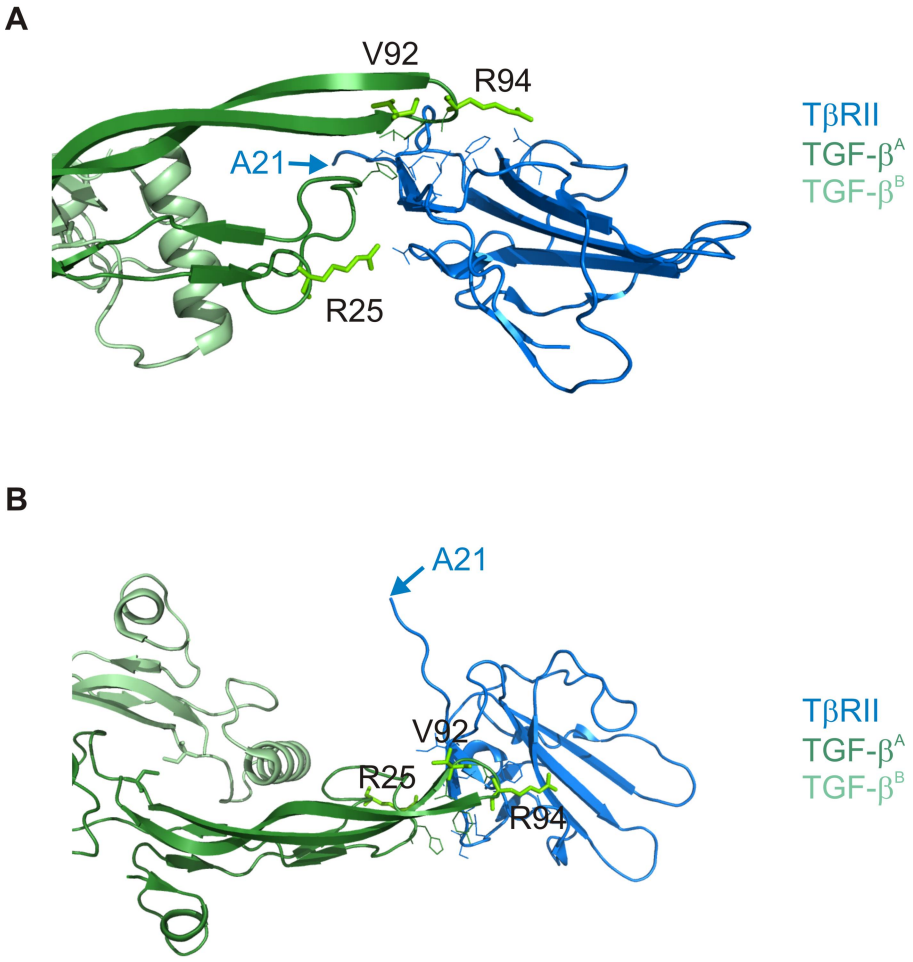

Fig. 3: Binding of TGF-β1 to TβRII. (A) Side view. TβRII wedges between the fingertips of the monomer. Amino acids in TβRII (blue lines) interact with TGF-β^A residues (green lines). Three residues in TGF-β^A which contribute to the binding interface determine high affinity binding of TGF-β1 and TGF-β3 to TβRII. (R25, V92, R94 of the mature receptor; light green sticks). These residues are exchanged in TGF-β2. At the N-terminal end of the crystallographic structure of TβRII is A21 (Fig. 4). The upstream region is assumed unordered and thus is not included in any of the crystallographic structures. (B) Top view. Images were generated using PyMOL based on PDB 3KFD (Radaev et al., 2010).

Mice lacking TGF-β3 were born alive, but failed to suckle after birth and died within less than 24 hours after birth (Kaartinen et al., 1995; Proetzel et al., 1995). These mice showed cleft palate, but no other craniofacial abnormalities. Lung development seemed to be abnormal as represented by an immature pulmonary phenotype (Kaartinen et al., 1995).

The non-overlapping phenotypes as a consequence of TGF-β1, TGF-β2, and TGF-β3 deficiency, respectively, indicate that each TGF-β isoform has a distinct role *in vivo*. By contrast, TGF-β isoforms exhibit overlapping activities *in vitro*. TGF-β1 and TGF-β3 at least seem to have the same potential to induce TGF-β mediated responses in cell culture.

1.2.4 The TGF-β receptor II isoform TβRII-B and aim of the project: "Antibodies against TβRII-B"

Murine and human TβRII-B sequences were isolated from a murine brain cDNA library (Suzuki et al., 1994) and by RT-PCR from human vascular endothelial cells (Hirai and Fijita, 1996), respectively, as an isoform of human TβRII. A series of studies confirmed that TβRII-B was a functional TGF-β type II receptor that was expressed in a variety of cell lines (Hirai and Fijita, 1996; Parker et al., 2007; Rotzer et al., 2001). In mice TβRII-B was found to be ubiquitously expressed with the lowest levels in the brain (Krishnaveni et al., 2006). The cDNA sequence of TβRII-B reveals a 75-nucleotide insertion in the codon for V32 which is a result of alternative splicing between Exon 1 and Exon 2, which introduces an additional exon 1a. The remaining sequence is identical to TβRII (Rotzer et al., 2001). On the protein level the TβRII-B insert contains 26 amino acids replacing V32 which is V9 in the mature receptor after cleavage of the signal peptide (Fig. 4). The N-terminal portions of the insert are conserved in mice and human while the C-terminal sequences vary.

Fig. 4: N-terminal peptide sequences of TβRII and TβRII-B. TβRII-B contains an insert of 26 amino acids that replaces Val9 in the mature receptor. The N-terminus of the insert is conserved between mouse and human. The peptide sequence used for immunization is boxed.

It was shown by TGF-β binding and crosslinkin studies that TβRII-B associates with TβRI, TβRII, and betaglycan upon TGF-β1 stimulation. In human primary chondrocytes and chondrocyte cell lines TβRII-B was found to form heteromeric complexes with TβRI, and endogenous TβRIIIs betaglycan and endoglin in the presence and absence of

ligand (Parker et al., 2007). Both human and mouse TβRII-B were reported to form ligand independent heterodimers with TβRII (Krishnaveni et al., 2006; Parker et al., 2007).

TβRII has only low affinity for TGFβ2 (Lin et al., 1995; Cheifetz et al., 1990). TGF-β2 is bound by betaglycan wich presents the ligand to facilitate assembly and activation of the receptor signaling complex (López-Casillas et al., 1993). By contrast, TβRII-B was reported to bind TGF-β2 and to mediate Smad signaling induced by TGF-β2 as well as by the other TGF-β isoforms in the absence of betaglycan (Rotzer et al., 2001). Increased affinity for TGF-β2 did not involve alternative disulfinde bond formation of two cyteines in the peptide insert, nor glycosylation at a potential N-glycosylation site (N48). It was suggested that the peptide insert creates an additional binding site that establishes higher affininty for TGF-β2 without abolishing binding of TGF-β1 or TGF-β3 (Rotzer et al., 2001). Other reports failed to confirm increased binding of TGF-β2 by TβRII-B as compared to TβRII. In these cell-based studies, however, the presence of betaglycan significantly hampered interpretation of results (Krishnaveni et al., 2006; Parker et al., 2007). *In-vitro* binding assays on the other hand, showed that the soluble Fc-fused extracellular domain of TβRII-B (sTβRII-B-Fc) is unable to bind directly to TGF-β2 and does not differ in this respect from sTβRII-Fc (del Re et al., 2004). Moreover, if TβRI was included in those assays, allowing for the formation of type I:type II receptor complexes in solution, both TβRII-B but also TβRII exihibited significant binding to TGF-β2. It was suggested that the existence of pre-formed complexes of TGF-β type I and type II receptors may be of increased relevance specifically in TGF-β2 induced signaling (del Re et al., 2004; Radaev et al., 2010).

Signaling by TβRII-B has been investigated by ligand binding and crosslinking studies which suffer from unspecific binding of TGF-β, most likely to TβRIII; using *in-vitro* binding assays which can not reproduce the complex environment of the cell membrane; by cell-based signaling studies in which requirement for overexpression of tagged TβRII-B and other receptors tends to distort the stoichiometric balance of receptor types and thus to generate artefacts. To characterize signaling of TβRII-B in more detail in order to solve some of the decribed contradictions, and to uncover its physiological role, the ability to visualize TβRII-B *in situ*, i.e. in tissues and on cells at endogenous levels, is highly desirable. Moreover, specific interference with TβRII-B signaling could create evidence of its functions and roles in TGF-β regulated processes. The generation of two mouse monoclonal antibodies for TβRII-B is described here. Their specificity and applicability as immunological tools and as inhibitors to target TGF-β2-TβRII-B signaling are reported.

1.2.5 Activation of Smad signaling by TGF-β receptors

The cytoplasmic domains of TβRI and TβRII are dominated by a protein kinase domain of the tyrosine kinase-like (TKL) family (Hanks and Hunter, 1995). Although

originally described a serine-threonine kinases, structural and sequence similarities to tyrosine kinases suggest that TGF-β type I and type II receptors of the TGF-β superfamily are dual-specificity kinases that are able to phosphorylate on serines, threonines and tyrosines (1.2.7) (Han et al., 2007; Hanks and Hunter, 1995; Huse et al., 1999).

The highly conserved structure of eukaryotic kinases is organized into a smaller N-terminal lobe (N-lobe) consisting mainly of β-sheets, and the larger C-terminal lobe (C-lobe) which is predominantly α-helical (Knighton et al., 1991). The active site of the kinase is located in a deep cleft between both lobes. The function of the N-lobe is to coordinate and to regulate ATP binding whereas the C-lobe recognizes and positions the kinase substrate. In addition, both lobes serve as interaction sites for accessory proteins. In spite of high structural homology with other protein kinases, the regulation and activation of TβRII and especially TβRI kinase activity varies from classical activation mechanisms (Engh and Bossemeyer, 2001). The kinase domain of TβRII is considered constitutively active and phosphorylated on serines, threonines, and tyrosines (Wrana et al., 1994; Lawler et al., 1997). Full activation was shown to require autophosphorylation at S213 upstream of the kinase domain and S409 in the activation loop of the kinase, which occur in cis (intramolecular autophosphorylation by the same peptide chain) or trans (intermolecular autophosphorylation), respectively (Luo and Lodish, 1997). In addition, tyrosine autophosphorylation of TβRII on Y259, Y336, and Y424 was reported to be critical for TβRII kinase activity (Lawler et al., 1997).

Binding of TGF-β to TβRII promotes recruitment of TβRI into the oligomeric receptor complex in which TβRI is activated through transphosphorylation by TβRII (Fig. 1) (Wrana et al., 1994). TβRI activity is regulated by phosphorylation of multiple serines and threonines in a TTSGSGSG sequence in its glycine/serine rich (GS) domain which is immediately upstream of the kinase domain (Souchelnytskyi et al., 1996; Wrana et al., 1994). In the absence of GS-domain phosphorylation TβRI is found in a catalytically inactive conformation as a consequence of a rotation of the N-lobe with respect to the C-lobe which results in shearing of the active site (Huse et al., 1999). The inactive conformation is stabilized by binding of the immunophilin FKBP12 to the unphosphorylated GS domain. FKBP12 is thought to suppress basal levels of TβRI activity in the absence of ligand. Conversely, phosphorylation of a threonine and three serines in the GS domain was demonstrated to abolish binding of FKBP12 (Huse et al., 2001). In the absence of FKBP12 repression TβRI can adopt a catalytically active conformation. Moreover, phosphorylation of the GS domain establishes binding sites for TβRI substrates, Smad2 and Smad3.

Smad proteins comprise a conserved N-terminal MAD-homology 1 (MH1) domain which promotes DNA binding either directly or by contacting DNA-binding cofactors (Shi and Massagué, 2003). The likewise conserved C-terminal MH2 domain mediates protein-

protein interactions such as association with the type I receptors, with the MH2 of other Smad proteins, and with DNA-binding cofactors or transcriptional co-activators or co-repressors. MH1 and MH2 domains are connected by a variable and flexible linker domain. R-Smads, Smad1/2/3/5/8 feature a SXS motif at their very C-terminus which is phosphorylated by the type I receptor upon interaction (Fig. 1) (Macías-Silva et al., 1996). Smad2 and Smad3 are phosphorylated on S465 and S467 and on S423 and S425, respectively (Ross and Hill, 2008).

Recruitment of Smads to the activated receptor complex is facilitated by adaptor proteins such as SARA (1.2.8) (Tsukazaki et al., 1998), Disabled-2 (Dab-2) (Hocevar et al., 2001), and Axin (Furuhashi et al., 2001), and was shown to involve kinesin-mediated transport along microtubules (Batut et al., 2007).

Once phosphorylated R-Smads dissociate from the receptor complex and form dimeric or trimeric aggregates with other R-Smads and/or Smad4 (Fig. 1) (Chacko et al., 2001; Wu et al., 2001). In these complexes, MH2 domains arrange in a head-to-tail fashion in which the C-terminal pSXpS motif of one molecule interacts with the basic surface pocket of another monomer (Wu et al., 2001).

The specificity of TGF-β superfamily Smad signaling was originally assigned to a specific interaction of each of seven ALKs with either TGF-β- or BMP activated R-Smads (Miyazawa et al., 2002). Following phosphorylation by TβRII, the GS domain of TβRI was demonstrated to bind to a basic surface pocket in the MH2 domain of R-Smads, which is thought to promote the interaction but not to confer specificity (Shi and Massagué, 2003; Wu et al., 2000). The specificity of receptor-Smad interaction is established by interactions of the loop between β-sheets 4 and 5 (L45 loop) in the type I receptor and the L3 loop in the MH2 domain of Smads, and experimental variations in the L45 loops of type I receptors were demonstrated to be sufficient to alter Smad specificity (Chen et al., 1998; Feng and Derynck, 1997). According to this model, ALK1,ALK2, ALK3, and ALK6 activate BMP-Smads, Smad1/5/8, and ALK4, ALK5, ALK7 phosphorylate TGF-β-Smads, Smad2/3.

Recently, this dinstinction has been challenged by findings that TGF-β induces phosphorylation of Smad1/5 in a series of cell lines. In one study, TGF-β induced Smad1/5 phosphorylation required the contribution of a BMP type I receptor (ALK2 or ALK3) activity in addition to TβRI and TβRII (Daly et al., 2008). This scenario resembles a previously published model for TGF-β stimulated Smad1/5 phosphorylation in endothelial cells which involved ALK1 and the TβRIII endoglin in addition to TβRI and TβRII (Goumans et al., 2003; Lebrin et al., 2004). These findings suggested a lateral signaling between TGF-β- and BMP-type I receptors. However, other groups found a BMP-type I receptor independent activation of Smad1 or Smad1/5 in non-endothelial cell lines (Liu et al., 2009; Wrighton et al., 2009b). The L45 loop of ALK5 and ALK5 kinase activity were shown to be

crucial for TGF-β induced Smad1/5 phosphorylation in these studies and, moreover, it was demonstrated that ALK5 was capable of directly phosphorylating Smad1 in *in-vitro* kinase assays in spite of their assumed incompatibility of the L45 and L3 loops (Liu et al., 2009; Wrighton et al., 2009b). *In vivo*, however, requirement of BMP type I receptors for TGF-β induced Smad1/5 activation appeared to be dependend on the cell type, and further studies are required to characterize the quanitative, functional and context-specific roles of this pathway (Wrighton and Feng, 2008).

1.2.6 TGF-β signaling through Smads

Unphosphorylated R-Smads are found predominantly in the cytoplasm, whereas Smad4 is evenly distributed throughout the cell. Upon phosphorylation, R-Smads accumulate in the nucleus to regulate transcription in concert with transcriptional co-factors, co-activators, and co-repressors (Fig. 1) (Ross and Hill, 2008).

Nuclear import of TGF-β Smads seem to require both importin-dependent and -independent mechanisms. An active nuclear localization signal has been identified in the MH1 domain of Smad3 and Smad4 (Kurisaki et al., 2001; Xiao et al., 2000a,b, 2003). Motifs for direct interaction with nucleoporins were revealed in the MH2 of both Smad2 and Smad3 (Xu et al., 2002, 2003). While nuclear export of Smad4 requires a nuclear export signal in the linker region of Smad4 which interacts with exportin-1, export of Smad2 and Smad3 again is mediated by karyopherin-dependent and -independent mechanisms (Pierreux et al., 2000; Kurisaki et al., 2006; Watanabe et al., 2000; Xu et al., 2002).

In the current model, all Smads are constantly shuttling in and out the nucleus, and the subcellular distribution of Smads depends on the balance of import- and export rates of R-Smads and Smad4 (Schmierer and Hill, 2005, 2007). While for Smad4 steady-state import and export rates are similar, export rates of Smad2/3 dominate over import, leading to a predominantly cytoplasmic localization of R-Smads. Upon ligand stimulation, kinetic analysis of Smad shuttling suggested primarily a decreased nuclear export rate to shift the balance to the nucleus (Schmierer and Hill, 2005). Reduced export was assigned to enhanced nuclear retention by binding of activated Smad complexes to DNA and transcription factors such as the transcriptional regulators TAZ and the transcriptional co-factor ARC105 (Varelas et al., 2008). In addition, mathematical modeling revealed that an increased import rate contributes to the nuclear accumulation of R-Smads (Schmierer et al., 2008), which was proposed to be based on exposure of a Smad3 NLS following C-terminal phosphorylation (Kurisaki et al., 2001; Xiao et al., 2000b). The termination of Smad signaling in the nucleus was demonstrated to involve degradation of nuclear Smads (Lo and Massagué, 1999) or dephosphorylation by nuclear Smad phosphatases such as PPM1A which may promote nuclear export of Smads (Lin et al., 2006). The

dynamic system of permanently cycling activation, shuttling, and deactivation of Smads is thought to allow for quick and continuous sensing of receptor activation, which is critical with regard to the highly quantitative nature of Smad signaling (Inman et al., 2002).

In addition to C-terminal phosphorylation, both BMP Smads and TGF-β Smads can be phosphorylated by a variety of protein kinases such as ERK, p38 MAPK, JNK, and GSK3β at sites in the Smad linker (Wrighton et al., 2009a). For Smad2/3 in addition phosphorylation in the MH1 domain by ERK, CDK, PKC, GSK3β was shown. These phosphorylations regulate Smad activity by influencing nuclear translocation, transcriptional activity, and protein stability, however, many of these effects are assumed to be cell type specific (Alarcón et al., 2009; Gao et al., 2009). Further post-translational modifications of Smads include sumoylation, which has been described for the MH1 and linker domains in Smad4, and acetylation of Smad2 and Smad3 (Ross and Hill, 2008). Acetylation of Smad2 in the MH1 domain and of Smad3 in MH1 and MH2 were shown to increase transcriptional activity by attenuating nuclear export or by increasing DNA binding, respectively (Simonsson et al., 2006; Tu and Luo, 2007). Importantly, Smads were shown to be ubiquitinated by a series of ubiquitin E3 ligases which target them for degradation. Smad ubiquitin regulatory factor-1 (Smurf-1) and Smurf-2 interact with Smad1/5 or with Smad1/5 and Smad2/3, respectively, and this is followed by proteasomal degradation of Smad1 and Smad2 (Lin et al., 2000; Zhang et al., 2001; Zhu et al., 1999). Additional E3 ligases that were shown to associate with and to ubiquitinate Smads are neuronal precursor cells expressed, developmentally downregulated 4-2 (NEDD4-2) and WW domain containing E3 ubiquitin ligase 1/TGIF-interacting ubiquitin ligase 1 (WWP1/TiuL1) (Komuro et al., 2004; Seo et al., 2004).

1.2.7 Non-Smad signaling by TGF-β

In parallel to its canonical pathways in which Smads relay the TGF-β signal from the membrane to the nucleus and execute transcriptional responses by binding to DNA, TGF-β stimulates additional pathways without direct involvement of Smads (Derynck and Zhang, 2003; Moustakas and Heldin, 2005; Zhang, 2009), including ERK-MAPK, p38 MAPK, JNK, PI3K/Akt and Rho-like GTPase pathways. These pathways are thought to originate at TGF-β receptor complexes and thus require ligand induced formation of TβRI:TβRII complexes and, in some cases, kinase activity of one or both receptor types. TGF-β non-Smad pathways add another layer of complexity to the regulation of TGF-β signaling since in some cases crosstalks to the TGF-β-Smad pathways have been identified.

ERK phosphorylation is induced by TGF-β through mechanisms similar to activation by receptor tyrosine kinases. While originally classified as serine-threonine kinases,

TGF-β receptors were shown to have weak but significant tyrosine kinase activity. Structural similarities with tyrosine kinases (Huse et al., 1999) as well as findings that TβRII autophosphorylates on tyrosines 259, 336, and 424 (Lawler et al., 1997) have provided evidence that TGF-β receptors are dual specificity kinases able to phosphorylate specific substrates on serines, threonines and tyrosines (Hanks and Hunter, 1995). Following TGF-β stimulation TβRI is phosphorylated at serines, threonines and tyrosines, however, it has not been clarified to date to which extent tyrosine phosphorylations are established by auto- or transphosphorylation events in TβRI and TβRII. Activated TβRI was shown to associate with and to phosphorylate ShcA on serine and tyrosine residues (Lee et al., 2007). ShcA phosphorylation is dependent on the kinase activity of TβRI and TβRII. Phosphorylation of ShcA at the receptor complex is thought to enable binding sites for Grb2 and the Ras-guanine nucleotide exchange factor Sos, which in turn activates membrane-bound Ras, the upstream activator of the MAPK kinase cascade. In addition to this direct activation of ERK which, dependent on the cell type, becomes detectable after 5 to 45 minutes, there is also a delayed activation of ERK by TGF-β after several hours which is likely to involve transcriptional or translational events events.

TGF-β induces phosphorylation of p38 MAPK and JNK through a direct and rapid mechanism that involves the MAPKKK TGF-β activated kinase 1 (TAK1) and the RING finger E3 ligase TRAF6 (Sorrentino et al., 2008; Yamashita et al., 2008). TAK1 interacts directly with TβRII and was reported to be indispensable for JNK activation in response to TGF-β (Shim et al., 2005; Watkins et al., 2006). TRAF6 associates with TβRI and TβRII through its C-terminal TRAF domain. Once bound to the activated receptor complex TRAF6 autoubiquitinates by K63-polyubiquitination. TRAF6 polyubiquitination recruits TAK1 which is followed by TAK1 K63-polyubiquitination and activation (Sorrentino et al., 2008; Yamashita et al., 2008). TAK1 is a MAPKKK directly upstream of the MAPKKs MKK3/6 and MKK4 which in turn are upstream activators of p38 MAPK and JNK, respectively. Smad signaling is dispensable for the rapid activation of p38 and JNK by TGF-β. In addition, mutations of the L45 loop in TβRI that disrupt TβRI Smad signaling activity did not affect p38 nor JNK activation (Itoh et al., 2003; Yu et al., 2002). By contrast, it is not entirely clear whether the kinase activity of TβRI is required to activate TRAF6 and TAK1 in response to TGF-β. In HEK293T cells treatment with two different inhibitors of ALK5 kinase abolished Smad2 but not p38 phosphorylation in response to TGF-β, suggesting that ALK5 kinase is dispensable (Sorrentino et al., 2008). By contrast, in another study the requirement for an active ALK5 kinase was emphasized, as introduction of wildtype but not of a kinase defective ALK5 into ALK5 deficient mink lung cells restored ubiquitination of TRAF6 (Yamashita et al., 2008).

Additional mechanisms which lead to a delayed activation of p38 and JNK seem to involve transcriptional effects of the Smad pathway. p38 was reported to be activated

following TGF-β stimulation through Smad-dependent expression of GADD45β which binds to and activates MEKK4. MEKK4 is an upstream kinase of both MKK4/7 and MKK3/6 (Takekawa et al., 2002).

The PI3K/Akt pathway is another non-Smad pathway which can be rapidly stimulated by TGF-β in the absence of Smad activity (Bakin et al., 2000; Wilkes et al., 2005). Class IA PI3K bind to tyrosine phosphorylated activated receptor tyrosine kinases through interaction of their p85 regulatory subunit with phosphorylated tyrosines in a pYXXM context (Engelman et al., 2006). Upon binding to RTKs repression of the p110 catalytic subunit by the regulatory subunit is relieved, and PI3K promotes the production of phosphatidylinositol 3,4,5 triphosphates (PIP3) from phosphatidylinositol-4,5-bisphosphate (PIP2). PIP3 provides a docking site for the Akt pleckstrin-homology (PH-) domain to the plasma membrane. Akt is subsequently phosphorylated by a phosphoinositide dependent kinase 2 (PDK2) on S473, and by PDK1 on T308 enabling activation of Akt kinase. The p85 subunit of PI3K was shown to be constitutively associated with TβRII while interaction with TβRI required ligand stimulation (Yi et al., 2005). Stimulation with TGF-β induced Akt phosphorylation at S473 in fibroblast but not in epithelial cell cultures (Wilkes et al., 2005) whereas is was observed in NMuMG mammary epithelial cells by others (Bakin et al., 2000; Lamouille and Derynck, 2007). The kinase activity of ALK5 appears to be required for Akt phosphorylation since the latter could be blocked by an ALK5 inhibitor. TGF-β also led to activation of a downstream effector of Akt, mammalian target of rapamycin (mTOR), which in turn promoted phosphorylation of S6 kinase (S6K) to regulate protein synthesis (Lamouille and Derynck, 2007) . Of note, Akt was shown to directly interact with and to sequester unphosphorylated Smad3 in the cytosol which resulted in inhibition of Smad3 dependent transcription. Thereby Akt antagonizes TGF-β signaling to protect cells from TGF-β induced apoptosis and cell cycle arrest (Conery et al., 2004; Remy et al., 2004).

1.2.8 Endocytic regulation of TGF-β signaling

Endocytosis of cell surface receptors is a common theme in the regulation of signaling pathways; however, variations are observed regarding the function and outcomes of receptor internalization. Internalization of G protein-coupled receptors (GPCR) serves to downregulate the number of membrane receptors after agonist stimulation and thus allows for signaling termination and desensitization (Luttrell and Lefkowitz, 2002). In other pathways receptor endocytosis is not only a means to regulate receptor surface levels, but is actually required for signaling propagation, and endocytic routing is a determinant for signaling specificity and intensity, as shown for epidermal growth factor receptors (EGFR) (Roy and Wrana, 2005; Sigismund et al., 2008; Vieira et al., 1996).

The TGF-β receptors were demonstrated to be rapidly internalized together with bound TGF-β (Massagué and Kelly, 1986). In contrast to GPCRs and EGFR, endocytosis of TGF-β receptors depends on constitutive internalization and recycling and is not induced nor promoted by ligand binding (Ehrlich et al., 2001; Mitchell et al., 2004). TGF-β receptors are endocytosed through clathrin dependent and clathrin independent mechanisms, and the specific routes of trafficking were suggested to be regulatory switches in the TGF-β pathway (Di Guglielmo et al., 2003).

In clathrin dependent endocytosis TβRII binds to apaptor protein-2 (AP2) with a [DE]XXXL[LI] di-leucin motif in its cytoplasmic domain (Ehrlich et al., 2001; Yao et al., 2002). AP2 is a central adaptor which associates with PtdIns(4,5)P_2 in the plasma membrane and by binding to clathrin promotes the polymerization of triskelial clathrin to form the coat scaffold (Bonifacino and Lippincott-Schwartz, 2003). AP2 also recruits TGF-β receptors into coated membrane domains by directly or indirectly binding of the β2 subunit of AP2 to the I218-I219-L220 di-leucine motif in TβRII (Ehrlich et al., 2001).

Classical internalization signals are absent in TβRI. Instead, a C-terminal sequence including R482 to L492, termed non-activating-non-downregulating (NANDOR) box, was reported to be critical for internalization (Garamszegi et al., 2001; Zhou et al., 2004). Deletion of the TβRI NANDOR box in addition abolished transphosphorylation by TβRII and rendered TβRI inactive (Garamszegi et al., 2001).

Clathrin endocytosis of TGF-β receptors has been linked to active TGF-β-Smad signaling (Chen, 2009; Di Guglielmo et al., 2003; Penheiter et al., 2002). Following clathrin endocytosis TGF-β receptors are found in early endosome antigen-1 (EEA1) positive early endosomes (Di Guglielmo et al., 2003; Hayes et al., 2002). The TGF-β signaling-promoting Smad anchor for receptor activation (SARA) colocalizes with EEA-1 positve early endosomes. SARA was demonstrated to facilitate TβRI mediated R-Smad phosphorylation by targeting Smads to the activated receptor complex (Itoh et al., 2002; Tsukazaki et al., 1998). Internalized receptors can be shifted back to the membrane in Rab11 positive recycling endosomes (Di Guglielmo et al., 2003; Mitchell et al., 2004).

In parallel to clathrin dependent endocytosis TGF-β receptors were reported to undergo internalization in caveolin positive vesicles. This endocytic pathway is thought to originate from TGF-β-bound TGF-β receptors localized in lipid rafts. These dynamic microdomains are enriched in cholesterol and sphingolipids (Lingwood and Simons, 2010; Roy and Wrana, 2005). The raft-associated protein caveolin-1 promotes formation caveolin-rich vesicles, termed caveolae; however, the exact mechanisms by which caveolae are formed have not been elucidated to date (Chen, 2009). TβRI was found to interact with caveolin (Razani et al., 2001), and caveolar endocytosis of TGF-β receptors has been reported to shift TGF-β receptors towards a degradative pathway that antagonizes TGF-β signaling (Di Guglielmo et al., 2003). This has been suggested from findings that

caveolin-1 positive vesicles were positive for the inhibitory Smad7 and the HECT E3 ligase Smurf which targets TGF-β receptors for degradation (Di Guglielmo et al., 2003; Hayashi et al., 1997; Kavsak et al., 2000; Nakao et al., 1997).

An additional mechanism of TGF-β receptor endocytosis was shown to involve the adaptor protein β-Arrestin (β-Arr) (Lohse et al., 1990). β-Arr is known to regulate internalization and signaling in G protein-coupled receptors (Pitcher et al., 1998) and to interact with clathrin and AP2 (McDonald and Lefkowitz, 2001). TβRIII was shown to directly associate with β-Arrestin (Chen et al., 2003). This interaction was triggered by phosphorylation of the TRIII cytoplasmic domain by TβRII. As a consequence, TβRII and TβRIII were internalized to downregulate TGF-β signaling (Chen et al., 2003). Recently, TβRII was shown to form parathyroid hormone (PTH) induced complexes with the PTH receptor (PTH1R) and to undergo β-Arr mediated internalization which suppressed Smad signaling (Qiu et al., 2010). The mechanisms, however, by which TGF-β signaling is repressed in the context of β-Arr mediated internalization remains to be elucidated in future studies (Chen, 2009).

It is, however, still under debate whether partitioning of TGF-β receptors into membrane microdomains and/or endocytic routes is a general regulatory mechanism in TGF-β signaling, and how the TGF-β receptors are targeted for either clathrin or caveolin endocytosis (Kang et al., 2009). Moreover, the significance of TGF-β receptor endocytosis in the activation of the signaling pathways is discussed controversely.

1.3 Marfan Syndrome and MFS-related diseases

1.3.1 Classical Marfan Syndrome

Marfan syndrome (MFS), first decribed by french pediatrician Antoine Marfan, is an autosomal hereditary connective tissue disorder with an estimated prevalence of one case in 3000 to 5000 individuals (Marfan, 1896; Judge and Dietz, 2005). Clinical manifestations of MFS involve the skeletal, ocular, and cardiovascular sytem, and diagnosis is based on specific criteria following the 1996 Ghent nosology (Paepe et al., 1996). Patients often display tall statue, long and slender limbs, disproportionate outgrowth of the long bones, arachnodactyly, scoliosis and pectus excavatum or carinatum (hollowed or pigeon chest). Ectopia lentis is the most prominent ocular feature. Defects in the cardiovascular system include left ventricular dilatation and mitral valve abnormalities. The most severe complications, representing the primary cause of premature mortality, are dilatations of the ascending aorta that predispose to the formation of ascending aortic aneurysms and eventually dissections due to a decreased stability and elasticity of the aortic walls. MFS is linked to mutations in the gene encoding fibrillin-1 (*FBN1*) on chromosome 15q21.1 (Dietz et al., 1991).

To date more than 800 mutations in *FBN1* have been identified, including missense-, premature stop codon- (PTC-), frameshift- and splicing mutations (Faivre et al., 2007; Robinson et al., 2006). Among missense mutations, which account for two-third of all mutations, 61% are cysteine-related.

Fibrillin-1 is as 350-kDa glycoprotein that contains multiple repeats of calcium-binding epidermal growth factor (cbEGF)-like modules interspersed with eight-cysteine TB/8 motifs that are unique to fibrillins and LTBPs (Robinson et al., 2006). Fibrillin monomers polymerize to form microfibrils forming a lattice by head-to-tail and lateral interactions. Microfibrils can either associate with cross-linked elastin in elastic fibers or grow into large aggregates devoid of elastin (Ramirez and Dietz, 2009). In the medial layer of the aortic wall microfibrils associate with elastin to form lamellae surrounding and separating individual vascular smooth muscle cell (VSMC) layers. In addition, elastin-free microfibrils connect lamellar rings to one another, to VSMCs, and to the endothelial basement membrane (Ramirez and Dietz, 2007). Mutations in FBN1 result in an aberrant formation of elastic fibers and disruption of microfibril-mediated connections between cells and elastic lamellae which causes reduced stability and elasticity of the aortic walls.

In addition to its architectural function, fibrillin-rich microfibrils are involved in the regulation of activation and bioavailability of growth factors, including latent TGF-β and pro-BMPs, by sequestering them to extracellular matrix: LTBP1, which is associated with TGF-β in the LLC (1.2.1) was demonstrated to associate with fibrillin, and the interaction was mapped to three C-terminal domains of LTBP1 and four N-terminal domains of fibrillin (Isogai et al., 2003). In turn, fragments of fibrillin-1 (exons 44-49) were shown to promote the release of TGF-β from the ECM by competing with the C-terminus of LTBP for binding to the N-terminus of fibrillin, which resulted in increased phosphorylation of Smad2 (Chaudhry et al., 2007). Furthermore, the pro-domains of BMP2, BMP4, BMP7, BMP10 and GDF5, but not GDF8 are bound with high affinity directly by the N-terminus of fibrillin-1, suggesting that the growth-factor:pro-domain complexes of BMP4 (with the full-length pro-peptide), BMP7, BMP10, and GDF5 are targeted to fibrillin-rich microfibrils as well (Gregory et al., 2005; Sengle et al., 2008).

The role of fibrillin-1 in the regulation of TGF-β bioavailability was emphasized by mouse models of MFS. Mice in wich *FBN1* expression was abolished by targeted deletions of exons 19-24 ($mg\Delta/mg\Delta$) (Pereira et al., 1997) displayed enhanced TGF-β activation and signaling leading to apoptosis in the developing lung which could be rescued by perinatal administration of a TGF-β neutralizing antibody (Neptune et al., 2003). Another mouse model of MFS comprises one hypomorphic allele of *FBN1* arising from a cysteine substitution ($FBN1^{C1039G/+}$). These mice develop progressive aortic aneurysms and non-cardiovascular symptoms of MFS, accompanied by signs of elevated TGF-β signaling, i.e. increased collagen deposition, Smad phosphorylation and nuclear translocation (Habashi

et al., 2006). Inhibition of TGF-β signaling by treatment with a TGF-β neutralizing antibody or a angiotensin II type 1 receptor (AT1R) blocker (ARB, Losartan) prevented the development of aortic aneurysms. Angiotensin II binding to AT1R has been shown to increase TGF-β1 mRNA levels by a NADPH oxidase/p38 MAPK/AP1 signaling cascade (Wenzel et al., 2001), and also to upregulate Thrombosponin 1, an activator of latent TGF-β (Zhou et al., 2006). Alternatively, Angiotensin II was reported to promote TGF-β independent Smad2 phosphorylation in VSMCs through an AT1R mediated mechanism (Rodríguez-Vita et al., 2005). The role of TGF-β1 in the development of aortic aneurysms was emphasized by analyses of aneurysmal aortic specimens from patients which displayed aberrant distribution of TGF-β1, elevated levels of phosphorylated Smad2, and increased PAI-1 expression, which were accompanied by a breakdown of elastic fibers (Gomez et al., 2009).

Although the mechanisms by which increased TGF-β signaling promotes the development of aneurysms remain to be elucidated, it seems clear that dysregulation of TGF-β signaling which may result from defective sequestration and activation of latent TGF-β in the ECM critically contributes to the development of the MFS disease phenotype.

1.3.2 Marfan syndrome type II, Loeys-Dietz syndrome and Thoracic Aortic Aneurysms and Dissections syndrome

During the past years an increasing number of patients were reported to display a Marfan-like phenotype in the absence of mutations in *FBN1*. The disease phenotypes in those patients were similar to classical Marfan syndrome, but revealed distinct and non-overlapping features which set them apart both from classical MFS and from each other (Robinson et al., 2006). The genetic basis common to these diseases, Marfan syndrome type II (MFS2), Loeys-Dietz syndrome (LDS) and familial thoracic aortic aneursms and dissections syndrome (TAAD), are heterozygous mutations in the genes for the TGF-β type I or type II receptors, (*TGFBR1*, *TGFBR2*) (Loeys et al., 2005, 2006; Mizuguchi et al., 2004; Pannu et al., 2005; Robinson et al., 2006).

A second locus for Marfan syndrome in a french family was first mapped on chromosome 3p24.2-25 (Collod et al., 1994). This syndrome was very similar to classical MFS as it comprised aneurysms and dissections and skeletal features characteristic for classical MFS, but without an ocular phenotype. The syndrome was thus termed type 2 Marfan syndrome (MFS2). In 2004 analyses the same family revealed a mutation in the gene for TβRII (*TGFBR2*) (Mizuguchi et al., 2004). A synonymous nucleotide substitution (1524G→A, Q508Q) is located at the last nucleotide of Exon 6 and promotes aberrant splicing of *TGFBR2* which creates a premature stop codon. In the same study three nonsynonymous mutations were identified in four unrelated patients (L308P, S449F, R537C).

The phenotypes of Loeys-Dietz syndrome (LDS) are more severe as compared to MFS or MFS2. LDS features overlap with classical MFS in aortic aneurysms, arachnodactyly and dural ectasia, but comprise additional manifestations such as hypertelorism, bifid uvula, cleft palate, widespread vascular aneurysms and dissections and general arterial tortuosity (Loeys et al., 2005). Mutations in patients diagnosed for LDS were found in the kinase domain of TβRI (T200I, M318R, D400G, R487P) and TβRII (Y336N, A355P, G357W, R528H, R528C) (Loeys et al., 2005). A subtype of LDS, LDS2, was diagnosed in a subset of patients that display additional features such as vascular rupture, uterine, splenic, or intestinal rupture, translucent skin, and atropic scars (Loeys et al., 2006). The LDS2 phenotype resembles that observed in vascular Ehlers-Danlos-syndrome which is caused by mutations in the *COL3A1* gene encoding type III collagen (El-Hamamsy and Yacoub, 2009).

At the mild end of the clinical spectrum, familial non-syndromic thoracic aortic aneurysms and dissections (TAAD) display isolated aortic aneurysms and no or only mild unspecific additional features. For the the development of TAAD six different loci have been recognized. One mutation, R460C, in *TGFBR2* (the *TAAD2* locus) was identified in TAAD (Hasham et al., 2003; Pannu et al., 2005). In addition to mutations in *TGFBR2*, isolated aortic aneurysms were found associated with loci including the genes for smooth muscle α-actin (*ACTA2*, locus *TAAD4*), smooth muscle myosin heavy chain (*MYH11*, *TAAD/PDA*), ALK5 (*TGFBR1*, *TAAD5*), and with three loci which have not been mapped to a gene (chromosomes 5q13-14, *TAAD1*; 15q24-26, *TAAD3*; 11q23-24, *FAA1*) (Milewicz et al., 2008).

An additional number of mutations were identified in *TGFBR1* and *TGFBR2*, which were diagnosed in MFS2, LDS, or TAAD (Mátyás et al., 2006). Notably, a series of MFS related disease mutations studied in this work have been associated with different syndromes, depending on patient and investigator (Tab. 1).

Classification of MFS2, LDS and TAAD is complicated by a significant degree of clinical heterogeneity in persons with mutations in *TGFBR2* (Attias et al., 2009). In addition, histological data of alterations in the aortic wall in different MFS related diseases are rare, mainly due to limited availability of tissue samples (Gomez et al., 2009).

Dysregulated TGF-β signaling, however, is considered the common basis shared by MFS and MFS related diseases. In aortic samples of LDS patients signs of elevated TGF-β signaling were apparent from increased levels of phosphorylated Smad2 and connective tissue growth factor (CTGF), which is induced by TGF-β, in the aortic media (Gomez et al., 2009; Loeys et al., 2005). Only a few of the *TGFBR2* mutations in MFS related diseases have actually been tested *in vitro* for TGF-β signaling activity in the context of MFS or cancer (Grady et al., 1999; Lawler et al., 1997; Mizuguchi et al., 2004). A series of mutations were subjected to an *in-silico* analysis to predict their activity (Mátyás et al., 2006). Based

Tab. 1: Reported clinical phenotypes of patients with the *TGFBR2* mutations studied in this work. TAAD: Familial thoracic aortic aneurym/dissection with no or only mild skeletal features (Pannu et al., 2005). MFS2: Aortic and skeletal features resembling those of classic Marfan syndrome without ectopia lentis and without other clinical features specific for LDS (Mizuguchi et al., 2004). LDS1/LDS2: Loeys-Dietz syndrome.*personal communication Eloisa Arbustini

Mutation	TAAD	MFS2	LDS1	LDS2	References
L308P	0	1	0	0	Mizuguchi et al. (2004)
Y336N	0	0	1	0	Loeys et al. (2005)
S449F	0	2	0	1	Mizuguchi et al. (2004); Loeys et al. (2006)
R460C	16	4	0	0	Hasham et al. (2003); Pannu et al. (2005); Singh et al. (2006)
R460H	29	3	23	1	Pannu et al. (2005); Law et al. (2006); Disabella et al. (2006); Loeys et al. (2006)
R528C	0	0	4	0	Loeys et al. (2005, 2006); LeMaire et al. (2007)
R528H	0	0	6	0	Loeys et al. (2005, 2006)
R537C	0	9	1	0	Mizuguchi et al. (2004); Loeys et al. (2006)
R537P	0	1	1	0	*

on these studies it was assumed that mutations in TβRI and TβRII which are known to cause one of the MFS related disease syndromes render the protein kinase inactive and result in non-functional receptors (Gordon and Blobe, 2008). This finding raised the question of how loss-of-function TGF-β receptors promote a paradoxical activation of TGF-β signaling, and, moreover, how different mutations in *TGFBR2* cause distinct clinical phenotypes.

1.4 Pathological remodeling in the aortic media and the development of aortic aneurysms

The aortic wall consists of three layers. The thin inner layer, the tunica intima, is formed by tightly packed endothelial cells (EC) lining the lumen of the vessel, and an underlying thin layer of connective tissue, the basal lamina (Fig. 5). Adjacent to the intima, the medial layer, tunica media, confers strength and elasticity to the aortic wall. The media is formed by layers of VSMCs which are sandwiched between elastin fibers, bundles of collagen and connected and surrounded by extracellular matrix of microfibrils and proteoglycans (El-Hamamsy and Yacoub, 2009). The outermost layer in the aortic wall is the tunica adventitia, which is rich in collagens and comprises fibroblasts, nerves and capillaries.

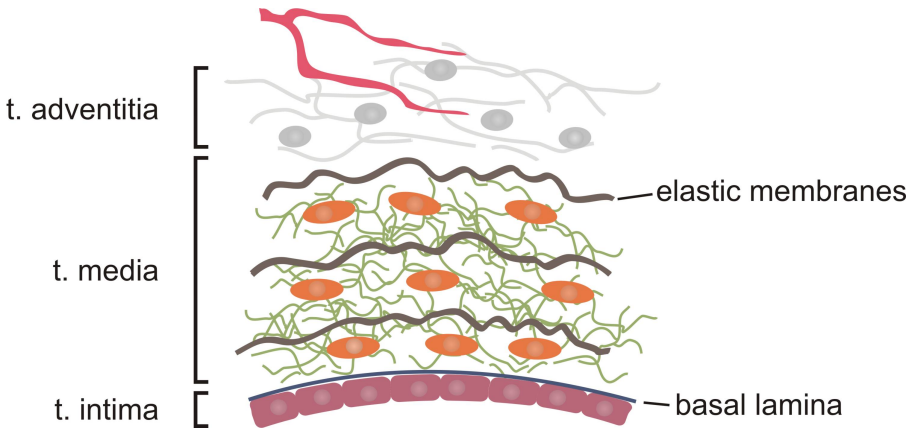

Fig. 5: Composition of the aortic wall. Lining the vessel lumen, the tunica intima consists of endothelial cells. The basal lamina separates the tunica intima from the tunica media which consists of longitudinally oriented smooth muscle cells dispersed between with concentrically arranged elastic membranes and extracellular matrix proteins. The outer layer, tunica adventitia, contains fibroblasts, nerves, and capillaries in a collagen-rich matrix.

VSMCs are not terminally differentiated cells even in the adult organism, and they can alternate between proliferative, contractile, secretory or quiescent states. Depending on the respective state, VSMCs are characterized by specific morphologies, proliferative and migrative properites, and the expression of marker proteins (Owens et al., 2004; Rensen et al., 2007). VSMCs in the aortic wall fulfill two major functions.

First, VMSC of the contractile phenotype regulate blood pressure and hemodynamics in reponse to the pulsatile blood flow. Contractions depend on the interaction of the contractile complex comprising smooth muscle α-actin (encoded by *ACTA2*) and β-myosin heavy chain (*MYH11*) which are connected to the cell membrane through anchor proteins (El-Hamamsy and Yacoub, 2009). As described, mutations in *ACTA2* and *MYH11* are associated with TAAD (1.3.2). Second, secretory VSMCs synthesize ECM components such as collagens I and III, elastin, fibrillin and fibulin and proteoglycans, thereby controlling mechanical properties of the vascular wall. In addition, VSMCs secrete a large number of cytokines including TGF-β, PDGF and VEGF (Gerthoffer and Singer, 2002). The state of VSMCs is regulated by mechanical cues such as radial stretch and ECM interactions, by inflammatory and oxidative stress, and, importantly, by biochemical factors such as platelet-derived growth factor (PDGF) and TGF-β (Owens et al., 2004).

This plasticity of the tunica media enables blood vessels to respond to hemodynamic stimuli through vascular remodeling, an adaptive process that induces enduring changes in the composition and size of the vessel (Jones et al., 2008). In addition, vascular remodeling allows for repair following vascular injury. Aortic aneurysms linked to MFS and related diseases are regarded to be a consequence of pathological vascular remodeling in the aorta which leads to a degeneration of the medial layer. The hallmark of this pathological process is an increased fragmentation of elastic fibers. In addition, in

aortic aneurysms an increased rate of apoptosis and disturbed VSMC arrangement are observed (El-Hamamsy and Yacoub, 2009).

Degenerative processes in the tunica media are assumed to include deregulated matrix-metalloprotease (MMP) mediated degradation of elastin and later of collagen (Thompson et al., 2002). Pathological vascular remodelling in TAAD can at least in part be attributed to overactivation of MMP-activation (Jones et al., 2008). On the other hand, a dysregulated production of ECM by VSMCs may contribute to pathological remodeling. Furthermore, VSMC proliferation and apoptosis, as well as their differentiative state are relevant for the development of aortic aneurysms.

Together these pathological alterations are thought to constitute a medial atropy in TAAD. Since the weakened aortic wall can not withstand the blood pressure, dilatations of the aortic wall develop which further proceed into aneurysms. Aortic dissections occur if blood enters the medial layer through lesions in the endothelial barrier and the blood flow disrupts the aortic wall, resulting in life threatening internal hemorrhagic complications (Milewicz et al., 2008).

1.5 Role of TGF-β in vascular remodeling

The role of TGF-β superfamily signaling in vascular development is well documented (Pardali et al., 2010). Targeted deletions of ALK1 (*ACVRL1*), ALK5 (*TGFBR1*), TβRII (*TGFBR2*), or endoglin (*ENG*) in knockout mice generated similiar phenotypes. Deficiency of any of these receptors resulted in embryonic lethality at mid-gestation and was associated with defective vascular development (Larsson et al., 2001; Oshima et al., 1996; Urness et al., 2000). Heterozygous mutations in genes for ALK1 or endoglin result in a phenotype of hereditary haemorrhagic telangiectasia type 2 (HHT2) or HHT1, respectively. These mutations are assumed to interfere with proper receptor folding and expression and thus lead to haploinsufficiency (Gordon and Blobe, 2008). HHT is an autosomal dominant disorder characterized by vascular dysplasia resulting in telangiectasias (appearance of small dilated blood vessels in mucocutaneous skin) and arteriovenous malformations (AVM). However, the molecular mechanism underlying HHT has not been entirely elucidated to date (Gordon and Blobe, 2008; Pardali et al., 2010).

TGF-β signalling is directly connected with the regulation of extracellular matrix homeostasis (Fig. 6) (Jones et al., 2008; Verrecchia and Mauviel, 2002, 2007). TGF-β is known to be a strong promoter of ECM deposition by induction of various collagens (type I, III, V, VI, and VII) as well as of other ECM components such as fibronectin and proteoglycans (Ignotz and Massagué, 1986; Rossi et al., 1988; Varga and Jimenez, 1986; Verrecchia and Mauviel, 2002), moreover, TGF-β was reported to upregulate elastin by stabilizing tropoelastin mRNA (Kähäri et al., 1992; Kucich et al., 2002). By inducing expression of con-

nective tissue growth factor (CTGF) TGF-β stimulates fibroblast proliferation, migration, adhesion, and extracellular matrix formation (Moussad and Brigstock, 2000).

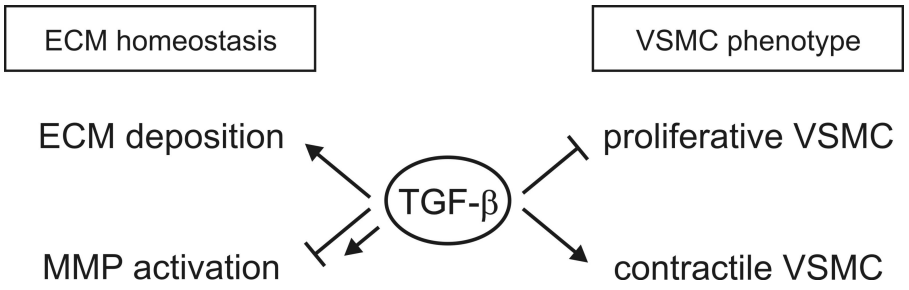

Fig. 6: TGF-β control of vascular remodeling. TGF-β stimulates synthesis of ECM proteins and antagonizes MMP activation in most contexts, and promotes SMC differentiation into the contractile phenotypes.

Concurrent with its positive effect on matrix production, TGF-β was shown to counteract MMP-mediated matrix degradation by directly or indirectly inhibiting MMP activity (Fig. 6). TGF-β was reported to induce expression of tissue inhibitors of metalloproteases (TIMP), TIMP-1 and TIMP-3 in fibroblast cells (García-Alvarez et al., 2006; Kwak et al., 2006). TGF-β might directly repress MMP expression through TGF-β inhibitory elements (TIE) in the promoter of MMPs 1, 7, and 13 (Chakraborti et al., 2003; Yan and Boyd, 2007). Furthermore, plasminogen activator inhibitor (PAI-1) is a well established target gene induced by TGF-β. PAI-1 inhibits tissue- and urokinase plasminogen activators (tPA, uPA) which convert plasminogen to plasmin. The serine protease plasmin, in addition to its function as an upstream activator of MMPs (Lijnen, 2001; Ramos-DeSimone et al., 1999; Yang et al., 2005), has been shown to induce VSMC apoptosis and anoikis by mechanisms that involved direct binding of plasmin to the surface of VSMCs (Chen et al., 2006; Rossignol et al., 2006). Expression of PAI-1 in VSMCs interfered with plasmin-mediated apoptosis and promoted VSMC proliferation. However, the role of TGF-β has been rendered more complex by reports that demonstrated an opposite effect of TGF-β. In skin MCF10 breast cancer cells type and skin fibroblasts, TGF-β was shown to actually induce MMPs or plasminogen activator, respectively (Kim et al., 2004; Laiho et al., 1986).

In addition to its role in ECM metabolism as a regulator of ECM secretion and MMP activity, TGF-β functions to control VSMC proliferation and differentiation (Fig. 6). TGF-β was reported to promote SMC differentiation in vitro by upregulation of contractile proteins like SMC specific α-actin and myosin heavy chain (Adam et al., 2000; Hautmann et al., 1997; Owens et al., 2004). Moreover, TGF-β promoted the differentiation of SMCs from mesenchymal cells (Sinha et al., 2004). Conversely, TGF-β inhibited proliferation of VSMCs in a Smad2/3- and p38 dependent mechanism and thereby appears to promote VSMC differentiation (Owens et al., 1988; Seay et al., 2005).

1.6 State of research on TGF-β type II receptor mutations and aim of the project: "*TGFBR2* mutations in MFS related diseases"

As described above, TGF-β signaling is regulated on various levels of the pathway, and the signaling outcomes are highly context specific. To date there is little information that may serve to elucidate whether the observed paradoxical activation of TGF-β results from cell-autonomous mechanisms or if it develops as a secondary effect of abnormal receptor activity during tissue homeostasis, or from a combination of both. In the first scenario, a receptor with a mutation may for instance contribute to ligand binding and thus function as an accessory receptor to enhance signaling (Jones et al., 2008). By altering receptor trafficking and endocytosis, or by shifting endocytotic routes a mutant TGF-β receptor may promote activity of the wildtype receptors. With respect to the pleiotropic effects on non-Smad pathways it seems also possible that distinct mutations differentially affect non-Smad pathways leading to direct or secondary effects on the TGF-β pathway. Mutations in the cytoplasmic domain may further affect interaction with accessory proteins involved in the regulation of the pathway. All these effects may be depending on the nature of the respective mutations. In order to gain information on individual features of single mutations which were identified in TGF-β receptors, this study was set out to comprehensively characterize a series of nine mutations in *TGFBR2* in biochemical and cell based assays. Its results may serve to reveal a potential mechanism for paradoxical activation of TGF-β signaling and thus provide new insights into pathway dynamics. Moreover, by comparing a number of mutations it may contribute to elucidate the mechanisms by which TGF-β signaling promotes the development of distinct phenotypes which are caused by different mutations.

2 Materials and Methods

Reagents were purchased from Carl Roth Laborbedarf, VWR, neolab, or Merck unless otherwise stated. Lab and cell culture plasticware and consumables were obtained from Eppendorf, Greiner Bio-One, Nunc, or Hartenstein Laborbedarf.

2.1 Molecular biology

2.1.1 Cloning, mutagenesis, plasmid preparation

All standard techniques of molecular cloning were performed according to Sambrook (2001).

The coding sequence of TβRII with an N-terminal HA-tag, or a FLAG-tag at the C-terminus was excised from its source plasmid pcDNA1 using *NotI* and *BamHI* and subcloned to the pcDNA3.1 vector. Plasmid charts can be found in Appendix A.1. Mutant constructs were generated using the GeneTailor Site-Directed Mutagenesis kit (Invitrogen) according to manufacturer´s protocols. Primers used are listed in Appendix A.2. Bacterial amplification and purification of plasmid DNA was done using the Qiaprep Mini and Midi Kits (Qiagen) or the Promega Mini Kit (Promega), respectively, according to manufacturer's instructions. The concentration of purified plasmid DNA was determined on a NanoDrop spectrophotometer (Peqlab).

2.1.2 RNA preparation, reverse transcription

RNA preparation was done using either PeqGOLD TriFast reagent (Peqlab) or the the TotalRNA Kit (Peqlab), respectively, according to manufacturer's protocols. DNA contaminations were removed by on-column digestion with DNaseI (Peqlab). RNA purity was determined on a NanoDrop spectrophotometer (Peqlab). Isolated total RNA was stored at -80°C. 0.5-1 μg of total RNA per sample was employed for reverse transcription. Reverse transcription was done using MMLV-reverse transcriptase (Promega) and anchored NV-oligo-dT primers (Invitrogen). Each 12 μl of RNA denaturation mix were incubated at 70°C for 5 minutes and placed on ice immediately. Per sample 13 μl of reverse transcriptase mix were added, and the reaction was performed at 42°C for 50 minutes before the transcriptase was inactivated by heating to 70°C for 15 min. cDNA quality was checked by agarose gel electrophoresis.

Buffers and reagents

- RNA denaturation mix: 1 μg RNA template, 0.5 μl NV-Oligo-dT (100 pmol/μl), ad 12 μl DEPC-H_2O
- Reverse transcriptase mix: 1.25 μl dNTPs (10 mM; qbiogene), 5 μl 5$\times$ MMLV-RT buffer (Promega), 1 μl RNasin RNase Inhibitor (Promega), 1 μl MMLV reverse transcriptase (Promega), 4.25 μl DEPC-H_2O
- DEPC-H_2O: 100 μl DEPC, 100 ml MP-H_2O; mixed, incubated for 15 minutes (uncovered, fume hood), mixed again, incubated overnight (closed, fume hood), autoclaved

2.1.3 Quantitative RT-PCR

Appropriate dilutions of sample cDNAs (usually 1:2-1:16 in MP-H_2O) were used as templates in fluorescence-based quantitative PCR reactions. A master mix for all samples was prepared first, which was then distributed to different samples in 96-well white qPCR Plates (AbGene). Oligonocleotide primer sequences are listed in Appendix A.3. SYBR-Green qPCR was done in an Opticon Monitor (MJ Research/Bio-Rad) with the following thermal profile:

1. initial denaturation: 95°C for 5 min
2. 35 cycles: 95°C for 30 seconds (denaturation), 60°C for 30 seconds (annealing), 72°C for 30 seconds (elongation), 78°C for 5 seconds (fluorescence recording)
3. melting curve: 65-95°C, hold 5 s

C_T values were calculated by Opticon Monitor software (MJ Research). Relative expression values were obtained using the $\Delta\Delta C_T$ method (Livak and Schmittgen, 2001), or determined by calculation of mean normalized expression using the qDE qPCR data evaluation template (Daniel Horbelt) which incorporates reaction efficiencies (Pfaffl, 2001; Simon, 2003).

Buffers and reagents

- Taq polymerase incubation mix: 2 μl cDNA (diluted appropriately), 0.6 μl dNTPs (10 mM; qbiogene), 2.5 μl Taq buffer (10$\times$, containing 15 mM $MgCl_2$; qbiogene), 1 μl $MgCl_2$ (25 mM; qbiogene), 1.3 μl SYBRGreen (5$\times$; Cambrex Bioscience), 0.3 μl Taq polymerase (5U/μl; qbiogene), 15.3 μl MP-H_2O
- Primers: 10 mmol/μl in MP-H_2O

2.2 Protein biochemistry

2.2.1 SDS-PAGE and Western blotting

For SDS-polyacrylamide gel electrophoresis and Western blotting the Mini Protean System (Bio-Rad) was used. Polyacrylamide Gels were cast at least 12 h before use and stored at 4°C. Samples and protein standards (PageRuler, Fermentas) were loaded on 10% or 12% gels in Laemmli SDS sample buffer. PAGE was performed at 180 V until samples had reached the separation gel, and further on at 150 V.

After PAGE gels were rinsed in blotting buffer before the blotting sandwich was assembled. Proteins were transferred to PVDF (Westran, Whatman) or nitrocellulose (Protran, Whatman) in a cooled tank at 100 V for 2 h. Membranes were washed briefly in washing buffer and blocked at RT in 3% non fat dry milk in washing buffer for 1 hour. Phosphoprotein Western blots were blocked in 5% BSA in washing buffer for 1 hour at RT. Primary antibodies were used as indicated in Tab. 2. Membranes were washed 3×5 minutes in washing buffer before incubation with secondary antibodies goat-anti-mouse-HRP (1:10000; Dianova) or goat-anti-rabbit-HRP (1:10000; Dianova), respectively, in washing buffer containing 3% non fat dry milk for 1-2 hours at RT. Chemoluminescent reactions were developed using Femto-Glo ECL reagents (P.J.K) and documented on a ChemiSmart 5000 digital imaging system (Vilber-Lourmat). Western blots were quantified by volumetric measurements using the Bio1D software (Vilber-Lourmat/Peqlab) on 16-bit raw digital images.

To stain proteins in gels after SDS-PAGE gels were shaken in Coomassie staining solution for 30 minutes and destained for 1-16 h.

Buffers and reagents

- polyacrylamide gels
  - 10% separating gels: 2 ml acrylamide:bis-acrylamide (40%, 29:1), 2 ml separating gel buffer, 4 ml dH_2O; 20 μl 40% APS, 7 μl TEMED
  - 12% separating gels: 2.5 ml acrylamide:bis-acrylamide (40%, 29:1), 2 ml separating gel buffer, 2.6 ml dH_2O; 8 μl 40% APS, 4 μl TEMED
  - separating gel buffer: 1.5 M Tris, 0.4% SDS, pH 8.8
  - stacking gels: 0.35 ml acrylamide:bis-acrylamide (40%, 29:1), 1 ml stacking gel buffer, 2.6 ml dH_2O
  - stacking gel buffer: 0.5 M Tris, 0.4% SDS, pH 6.8
- 6× Laemmli SDS sample buffer: 350 mM Tris pH 6.8, 40% (v/v) glycerol, 10% (w/v) SDS, 30% (v/v) β-mercaptoethanol, 0.001% (w/v) bromphenol blue

- 10× SDS PAGE buffer: 250 mM Tris, 1.9 M glycin, 1% SDS
- Western blot transfer buffer: 25 mM Tris, 190 mM glycin, 20% MeOH
- Western blot washing buffer (TBS-T): 50 mM Tris, 150 mM NaCl, 0.1% (v/v) Tween-20
- Coomassie blue staining solution: 0.2% (v/v) Coomassie R Brilliant Blue, 40% MeOH, 8% acetic acid
- Coomassie blue destaining solution: 10% 2-propanol, 10% acetic acid

Tab. 2: Primary antibodies for Western blotting. Suppliers were SA - Sigma-Aldrich, CS - Cell Signaling, KL - Knaus Lab, P - Promega, RD - R&D, SC - Santa-Cruz, ZY - Zymed, followed by catalogue number;
m - mouse, rb - rabbit, mAb - monoclonal antibody, pAb - polyclonal antibody; Incubation temperatures were 4°C for overnight (o/n) incubation, room temperature for 1 hours incubation.

Target	Supplier	Type	Blocking	Concentration	Incubation
FLAG-tag	SA F3165	m mAb	3% milk	1:2000	o/n or 1 h
HA-tag	SA H3663	m mAb	3% milk	1:1000	o/n
Myc-tag	KL	m mAb	3% milk	1:1000	o/n
TβRI	SC sc-9048	rb pAb	3% milk	1:1000	o/n
TβRII	SC sc-400	rb pAb	3% milk	1:1000	o/n
TβRIIB	RD AF1003	g pAb	3% milk	1:1000	o/n
TβRIII	SC sc-6199	g pAb	3% milk	1:1000	o/n
Smad2	CS 3122	rb mAb	3% milk	1:1000	o/n
Smad3	CS 9523	rb mAb	3% milk	1:1000	o/n
p-Smad2	ZY 40-0800	rb pAb	5% BSA	1:1000	o/n
p-Smad1/5/8	CS 9511	rb pAb	5% BSA	1:1000	o/n
p-ERK1/2	CS 9106	m mAb	5% BSA	1:1000	o/n
p-p38	P V1211	rb pAb	5% BSA	1:1000	o/n
GAPDH	CS 2118	rb mAb	3% milk	1:1000	o/n
Histone H3	CS 9715	rb pAb	3% milk	1:1000	o/n
β-actin	SA A5441	m mAb	3% milk	1:2000	o/n or 1 h
β-tubulin	SA T5201	m mAb	3% milk	1:2000	o/n

2.2.2 Protein quantification using the BCA protein assay

To enable equal loading of cell lysates, the bicinchoninic acid (BCA) protein assay was used to quantify protein concentrations in sample lysates. Clarified lysates were diluted 1:10 in MP-H_2O, and 20 μl were combined with 200 μl of BCA solution mix in a microtiter plate. Plates were incubated for 20-60 minutes at 56°C before absorbance was determined in a plate reader (Sunrise, Tecan) at 550 nm. Protein concentrations were calculated by extrapolating to a standard curve obtained in parallel.

Buffers and reagents

- BCA solution A: 1% (w/v) BCA , 1.35% (w/v) $NaHCO_3$, 0.58% (w/v) NaOH, 0.57% (w/v) $KNaC_4H_4O_6$ in MP-H_2O
- BCA solution B: 2.3% (w/v) $CuSO_4$ in MP-H_2O
- BCA solution mix: solution A:solution B = 49:1

2.2.3 Immunoprecipitation

L6 cells were washed with PBS (PAA) and harvested by scraping in TNE IP buffer. Following 45 minutes rotation at 4°C lysates triturated by pipetting and clarified by centrifugation (10 minutes, 15000g). Proteins were immunoprecipitated by addition of 0.5-1 μg antibody per 1×10^6 cells over night at 4°C. Antibody-protein complexes were precipitated by addition of 60 μl protein G-sepharose (1:1 in PBS; Sigma-Aldrich) for 1 hour at 4°C and pelleted by centrifugation (3 minutes, 300g). Following 3 washes in PBS pellets were resuspended in 50 μl 2× Laemmli SDS sample buffer.

Buffers and reagents

- TNE lysis buffer buffer: 20 mM Tris pH 7.4, 150 mM NaCl, 1 mM EDTA, 1% (v/v) Triton X-100
- TNE IP buffer: TNE lysis buffer, 1 mM PMSF, 1× complete protease inhibitor cocktail (Roche)
- Laemmli SDS sample buffer: see 2.2.1

2.2.4 ELISA

To evaluate binding and specificity of purified monoclonal TβRIIB antibodies an ELISA was performed in which the extracellular domains of either splice variant of TβRII, or the peptide that was used for immunization were employed as coating antigens. TβRII and TβRII-B ECDs were obtained from Joachim Nickel (Universität Würzburg). 96-well plates (Maxisorp, Nunc) were coated with a 2 μg/ml solution of the TβRIIB insert petide or TβRII ECD in sodium carbonate at 4°C over night. After washing 3× in PBS wells were blocked for 1 hour at 37°C. Wells were washed 3× in PBS and were incubated with the primary antibody in blocking solution on a plate shaker for 1 hour at 37°C. After washing (4× in PBS-T and once in PBS) a goat-anti-mouse-HRP or goat-anti-rabbit-HRP (1:10000 in blocking solution; Dianova) was allowed to bind for 1 hour at 37°C on a plate shaker. After washing 4× in PBS-T and once in PBS the peroxidase reaction was initiated by adding 100 μl peroxidase reaction mix. Absorbance was measured at 630 nm in a plate

reader (Sunrise, Tecan). If the reaction was very intense it was stopped by addition of 100 μl 1 M H_3PO_4, and absorbance was measured at 450 nm.

Buffers and reagents

- Sodium carbonate solution: 0.2 M, pH 9.4-9.7
- Blocking solution: TBS/1% BSA
- PBS: 137 mM NaCl, 2.7 mM KCl, 12 mM total phosphate, pH 7.2-7.4 (8 g NaCl, 0.2 g KCl, 0.24 g KH_2PO_4, 2.68 g $Na_2HPO_4 \cdot 7H_2O$, ad 1 l MP-H_2O
- PBS-T: PBS/0.1% Tween-20
- TBS: 150 mM NaCl, 20 mM Tris
- Peroxidase reaction mix: 5 ml citrate solution, 5 μl H_2O_2, 250 μl TMB solution
- Citrate solution: 50 mM, pH 4.25 (9.6 g citric acid in 1 l H_2O, adjust pH with Trisodiumcitrate solution (14.7 g in 1 l MP-H_2O)),
- TMB solution: 40 mg TMB, 9.9 ml MP-H_2O, 100 μl HCl_{conc}

2.2.5 *In-vitro* kinase assays

HEK293T cells were plated on 6-cm dishes at a density of 1.2-1.5$\times 10^6$ cells per dish 16-20 hours before transfection. Cells were transfected as described (2.3.1.2) with FLAG-tagged TβRII expression constructs (6 μg DNA per well). 20 hours after transfection (PEI) cells were harvested in TNE lysis buffer containing protease inhibitors. Receptors were immunoprecipitated over night with 2 μg/sample anti-FLAG M2 antibodies (Sigma-Aldrich) in TNE lysis buffer containing protease inhibitors followed by incubation for 1 hour with protein A-sepharose (Sigma-Aldrich). After extensive washing and centrifugation (2 minutes, 300g) sepharose pellets were resuspended in 20 μl kinase buffer. The reaction was started by addition of 5μl hot ATP mix containing 5 μCi [γ-^{32}P]-ATP (Hartmann Analytics) and incubated for 30 minutes at 30°C. Following SDS-PAGE and Western blot (section 2.2.1) signals were collected on film (Kodak). The total amount of receptors on the membrane was determined after decay of the radioactive ^{32}P signal using anti-FLAG and anti-TβRII antibodies as described above.

Buffers and reagents

- TNE lysis buffer: 20 mM Tris pH 7.4, 150 mM NaCl, 1 mM EDTA, 1% (v/v) Triton X-100

- TNE lysis buffer containing protease inhibitors: TNE, 1 mM PMSF, 1× complete protease inhibitor cocktail (Roche)
- 10× kinase buffer: 200 mM Tris pH 7.7, 1.5 M NaCl, 10 mM DTT, 100 mM NaF, 20 mM Na_3VO_4
- ATP mix: 500 μM ATP, 75 mM $MgCl_2$
- Hot ATP mix: per sample 4.5 μl ATP mix, 0.5 μl [γ-^{32}P]-ATP (10 μCi/μl; Hartmann Analytics)

2.2.6 Antibody Generation

2.2.6.1 Affinity purification

Antibodies were purified from hybridoma cell supernatants by protein G-sepharose affinity chromatography using ProPur vacuum columns (Nunc). 100 ml hybridoma supernatant were sterile filtered through 0.2 μm disc filters and diluted 1:1 with binding buffer. The protein G-sepharose resin was equilibrated with 10 ml binding buffer before the supernatant was applied at a rate of 4 ml/min. The column was washed with 20 ml binding buffer before bound antibodies were eluted with 10 ml elution buffer. Fractions of 0.9 ml (first fraction) or 1.8 ml (subsequent fractions) were collected, in tubes containing 0.1 or 0.2 ml of neutralization buffer, respectively. In a NanoDrop spectrophotometer (Peqlab) A_{280} was determined and fractions containing significant amounts of protein were pooled, and desalted and concentrated in PBS buffer in centrifugal filtration units (Vivaspin4, MWCO 30000, Vivascience/Sartorius). Fractions from all chromatography steps were analyzed by SDS-PAGE (section 2.2.1).

Buffers and reagents

- Binding buffer: 100 mM phosphate buffer, pH 7.4
- Elution buffer: 100 mM Glycin-HCl, pH 2.7
- Neutralization buffer: 1M Tris pH 8

2.2.6.2 AlexaFluor labeling

Labelling of purified monoclonal antibodies was performed using the AlexaFluor-488 mAb labelling kit (Invitrogen) according to the manufacturer´s instruction.

2.3 Cell biology and cell based assays

2.3.1 Cell Culture

2.3.1.1 Maintenance of cell lines

HEK293T embryonic kidney cells (*Homo sapiens*), COS7 kidney fibroblasts (*Cercopithecus aethiops*) and C2C12 myoblasts (*Mus musculus*) were maintained in Dulbecco´s MEM containing 10% FCS, 2mM L-Glutamine, and 100U/ml penicillin/streptomycin at 37°C in a 10% CO_2, humidified atmosphere. L6 skeletal myoblasts (*Rattus norvegicus*) and derived L6-TβRII/B inducible cell lines were cultured under the same conditions except for a 5% CO_2 humidified atmosphere. L6-HA-TβRII-B and L6-HA-TβRII cells were derived from parental L6 cells by retroviral infection (Lutz, 2002). Cells that had stably integrated the inducible constructs could be identified by constitutive expression of EGFP. Receptor expression was induced by addition of 1 μg/ml Doxycyclin for 24 hours. Mv1Lu lung epithelial cells (*Mustella vison*) and derived DR26 cells were grown in Earle´s MEM containing FCS, glutamine, and antibiotics as described, and supplemented with 1× non-essential amino acids, in a 5% CO_2 humidified atmosphere.

Cell cultures were passaged every 2 to 4 days. Cells were detached using Trypsin (PAA) for 1 to 10 minutes and 1/20 to 1/2 were plated for further culture.

Cell numbers were determined in a Neubauer hemocytometer by counting the number of cells in 2-4 16-square areas. The average number of cells in a 16-square area was multiplied by 10^4 to yield the number of cells per ml in the original cell suspension. Alternatively, cell numbers were determined in a CasyTT coulter counter (Roche).

Cryoconservation of cells was performed by resuspending 1×10^6 cells per vial in 1 ml cryo-medium (4°C) containing 20% FCS and 10% DMSO. Vials were transferred to -80°C and kept over night in styrofoam racks before they were transferred to <140°C liquid nitrogen tanks.

2.3.1.2 Transfection of cell lines

HEK293T cells and COS7 cells were transfected using polyethylenamine (PEI, Sigma-Aldrich) in the presence of serum and antibiotics. A PEI dilution in medium was added to plasmid DNA in medium at a ratio of PEI [μg]:DNA [μg] of 2:1. After vortexing for 30 seconds, complexes of polycationic PEI and DNA were allowed to form for 30 minutes at room temperature, before the transfection mix was distributed onto the cells. Cells were harvested 12 to 72 hours after transfection.

L6 cells were transfected using JetPEI (Polyplus Transfections), which is a PEI of a defined molecular weight range optimized for transfection. Transfection with JetPEI was performed in the presence of serum and antibiotics according to the manufacturer´s

instructions. The ratio of PEI [μg]:DNA [μg] was 2:1. Cells were harvested 12 to 48 hours after transfection.

C2C12 cells, Mv1Lu cells, and DR26 cells were transfected with Lipofectamine2000 in the absence of antibiotics according the manufacturer´s protocols. The a ratio of Lipofectamine2000 [μl]:DNA [μg] was 2:1. The medium containing the transfection reagents was replaced 5 hours post-transfection by growth medium not containing antibiotics. DR26 cells were also transfected using JetPEI as described for L6 cells.

2.3.1.3 Hybridoma cell culture and subcloning

Hybridoma cells were expanded in RPMI1640 medium with L-Glutamine containing 10% FCS, 100U/ml penicillin/streptomycin, 1$\times$ non-essential amino acids (PAA), and 50 μM 2-mercaptoethanol at 37°C in a 10% CO_2, humidified atmosphere.

For antibody production, cells were kept under the same conditions, but in the presence of only 5% FCS. Fresh medium was added to every 2 to 3 days until the maximum amount of medium for the respective tissue culture flask was reached. Supernatants were harvested after 10 to 20 days in culture when more than 90% of the cells had died.

Hybridoma subcloning was performed by limiting dilution to achieve single clones (Fuller et al., 2001). Cells were diluted to a statistical density of 0.8 cells per aliquot and plated in 96-well plates. Wells containing one single cell were marked, and the respective clones were expanded as described above.

2.3.2 Luciferase reporter gene assays

L6 cells were plated at 4000 cells per well in 96-well plates. 14-20 hours after plating cells were transfected with 150 ng of TβRII-B together with a TGF-β responsive $(CAGA)_{12}$ luciferase reporter gene construct (30 ng/well); in addition, the constitutively active thymidin kinase-driven renilla luciferase reporter (pRLTK-luc; 10 ng/well) was co-transfected. Transfections were done as described (2.3.1.2).

DR 26 cells were plated at 3000 cells per well and allowed to recover for 14-20 hours. Cells were co-transfected with TβRII WT and mutants at varying ratios, i.e. the fraction of WT was 100%, 75%, 50%, 25%, or 0% which was complemented to 100% by mutant TβRII or controls. The total amount of transfected plasmid DNA was constant (50 ng/well). The TGF-β responsive luciferase reporter gene constructs p3TP-luc or $(CAGA)_{12}$-luc (30 ng/well), and the RLTK-luc reporter (10 ng/well) were co-transfected with receptors as described (2.3.1.2).

16-24 hours after transfection, cells were starved for 2-4 hours in starvation medium containing 0-0.1% FCS. Cells were stimulated with 5-250 pM TGF-β1 (Peprotech) or TGF-β2 (R&D) for 12-20 h. Cells were lysed in passive lysis buffer (Promega), and luciferase activities were measured using the dual luciferase assay system (Promega)

according to manufacturer's instructions in a Mithras LB940 multimode plate reader (Berthold Technologies). Firefly luciferase activities were normalized to renilla luciferase to calculate relative luciferase units (RLU).

2.3.3 Subcellular fractionation

Subcellular fractionation was performed to determine the subcellular localization of Smad proteins and their nuclear translocation in response to TGF-β stimulation. HEK293T cells were plated at 350000 cells per well in 6-well plates 16-20 hours before transfection. Cells were transfected with TβRII receptor constructs (2 μg DNA per well) as described (2.3.1.2). 24 hours after transfection with HEK293T cells were starved for 3 to 5 hours in serum-free medium. Following stimulation or not with 200 pM TGF-β1 for 15 or 60 minutes, cells were harvested in ice cold PBS.

Fractionation was done using the ProteoJet Extraction Kit (Fermentas) buffers with modifications of the manufacturer's protocol: Briefly, the pellet was resuspended in 100 μl cytoplasmic lysis buffer, vortexed for 10 seconds and incubated on ice for 10 min. To prevent dephosphorylation of Smads 20 mM NaF were included in cell lysis buffer, nuclei washing buffer and nuclei storage buffer. After 10 seconds vortexing nuclei were pelleted by centrifugation (7 minutes, 1000g). The supernatant/cytosolic fraction was clarified by centrifugation (15 minutes, 20000g). Nuclei were washed twice and lysed in 75 μl storage buffer containing lysis reagent. After 15 minutes rotating at 4°C the nuclear fraction was clarified by centrifugation (10 minutes, 20000g). Fractionation was verfied by SDS-PAGE and Western blotting for nuclear and cytosolic marker proteins histone H3 and GAPDH, respectively (section 2.2.1). Subcellular localization of Smad2 or phospho-Smad2 was visualized by appropriate antibodies.

2.3.4 Immunocytochemistry

2.3.4.1 Surface staining

C2C12 cells were plated at 2000 cells per well in 16-well glass chamber slides (Nunc). Cells were transfected 14-20 hours after plating with 150 ng per well Myc-TβRII or Myc-TβRII-B expression constructs as described (2.3.1.2). 20 hours post-transfection cells were washed in PBS and fixed in 4% PFA for 20 minutes at room temperature. After washing 3× with PBS cells were incubated with blocking solution for 30 minutes at room temperature, followed by incubation with primary antibodies anti-Myc (1:50; KL) or anti-TβRII-B (4B4, 1:50 or 4B4-AF488, 1:50) in blocking solution over night at 4°C. Cells were washed in PBS and stained with secondary antibodies goat-anti-mouse IgG AF488 (1:400; Molecular Probes) in blocking solution, if applicable. After washing, nuclei were stained with DAPI (1:1000 in PBS) for 5 minutes at room temperature and washed again.

Coverslips were mounted with FluoromountG (Science Services). Image acquisition was done on an Axiovert 200 digital fluorescence microscope (Zeiss) using the Axiovision software (Zeiss).

Buffers and reagents

- PBS: see 2.2.4
- Blocking solution: 3% BSA in PBS

2.3.4.2 Smad nuclear translocation

Immunocytochemistry was used to visualize Smad nuclear translocation. DR26 cells were plated at 6000 cells per well 8-well glass or permanox chamber slides (Nunc). 14-20 hours after plating cells were co-transfected as described above (2.3.1.2) with HA-tagged receptor expression constructs (300 ng/well) and a green fluorescent protein vector pEGFP-N1 (60 ng/well). 20 hours post-transfection cells were starved for 4 hours in serum-free medium and stimulated with 250 pM TGF-β1 for 30 minutes. Cells were fixed in 4% paraformaldehyde, blocked and permeabilized simultaneously for 40 minutes at room temperature. Smad subcellular localization was visualized with anti-Smad2 antibodies (1:200; Cell Signaling), followed by goat-anti-rabbit IgG Alexa-Fluor594 conjugate (1:300; Molecular Probes). Coincidence of receptor expression and expression of co-transfected EGFP was confirmed by anti-HA staining (1:100; Sigma-Aldrich) followed by secondary detection with goat-anti-rabbit IgG Alexa-Fluor594 conjugate (1:300; Molecular Probes). Antibodies were diluted in blocking and permeabilization buffer. DAPI staining, mounting and image acquisition was performed as described in 2.3.4.1.

Buffers and reagents

- PBS: see 2.2.4
- Blocking and permeabilization buffer: 0.5% Triton X-100, 5% BSA in PBS

2.3.5 Phosphoprotein assays

HEK293T and DR26 cells were plated in 12-well plates at 150000 and 70000 cells per well, respectively. 14-20 hours after plating cells were transfected as described above (2.3.1.2) using 1 μg or 0.5-0.75 μg of TβRII expression constructs, respectively. 20 hours after transfection cells were starved for 4-6 hours in serum-free medium. Following stimulation with TGF-β1 (Peprotech) for 1-240 minutes cells were lysed in 1$\times$ Laemmli SDS sample buffer and analyzed by Western blotting (section 2.2.1).

2.3.6 Flow cytometry

2.3.6.1 Receptor expression and internalization

HEK293T cells were plated at 400000 cells per well in 6-well plates. 14-20 hours after plating cells were transfected with 3 μg of TβRII wildtype or mutant constructs as described (2.3.1.2). 20 hours post-transfection cells were harvested using 5 mM EDTA in PBS (PAA). N-terminally HA-tagged TβRII was stained with anti-HA7 (Sigma-Aldrich) at $1\mu g/10^6$ cells in HEPES-buffered DMEM/1% BSA for 40 minutes at 4°C. For measurement of cell surface expression, bound anti-HA7 was recognized by goat-anti-mouse IgG Alexa-Fluor488 conjugate ($1\mu g/10^6$ cells; Molecular Probes). Cells were resuspended in PBS containing propidium iodide ($1\mu g$/ml; Sigma-Aldrich) for dead cell discrimination before measurement in a Epics XL-MCL flow cytometer (Beckman-Coulter).

Flow cytometry on L6 cells was done basically as described for HEK293T cells. Receptor expression in L6-HA-TβRII and L6-HA-TβRII-B cells were induced with Doxycyclin as described (2.3.1.1). Cells were harvested by Accutase treatment for 2-10 minutes at 37°C.

To monitor receptor internalization, HEK293T cells were plated at 1.2-1.5$\times 10^6$ cells per well in 6-cm dishes. 14-20 hours after plating cells were transfected with 6 μg of TβRII wildtype or mutant constructs as described (2.3.1.2). 20 hours post-transfection cells were harvested, and surface TβRII was labelled with anti-HA7 as described. After washing with HEPES-buffered DMEM, cells were then either kept at 4°C or transferred to 37°C for various lenghts of time. Dynasore (160 μM; Sigma-Aldrich) was used to prevent receptor internalization in control cells. Antibody-labeled TβRII remaining at the cells surface was visualized with goat-anti-mouse IgG Alexa-Fluor488. Cells were resuspended in PBS/propidium iodide and measured as described. Flow cytometry data were evaluated using WinMDI (Joe Trotter) and FCSExpress (Denovo Software). Non-viable cells displaying low forward scatter and high side scatter, and permeable cells positive for PI staining were excluded from analysis as well as cell aggregates which were identified by high forward scatter signal (Fig. 7) (Shapiro, 1995).

2.3.6.2 Apoptosis and cell cycle flow cytometry

Changes in cellular DNA content during the cell cycle were determined by propidium iodide staining of DNA followed by flow cytometry. In a PI-histogram of cells from normal cell culture, two peaks represent 2n (G_0/G_1 phase cells) and 4n (G_2 phase cells) DNA content, respectively. A continuous population with a DNA content $2n \leq n \leq 4n$ represents cells in S-phase. Late apoptotic cells that have undergone DNA fragmentation lose some DNA due to diffusion of DNA fragments during permeabilization and thus are displayed with a DNA content <2n.

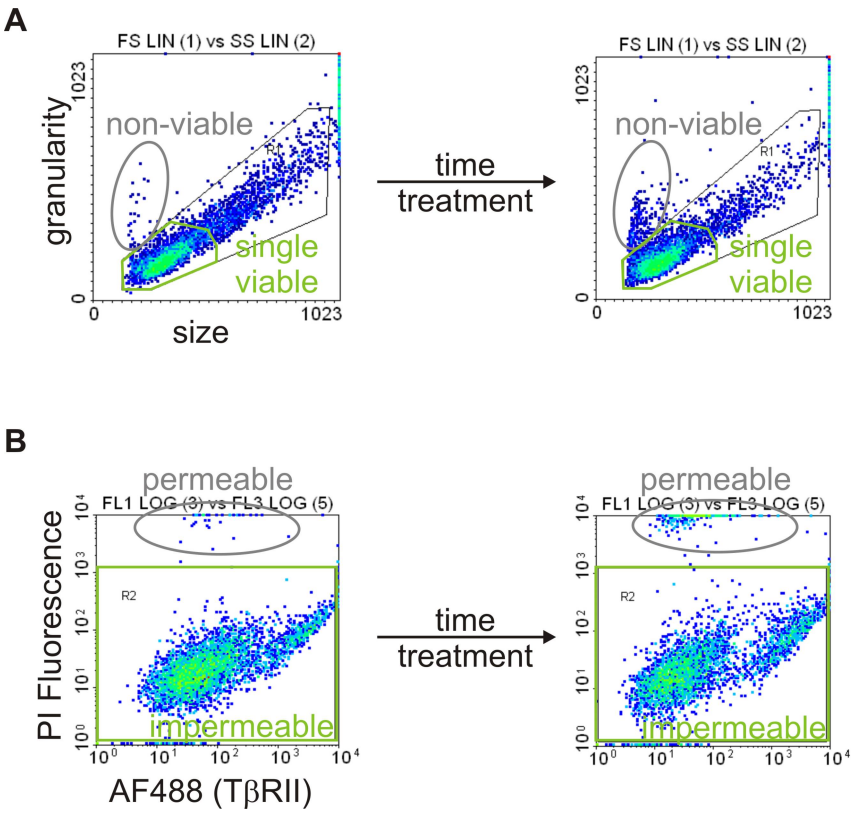

Fig. 7: Gating strategy for internalization measurements. (A) By forward scatter (FS; size) and side scatter (SS; granularity) gating single viable cells were identified and included in the analysis (green gate). During cell treatment a population of cells arised that displayed low FS and high SS (gray ovals). These cells were regarded apoptotic and/or non-viable. (B) Cells were counterstained with PI in addition to AF488 antibody staining of TβRII. The population of PI-positive cells increases with time/treatment and was excluded from analysis (gray ovals). Only PI negative cells that were impermeable were included in the analysis (green gate).

DR26 cells were plated at 45000 cells per well in 12-well plates. 14-20 hours after plating cells were transfected with 0.5 μg of TβRII expression constructs using JetPEI as described (2.3.1.2). 16 hours post-transfection medium was replaced to remove cells that had died from transfection. 40 hours after transfection, the medium supernatants were collected and combined with the respective cell samples that had been detached by Accutase treatment (PAA). Cells were pelleted by centrifugation (5 minutes, 300g). After washing cell aggregates were dissociated and resuspended in PBS by pipetting. Suspensions were added dropwise to 70% ethanol (-20°C), fixed and permeabilized simultaneously at least over night at 4°C. After fixation, cells were recovered by centifugation (5 minutes, 300g), washed in PBS, and resuspended in 500 μl PBS containing 2.5 μl RNaseA (10mg/ml; Sigma-Aldrich) to remove RNA. After 30 minutes incubation at 37°C, 25 μl propidium iodide (1mg/ml; Sigma-Aldrich) were added to stain cellular DNA. Following 5 minutes incubation at room temperature cells were kept on ice before PI fluorescence was determined in an Epics XL-MCL flow cytometer (Beckman-Coulter). Cell doublets and higher aggregates were identified by plotting the PI-peak area over peak height and excluded from analysis (Wersto et al., 2001) using WinMDI (Joe Trotter). Cell cycle distribution was quantified using Cylchred software (Terry Hoy).

3 Results: *TGFBR2* mutations in MFS related diseases

3.1 Mutations in the TGF-β receptor II kinase domain

A comprehensive analysis was performed of nine mutations from Marfan Syndrome-related diseases which are located in the core of the TβRII kinase domain (Fig. 8A). Since the structure of the TβRII kinase has not been published to date we generated a model based on the structure of the highly homologous activin receptor type IIB (ActRIIB) kinase domain (Han et al., 2007) using SWISS-MODEL (Arnold et al., 2006; Guex and Peitsch, 1997; Schwede et al., 2003). L308 is located at the beginning of beta-sheet 4 (β4), Y336 in α-helix D (αD), and S449 in αF (Fig. 8A) Arginine residues R460, R528, and R537 are highly conserved residues in the TGF-β receptor family (Fig. 9), and they contribute to preserving the kinase structure by a series of intramolecular polar interactions (Fig. 8B and 8C). Mutations of these residues are therefore very likely to alter the arrangement of the kinase structure and will potentially compromise kinase activity. In addition, R460 maps close to the substrate interacting regions. Mutations of R460 may thus directly affect substrate binding (Fig. 8).

3.2 Expression of mutant receptors

Mutations were introduced in TβRII wildtype expression constructs. Mutagenesis was performed by by Gao Guo (Charité, MPIMG, Berlin). Two sets of receptor mutants were generated, comprising either an N-terminal HA-tag, or a FLAG-tag at the C-terminus. Expression of the receptors was verified by Western blot from total lysates of transfected COS7 cells (Fig. 10A). Significant differences in receptor expression were found for all mutations when compared to wildtype receptors. Both the 75-kDa unglycosylated TβRII which represents the immature receptor in the endoplasmatic reticulum (ER), and the glycosylated forms of around 95-kDa representing the cell surface form of TβRII (Wells et al., 1997) were markedly reduced for all mutations when compared to the wildtype receptor (Fig. 10A). Quantitative RT-PCR confirmed that reduced expression is a consequence of these mutations on the protein level rather than an artefact of plasmid quality, since all mutated receptor mRNAs are present at levels comparable to the wildtype (Fig. 10B). Receptors with mutations Y336N and S449F were barely expressed and are likely to lead

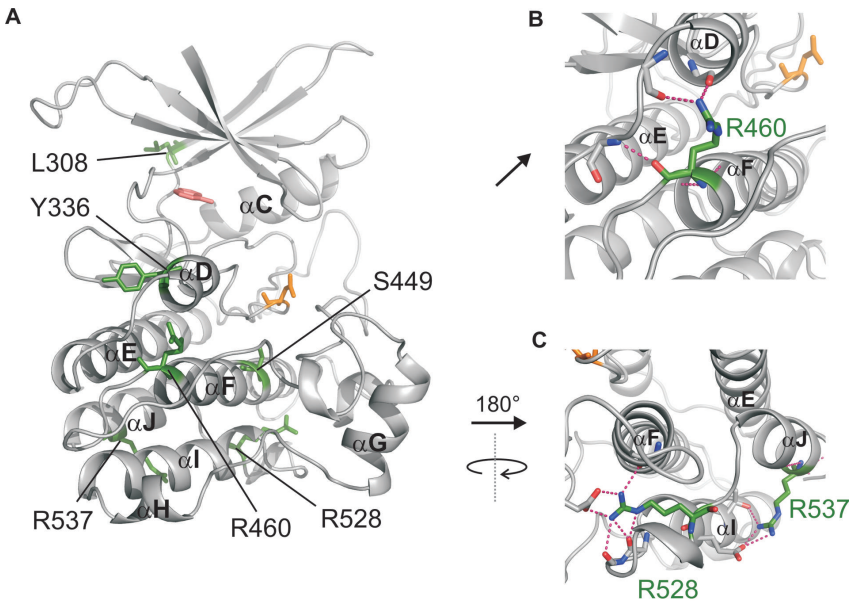

Fig. 8: Mapping of mutations in the kinase domain. (A) The nine mutations investigated in this study are shown in a model of the TβRII kinase domain. Except for L308 all mutations investigated map to the lower lobe of the kinase (represented as sticks, green). For orientation the position of the adenine moiety of ATP (from ActRIIB) and the catalytic aspartate are indicated in red and yellow, respectively. Helix nomenclature was adopted from ActRIIB. (B) Detail showing R460 (green) with intramolecular H-bonds (pink, dashed). The arginine residue at position 460 in TβRII RII is located at the C-terminal end of αF. This helix forms the central anchoring element in the architecture of eukaryotic kinases (Kornev et al., 2008). R460 is conserved among all type I and type II receptors of the TGF-β superfamily (Fig. 9) and contributes to the stability of the lower C-lobe by forming intramolecular H-bonds to backbone carbonyl oxygens in αD (Borders et al., 1994) and the downstream loop. (C) R528 and R537C (after 180° rotation of (A)). R528 is positioned between the αI and αJ in the lowermost part of the kinase, and this residue is conserved in all TGF-β superfamily receptors (Fig. 9). On the basis of homology to ActRIIB, R528 and R537 both are predicted to form hydrogen bonds to backbone carbonyls as well as salt bridges to conserved glutamate residues, which presumably is important for the stabilization of the kinase domain. The R528 side chain forms mutiple H-bonds to backbone carbonyls, and, in addition, a salt bridge with E428. This glutamic acid residue is conserved throughout the family, and the salt bridge is present in all TGF-β superfamily receptor kinase structures available to date (ActRIIB, ALK2, ALK5, BMPR2). R537 is situated in αJ at the far side of the substrate binding pocket and on the solvent surface. The arginine side chain H-bonds to T516 and forms a salt bridge to E519 in the neighboring αI. These bonds are present in TβRII and ActRIIB, however no such bonds are present in the structures of ALK2, ALK5, or BMPR2. In the type I receptors the arginine is replaced by a threonine residue whereas in BMPR2, which has an arginine at this position, αI-glutamate is exchanged to the smaller aspartate (Fig. 9). Figures were generated with PyMOL based on the model for the TRII kinase. Figure: Horbelt et al. (2010).

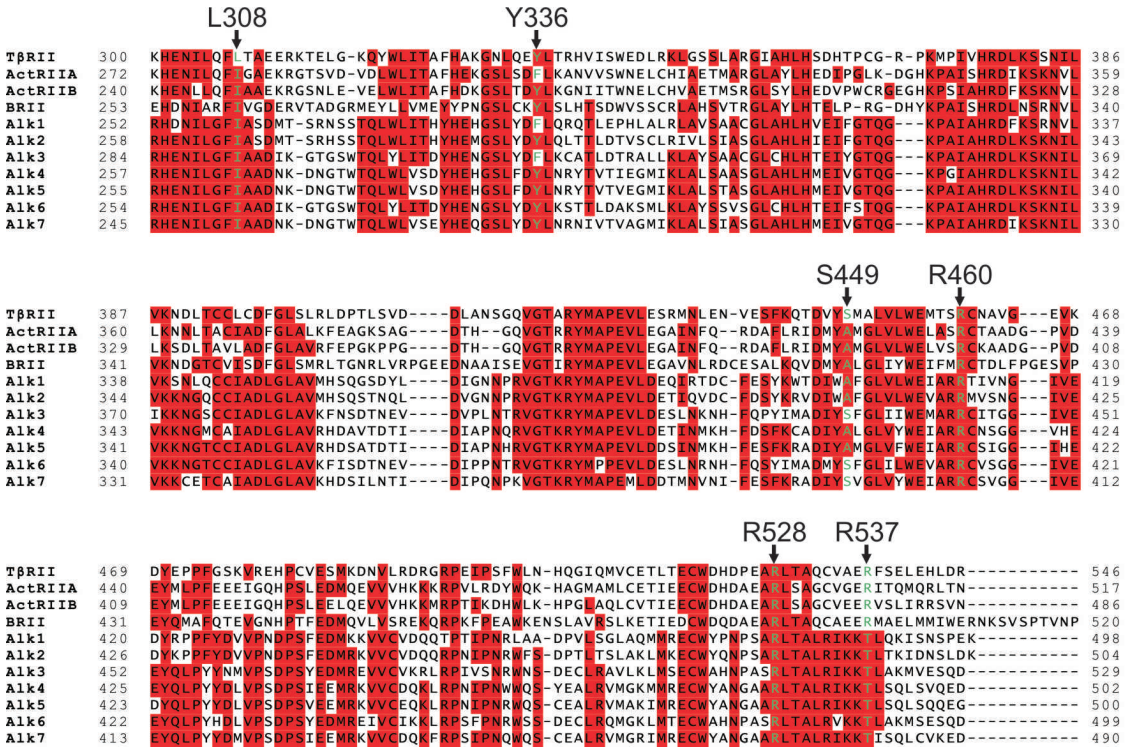

Fig. 9: Amino acid sequence alignment for human TGF-β superfamily type I and type II receptors. R460 and R528 are highly conserved among type I and type II receptors of the TGF-β superfamily, R537 is conserved in type II receptors. Figure: Horbelt et al. (2010).

to haploinsufficiency for TβRII. For the subsequent analysis, we focused on mutations of conserved arginines R460, R528, and R537.

To determine the actual amount of mutated TβRII at the plasma membrane, N-terminally HA-tagged receptors were overexpressed in HEK293T cells, and quantified by flow cytometry on non-permeabilized cells. Surface expression as determined by mean fluorescence intensity is reduced for all mutations investigated, ranging from 40% for R537C to 75% for R528C as compared to WT-TβRII (Fig. 11). Mutations of single amino acids in the kinase domain ot TβRII markedly affect expression and membrane localization of these receptors. However, it could be shown that all mutant receptor variants that were subject to further characterization are targeted to the plasma membrane at significant levels.

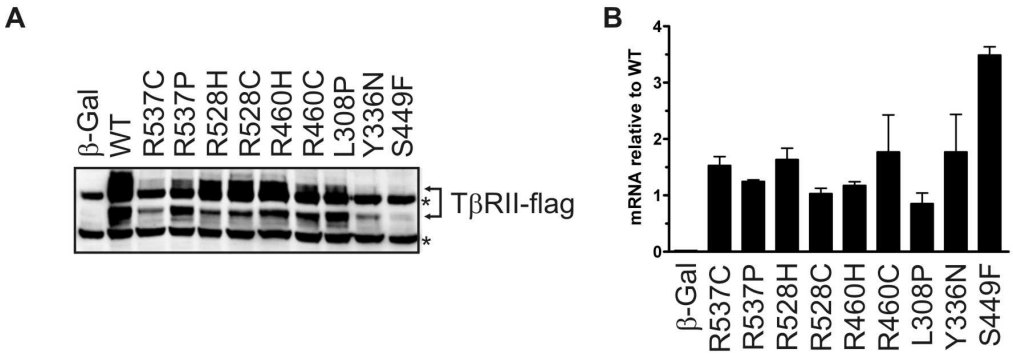

Fig. 10: Expression of TβRII mutants. (A) Western blot analysis of lysates from COS7 cells transfected with wildtype (WT) or mutants of TβRII, or control (β-Galactosidase); asterisks identify unspecific bands of the FLAG-antibody. (B) mRNA levels of TβRII mutant expression from constructs after transfection into HEK293T cells, relative to wildtype TβRII receptor construct. Cells were transfected with expression constructs, and cDNA was generated from isolated RNA; cDNA inputs were determined by quantitative PCR and relative amounts (WT=1) were calculated using the ΔΔCT method. Error bars represent SD from two independent experiments. Figure: Horbelt et al. (2010).

3.3 Receptor internalization

As described before endocytic internalization of receptors is regarded as a critical event in TGF-β signal transduction (Di Guglielmo et al., 2003), and inhibition of endocytosis was shown to alter cellular responsiveness to TGF-β (Runyan et al., 2005). Moreover, variation of internalization rates has been proposed to affect the dynamics of the TGF-β response (Vilar et al., 2006; Zi and Klipp, 2007). To address the question whether TβRII mutations affect receptor internalization, HEK293T cells were transfected with HA-tagged receptors. After labelling of surface TβRII at 4°C with primary antibodies cells were shifted to 37°C to allow for receptor internalization for different periods of time.

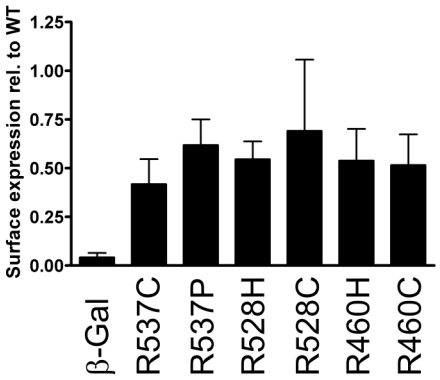

Fig. 11: Surface expression of TβRII mutants. Levels of surface expression of TβRII kinase mutants relative to wildtype after transfection into HEK293T cells. Epitope-tagged TβRII was stained on non-permeabilized cells and mean fluorescence intensity values were compared to wildtype (WT=1). Error bars represent SD of three independent experiments. Figure: Horbelt et al. (2010).

Labelled receptors remaining on the cell surface were then visualized with fluorescent secondary antibodies. Constitutive receptor endocytosis is represented by the decrease of surface fluorescence with internalization time. The application of this method to measure TGF-β receptor endocytosis was reported earlier (Ehrlich et al., 2001). In the present study, however, a series of experimental details were modified to improve sensitivity and reproducibility (Horbelt et al., 2010). Most importantly, non-viable cells, cell aggregates, and permeable cells were excluded from analysis by forward/side scatter gating and propidium iodide staining, respectively (Shapiro, 1995).

To validate the experimental strategy increasing amounts of WT-TβRII were transfected, and receptor internalization was quantified for 15, 45 and 90 minutes. Absolute surface expression of TβRII before internalization was not a linear function of plasmid amount since 4 μg (on 3×10^6 HEK293T cells) led to the same amount of surface TβRII as did 6 μg DNA (Fig. 12A, 0 minutes). Transfection of 2 μg DNA resulted in about 60% of receptor surface expression as compared to 4 μg or 6 μg, and with only 1 μg transfected the fluorescence signal could not be distingushed from background. Internalization of TβRII - represented by the derease of relative surface fluorescence - was the same whether 2 μg, 4 μg, or 6 μg plasmid were introduced, and even differences in initial receptor surface expression of almost 100% did not affect receptor internalization rates (Fig. 12B).

The internalization of wildtype and mutant TβRII was next quantified in a series of experiments. After 15 and 45 minutes 40% and 60% of wildtype TβRII were internalized, respectively (Fig. 13). The endocytosis rate, determined from the linear part of the internalization curve, was 0.025 min^{-1}. Both values match those published for TβRII (Ehrlich et al., 2001). Receptor internalization could be blocked by 160 μM of the dynamin GTPase inhibitor Dynasore (Fig. 13) (Macia et al., 2006). A mutant TβRII in which a di-leucine

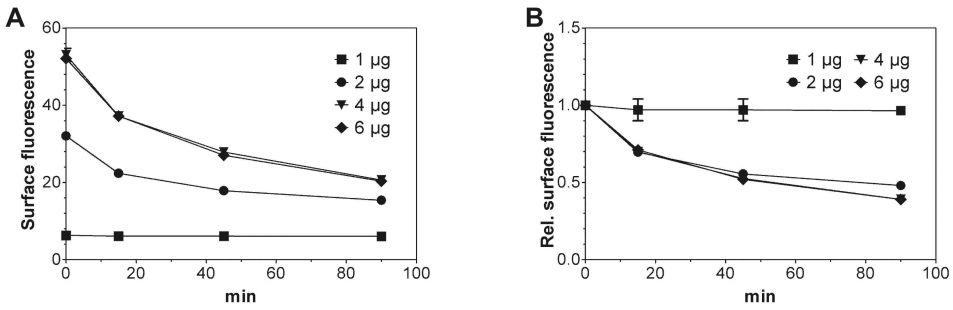

Fig. 12: Internalization of wildtype TβRII. HEK293T cells were transfected with variable amounts of HA-tagged wildtype TβRII. Cell surface receptors were labeled with an HA-tag specific antibody. After 0 to 90 minutes of internalization at 37°C antibody-receptor complexes remaining on the cell surface were recognized by fluorescent secondary antibodies and quantified by flow cytometry. (A) Absolute surface fluorescence (B) Receptor internalization expressed as the decrease in relative surface fluorescence. Error bars represent SD of duplicate measurements. Figure: Horbelt et al. (2010).

motif is mutated showed greatly reduced internalization as expected (Fig. 13H) (Ehrlich et al., 2001). Endocytosis of R537C and -P, R528H and R460C was mildly attenuated as compared to WT-TβRII but did not differ significantly (Fig. 13A-C and 13F) whereas R528C underwent endocytosis at a rate that was not distinguishable from the WT-TβRII (Fig. 13D). Internalization of R460H, however was severely compromised as only 15% and 30% of the receptors internalized after 15 and 45 minutes, respectively (Fig. 13E). Taken together, we found that as a consequence of various mutations in the TβRII kinase domain receptor turnover including expression, posttranslational processing, trafficking to the surface and receptor internalization are differentially affected depending on the site and nature of the mutation.

3.4 Autokinase activity of mutated receptors

In-vitro kinase assays were performed to analyze whether the enzymatic activity of the TβRII kinase is compromised by these mutations. HEK293T cells were transfected with FLAG-tagged receptor constructs. Overexpressed receptors were immunoprecipitated, and subjected to an *in-vitro* kinase assay using radioactively labeled [γ-^{32}P]-ATP to visualize autophosphorylation of TβRII (Fig. 14). Phosphorylated wildtype TβRII was detected in the autoradiogram at about 76 and 95 kDa. By contrast, none of the mutant TβRII displayed significant autokinase activity *in-vitro*.

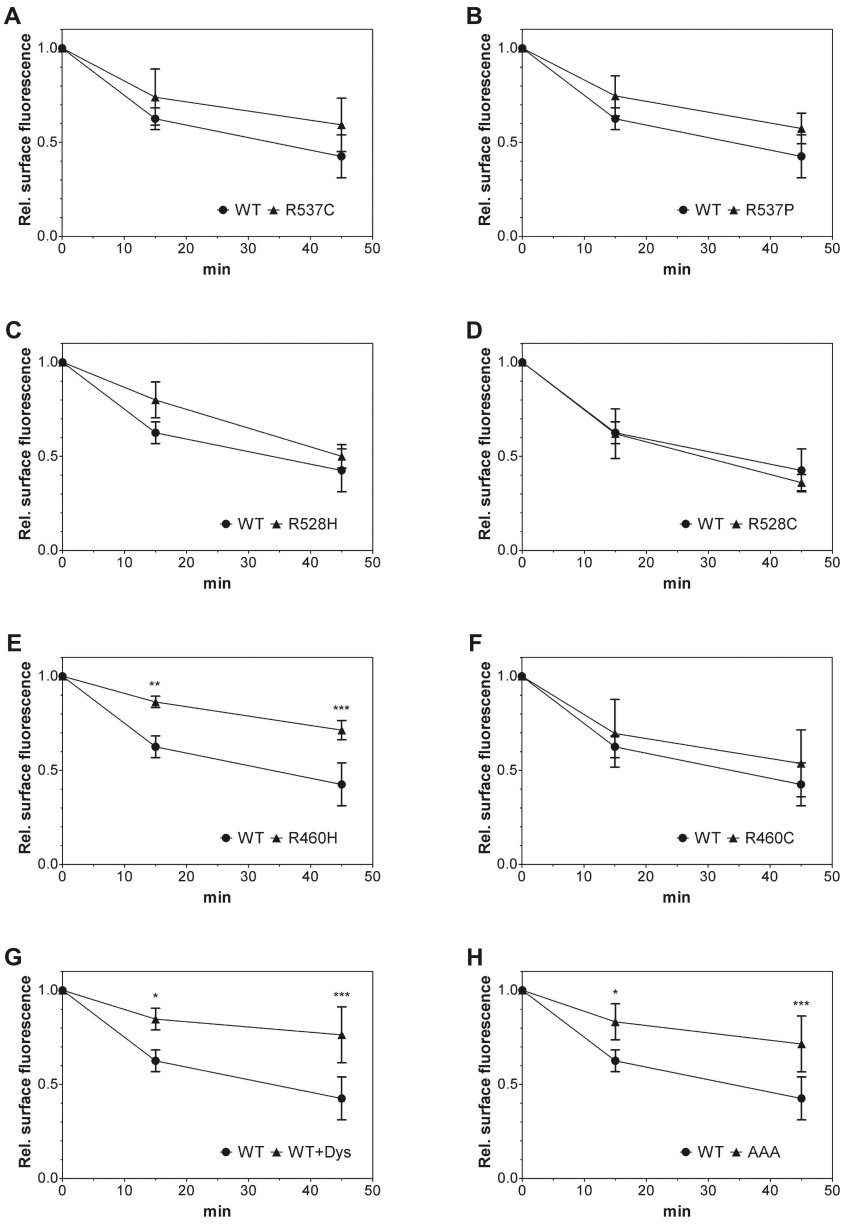

Fig. 13: Endocytosis of wildtype and mutant TβRII. HEK293T cells were transfected with HA-tagged wildtype or mutations, and internalization was determined after 15 and 45 minutes. Surface fluorescence of WT-TβRII transfected cells was decreased by 40% after 15 minutes of incubation at 37°C, and after 45 minutes 60% of receptors had been endocytosed. Internalization was slightly attenuated for R537C/P (A,B), R528H (C), R460C (F) whereas R528C (D) internalizes like WT-TβRII. Internalization of R460H (E) was substantially reduced and was comparable to Dynasore (Dys) treated WT-TβRII (G) and an internalization-defective TβRII mutant (AAA) (H). Data are shown as means of relative (±SD) median fluorescence intensities from three independent experiments. Asterisks indicate statistical significance (Two-way ANOVA followed by Bonferroni's post test for multiple comparisons): $p \leq 0.05$ (*), $p \leq 0.01$ (**), $p \leq 0.001$ (***). Figure: Horbelt et al. (2010).

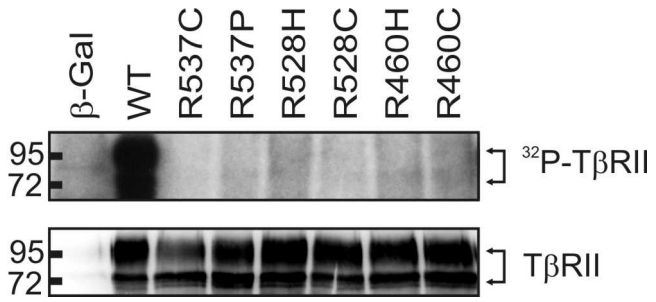

Fig. 14: Kinase activity of mutated TβRII. FLAG-tagged TβRII receptors were immunoprecipitated and subject to an *in-vitro* kinase reaction with [γ-^{32}P]-ATP. The autoradiogram shows 32P-phosphorylated TβRII (upper panel, arrows), Western blot (lower panel) indicates the amount of total TβRII in the immunoprecipitates. Figure: Horbelt et al. (2010).

3.5 Reporter gene activation by TβRII mutants

A series of experiments was performed to investigate the consequence of these mutations on TGF-β signal transduction. In order to dissect the impact on both Smad and non-Smad signaling two different reporter gene constructs were used. The $CAGA_{12}$-luc reporter contains 12 Smad binding elements (SBE) which bind activated Smad3/4 complexes; its activity thus depends exclusivley on active TGF-β-Smad signaling (Dennler et al., 1998). The 3TP-luc reporter contains a fragment from the human plasminogen activator inhibitor 1 (PAI-1) promoter following three Tetradecanoyl-phorbolacetate (TPA) response elements (Wrana et al., 1992). Responsiveness of the 3TP-luc reporter was shown to be promoted by non-Smad TGF-β induced JNK/ERK MAPK activity in addition to Smad signaling (Carcamo et al., 1995; Sirard et al., 2000).

In initial experiments the effect of TβRII mutations on endogenous TGF-β signaling was monitored by transfecting wildtype or mutated receptors into HEK293T cells (Fig. 15). Transfection of kinase deficient LDS mutation R528C repressed the 3TP luciferase response to the same amount as a dominant negative truncation of TβRII which lacks most of the cytotplasmic domain (TβRII-ΔCyt) (Wieser et al., 1993), suggesting a dominant negative effect of R528C. Subcellular fractionation (Fig. 16) and immunocytochemistry (Fig. 17) to visualize Smad2 phosphorylation and nuclear translocation further confirmed that R528C is an inactive receptor mutant that represses the TGF-β pathway in a dominant negative manner.

For further scrutinization of signaling activity DR26 mink lung epithelial cells were used. DR26 cells lack expression of endogenous TβRII (Wrana et al., 1992) and thus provide a system that allows to control the ratios between wildtype and mutated receptors by titrating transfected constructs. Cells were transfected with various amounts of wildtype

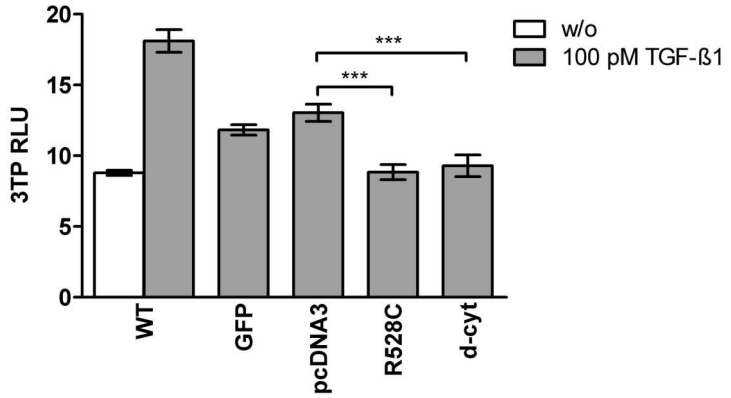

Fig. 15: Effect of dominant negative mutations of TβRII on reporter gene activity in HEK293T cells. TGF-β induced response on the 3TP-luc reporter in HEK293T cells after transfection with wildtype or mutated receptors, including a dominant negative TβRII lacking most of the cytoplasmic domain (d-cyt), or controls (GFP, pcDNA3). Error bars represent SD from triplicate measurements; asterisks indicate statistical significance (One-way ANOVA followed by Tukey's multiple comparison test): $p \leq 0.001$ (***). Figure: Horbelt et al. (2010).

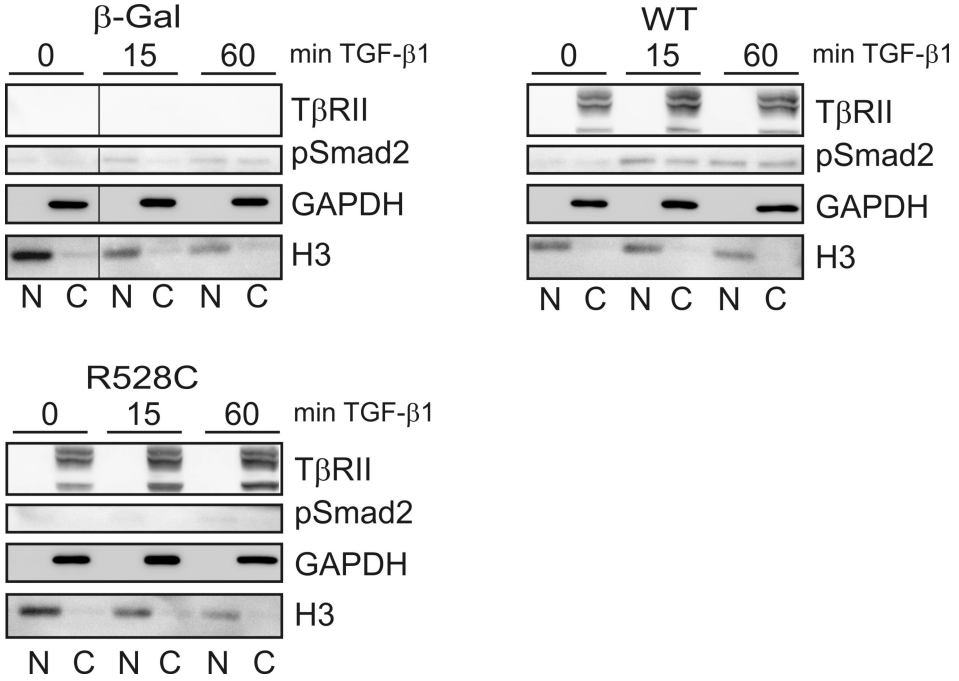

Fig. 16: Smad2 phosphorylation and nuclear translocation induced by R528C. Subcellular fractionation of TβRII transfected HEK293T cells. After stimulation with 250 pM TGF-β1 for 0-60 minutes, phosphorylated Smad2 was detected in nuclear (N) and cytosolic (C) fractions. In β-Gal transfected control cells, endogenous TGF-β receptors induce phosphorylation of Smad2 which is detectable in nuclear and cytosolic fractions. Expression of R528C dominantly represses Smad2 phosphorylation and nuclear translocation as compared to β-Gal transfected cells. Conversely, overexpression of WT-TβRII enhanced Smad2 phosphorylation and nuclear translocation. Figure: Horbelt et al. (2010).

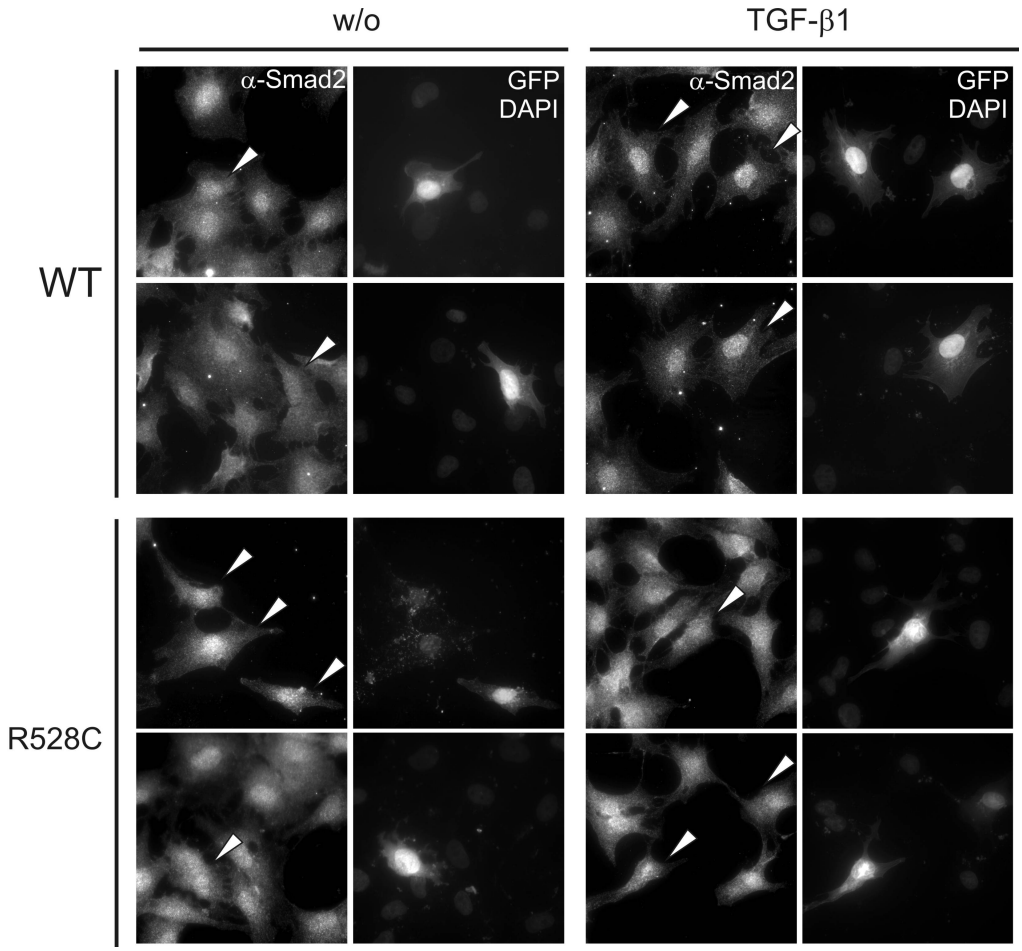

Fig. 17: Smad2 nuclear translocation induced by R528C. Immunocytochemistry on DR26 cells which lack expression of endogenous TβRII. Cells were co-transfected with the receptor and GFP to mark transfected cells. Smad2 was stained using an anti-Smad2 antibody. WT-TβRII restored responsiveness to TGF-β in transfected cells (arrowheads). Accumulation of Smads in the nucleus became apparent by clear demarkation of the nucleus in WT-transfected and stimulated cells in contrast to a more diffuse distribution in non-transfected cells. R528C was not able not promote nuclear translocation of Smad2. Figure: Horbelt et al. (2010).

TβRII plasmid ranging from 100% of total plasmid to 0%, which was complemented to 100% with plasmid DNA coding for receptor mutations or control plasmids. As in all following experiments of this type, the total amount of transfected DNA was kept constant to avoid overloading of the expression or signaling machinery. Activity of the 3TP-luc reporter only marginally decreased with diminished amounts of TβRII plasmid if empty vector, GFP, or the transmembrane receptor Ror2 where used as complement. Strikingly, with as little as 25% of the total DNA being wildtype the response was still about 75% of the wildtype-only signal (Fig. 18). On the contrary, titration with R528C repressed the reporter signal in a dominant negative fashion (Fig. 18). This finding strongly supports the conclusion that in this specific experimental setup the effect of a dominant negative mutation becomes manifest in a roughly linear function of reporter gene activity which decreases with increasing co-expression of a dominant negative receptor.

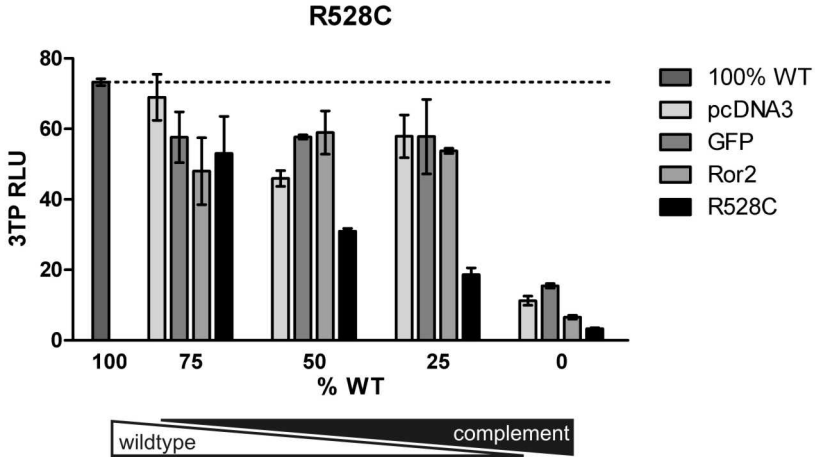

Fig. 18: Effect of dominant negative mutations of TβRII on reporter gene activity in DR26 cells. Response from 3TP-luc reporter in DR26 cells transfected with increasing ratios of mutated (R528C) or control complement DNA versus wildtype TβRII constructs. Cells were stimulated with 100 pM TGF-β1; error bars represent SD from triplicate measurements. RLU: relative luminescence units (3TP-luc/RLTK-luc). Figure: Horbelt et al. (2010).

DNA titration reporter gene assays were performed for mutations associated with MFS2 (R537C, R460H), LDS (R537P, R528H/C), or TAAD (R460C) using 3TP or $(CAGA)_{12}$ luciferase reporter constructs (Fig. 19, 20 and 21). For mutations of R537 a dominant negative effect manifested on the 3TP-luc and $(CAGA)_{12}$-luc reporter (Fig. 19). Interestingly, the dominant negative effect of R537P was more potent than that of R537C, leading to a more-than-linear decline of signal intensity with decreasing portions of transfected TβRII (Fig. 19B and 19D). Both mutations were incapable of mediating any TGF-β response in the absence of any wildtype receptor molecules.

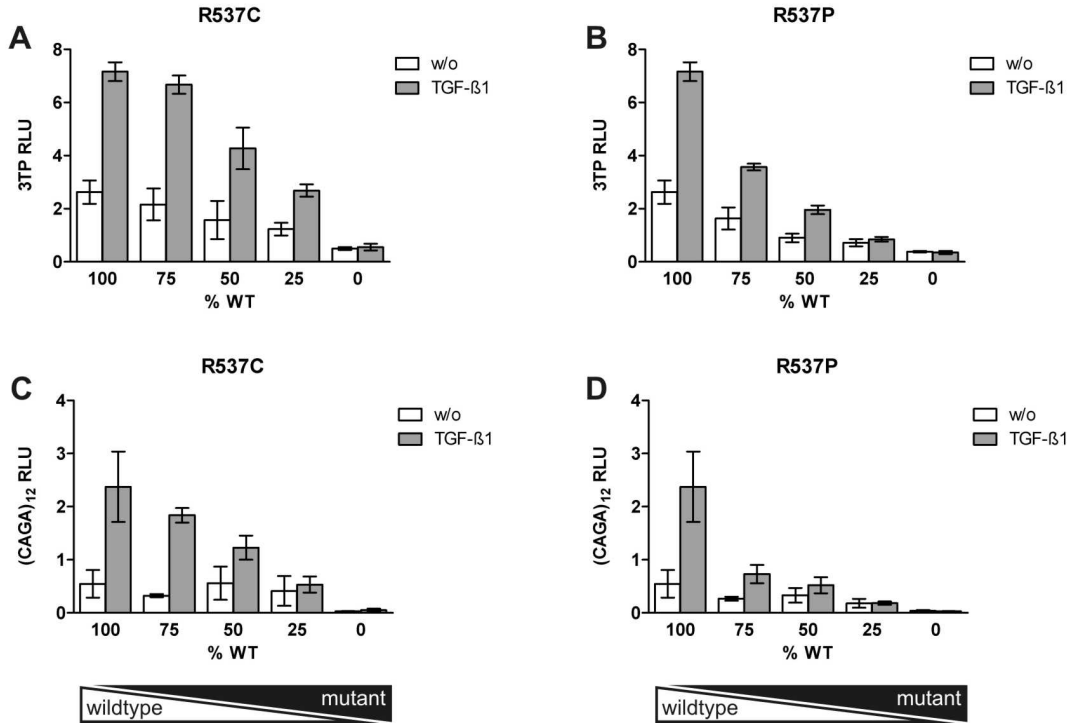

Fig. 19: Induction of 3TP-luc and $(CAGA)_{12}$-luc reporters after titration of wildtype versus R537C or R537P plasmids. DR26 cells were transfected with decreasing amounts of WT plasmid, complemented to 100% with the mutant construct. A dominant negative effect of R537 mutations on the 3TP-luc reporter construct as well as on a $(CAGA)_{12}$-luc reporter is indicated by a roughly linear decrease of the luminescent signal. Error bars represent s.d. from triplicate measurements. RLU: relative luminescence units (3TP-luc/RLTK-luc or $(CAGA)_{12}$-luc/RLTK-luc). Figure: Horbelt et al. (2010).

The latter finding held true also for mutations of arginine at position 528 (R528H/C), which were shown to be inactive on both 3TP-luc and $(CAGA)_{12}$-luc reporters (Fig. 20). In addition, as shown before in HEK293T and DR26 cells for R528C (Fig. 15 and 18), receptors carrying these mutations interfere with the activation of signaling by wildtype molecules in a dominant negative manner. The dominant negative potential of both mutants, however, was largely the same for R528C and R528H.

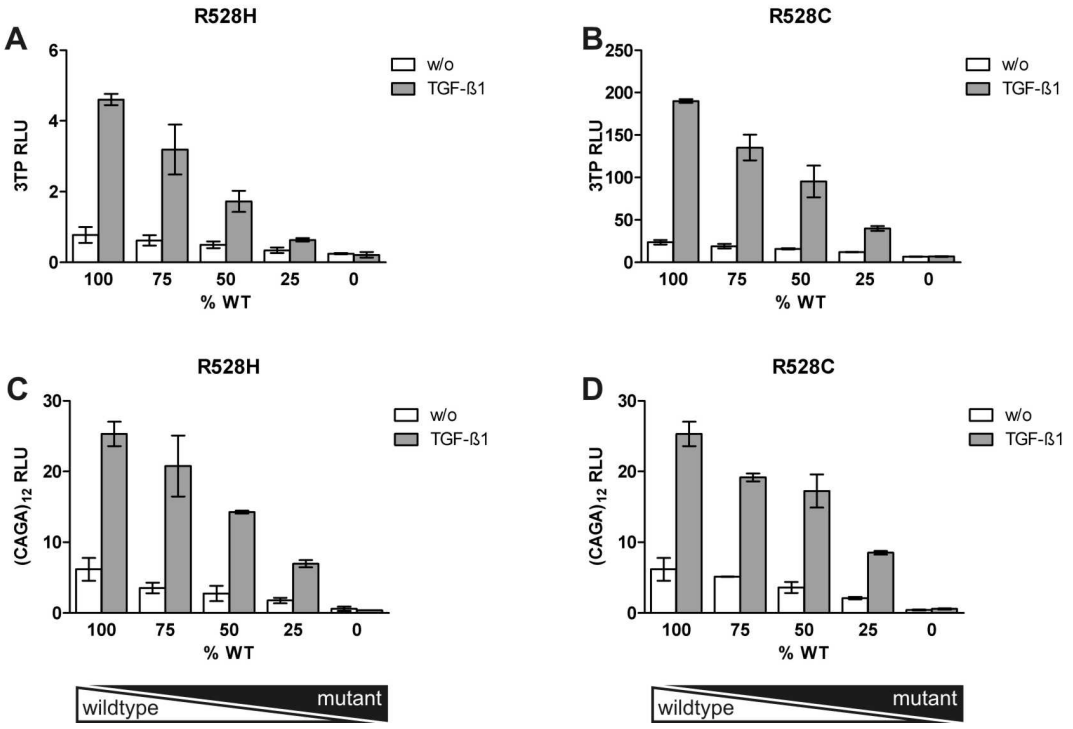

Fig. 20: Induction of 3TP-luc and $(CAGA)_{12}$-luc reporters after titration of wildtype versus R528H or R528C plasmids. Mutations of R528 exhibited a dominant negative effect on the 3TP and $(CAGA)_{12}$-luc luciferase reporter gene. Error bars represent SD from triplicate measurements. RLU: relative luminescence units (3TP-luc/RLTK-luc or $(CAGA)_{12}$-luc/RLTK-luc). Figure: Horbelt et al. (2010).

Finally, mutations of R460 to histidine (R460H) or cysteine (R460C) which have been found in MFS2/LDS and TAAD syndrome, respectively, were characterized using the same strategy. The R460H mutation also showed a dominant negative behavior in the absence of residual activity on any reporter (Fig. 21). By contrast, a cysteine in this position did not entirely abolish the responsiveness to TGF-β (Fig. 21B and 21D). This mutant retained some residual signaling activity even in the absence of WT-TβRII, and thus exhibited an only weak dominant negative effect on the signaling activity of wildtype TβRII on the Smad3/4 dependent $(CAGA)_{12}$-luciferase reporter (Fig. 21D). On the 3TP-

luc promoter which integrates both Smad and non-Smad pathways, R460C alone had only marginal activity, and the dominant negative effect was more pronounced (Fig. 21B).

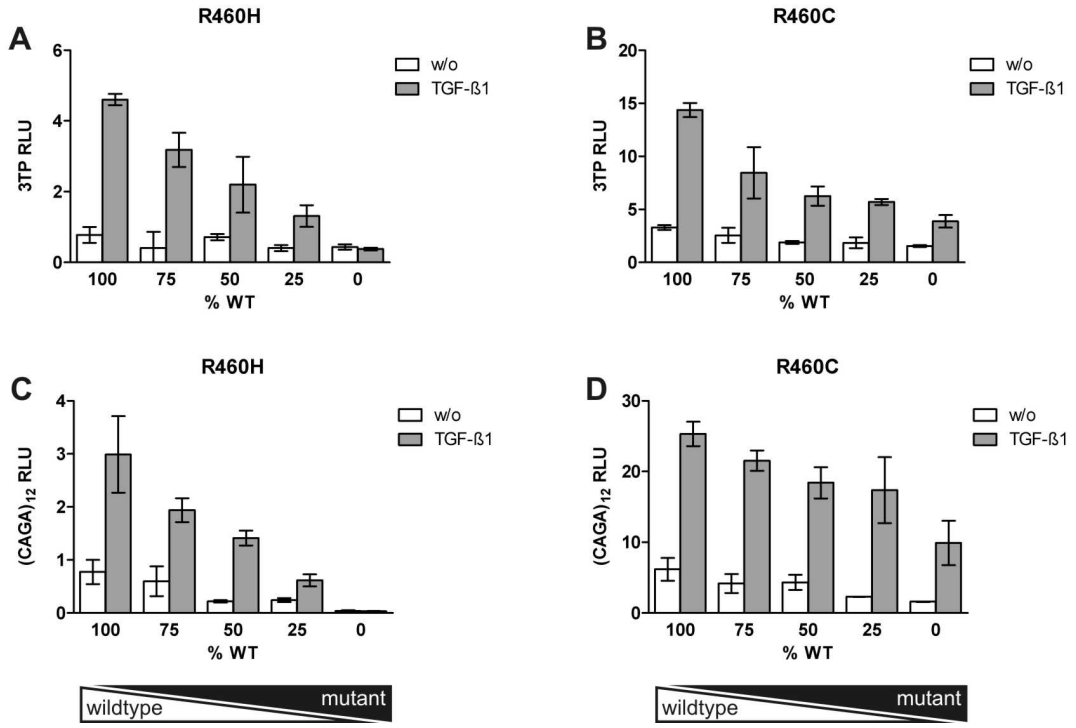

Fig. 21: Induction of 3TP-luc and $(CAGA)_{12}$-luc reporters after titration of wildtype versus R460H or R460C plasmids. 3TP-luc and $(CAGA)_{12}$-luc reporter activity in DNA titration experiments introducing R460H/C. (A,C) R460H had a dominant negative effect on the the TGF-β signal both on 3TP-luc and $(CAGA)_{12}$-luc reporters. (B) The R460C mutation affected 3TP-luc reporter activity in a dominant negative manner; when this mutation was expressed in the absence of wildtype TβRII it revealed residual activity. (D) On the $(CAGA)_{12}$-luc reporter the dominant negative effect was less pronounced, and the mutated receptor was able to induce significant reporter activity. Error bars represent s.d. from triplicate measurements. RLU: relative luminescence units (3TP-luc/RLTK-luc or $(CAGA)_{12}$-luc/RLTK-luc). Figure: Horbelt et al. (2010).

Taken together, all but one mutant TβRII were shown to interfere with transcriptional activity of TGF-β signaling in a dominant negative fashion. The TAAD mutation R460C was able to induce TGF-β signaling on both promoters to some extent. These findings prompted more detailed investigation of TGF-β induced signaling in order to dissect Smad and non-Smad signaling activities of these mutations.

In addition, mutations L308P, Y336N, and S449F were tested for their signaling capacity in the absence of WT-TβRII. These mutant TβRII were inactive on both $(CAGA)_{12}$ and 3TP reporters (Fig. 22).

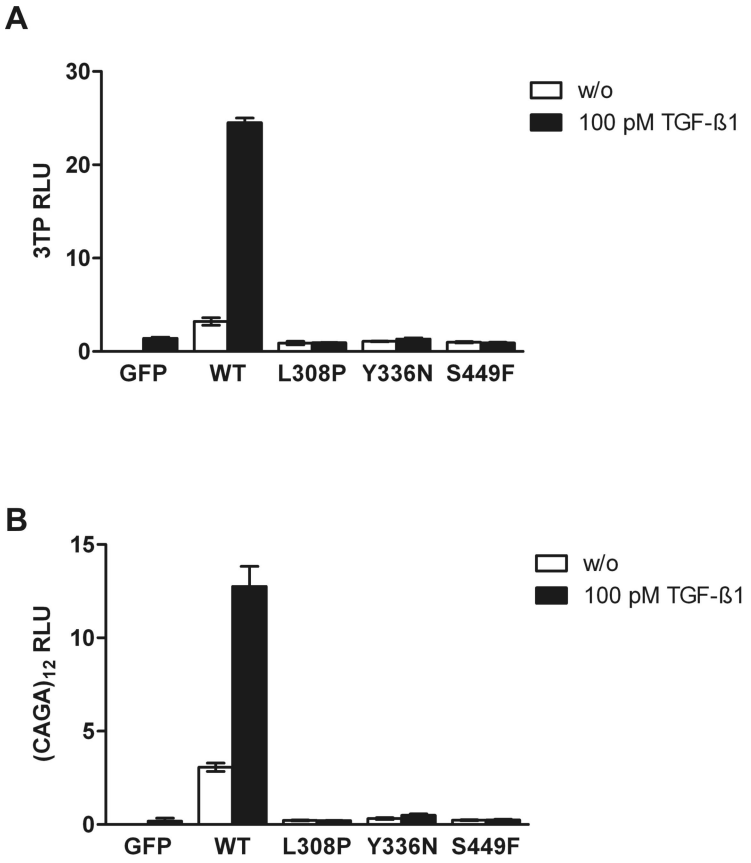

Fig. 22: Signaling activity of mutants L308P, Y336N, and S449F. Signaling activity of mutants L308P, Y336N, and S449F. DR26 cells were transfected with the respective constructs and stimulated with or without TGF-β1 for 20 hours. Introduction of WT-TβRII restored TGF-β signaling, but none of the mutated receptors mediated responsiveness to TGF-β. RLU: Relative luminescence units (normalized to RLTK-luc) of 3TP-luc (A) or $(CAGA)_{12}$ luciferase reporters (B). Error bars represent s.d. from triplicate measurements. Figure: Horbelt et al. (2010).

3.6 Activation of Smad- and non-Smad pathways

To determine the ability of TβRII mutations to mediate Smad2 phosphorylation DR26 cells were transfected with receptor constructs and Smad2 phosphorylation was determined after short term stimulation . While wildtype TβRII reconstitued phosphorylation of Smad2 after 5 to 40 minutes stimulation with TGF-β1, neither of the mutations investigated was able to do so to a similar extent (Fig. 23). After 15 and 40 minutes of stimulation, however, R460C induced weak phosphorylation of Smad2 suggesting that this mutation did not entirely demolish Smad activation. This correlates with findings in reporter gene assays (Fig. 21B and 21D).

TGF-β is able to directly induce activation of non-Smad signaling such as ERK and p38 MAPK pathways in most cells types (Zhang, 2009). Activation of ERK could be measured after 40 minutes of TGF-β stimulation if wildtype TβRII was introduced, while all mutations annihilated TGF-β induced activation of ERK (Fig. 23) in DR26 cells. In sum, only the R460C TAAD mutant was able to induce Smad activation to some extent whereas none of the TβRII mutants displayed ERK signaling activity.

TGF-β is known to rapidly activate the p38-MAPK pathway through interaction of the receptor complex with TAK and TRAF6 (Sorrentino et al., 2008; Yamashita et al., 2008). To test p38 activation DR26 cells were transfected with WT-TβRII or mutants. Following 4 hours starvation in serum-free medium cells were stimulated with 250 pM TGF-β from 1 minute to 40 minutes. No induction of p38 phosphorylation was detectable with any receptor construct (data not shown). In HEK293T cells, however, overexpression alone of WT-TβRII was sufficient to induce elevated levels of activated p38 in the absence of TGF-β, and stimulation with TGF-β did not further increase p38 phosphorylation (Fig. 24). Moreover, a correlation of p38 activation was observed with the expression levels of the receptor variants. It seemed that high levels of the membrane form of TβRII are sufficient to promote p38 activation in the absence of TGF-β and independent from the TβRII kinase activity.

3.7 TGF-β induced cell cycle arrest

TGF-β induces cell cycle arrest and in various cell lines including epithelial, endothelial, hemotopoietic, and glial cells (Siegel and Massagué, 2003). Since the antiproliferative effect of TGF-β may be of relevance in the development of connective tissue defects the functionality of mutant TβRII was assessed. DR26 cells were transfected with wildtype or mutant receptors and after 40 hours the cell cycle distribution in the respective populations was determined using flow cytometry to determine the cellular DNA content.

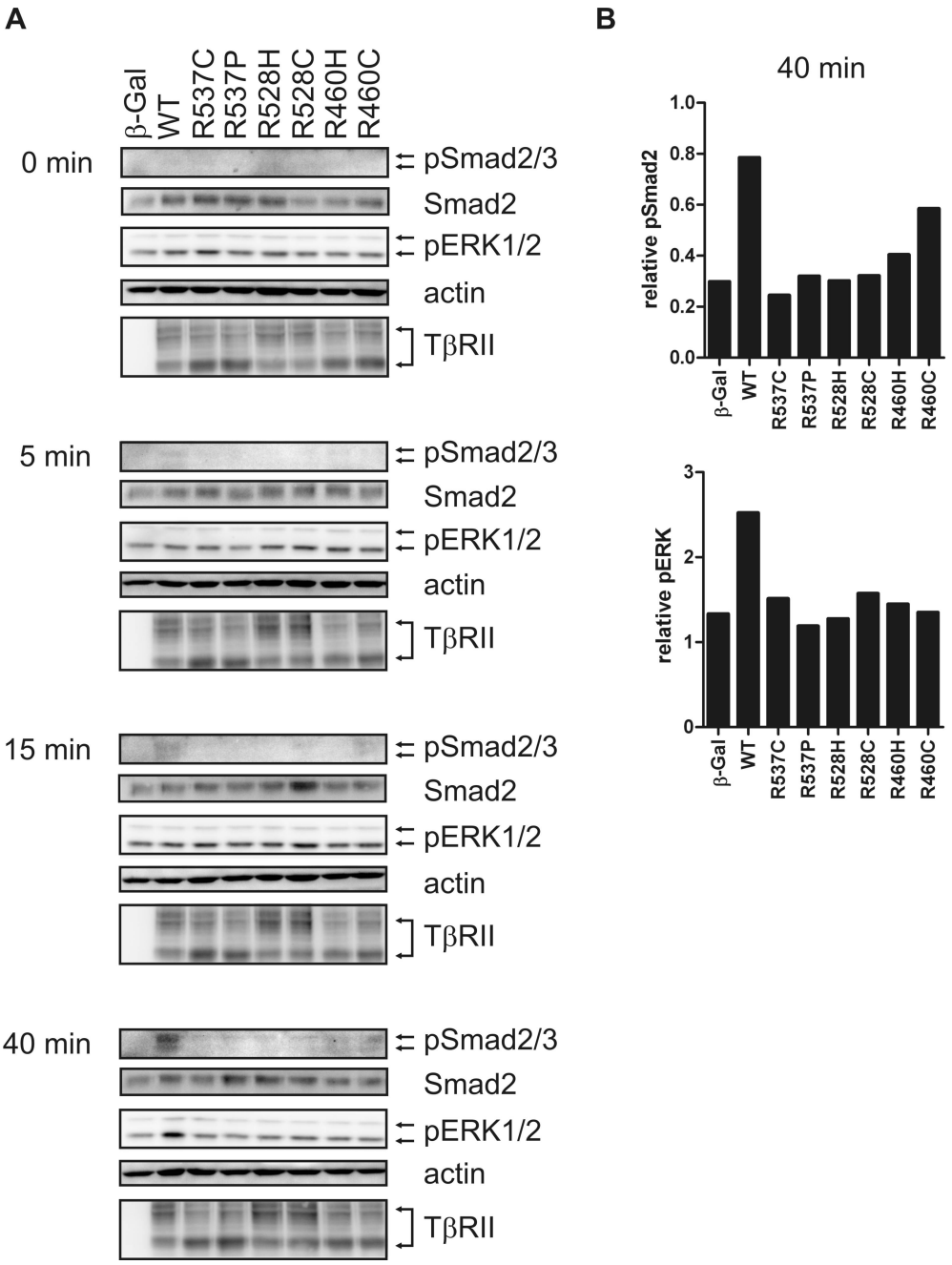

Fig. 23: Activation of Smad and ERK pathways by TβRII mutations. (A) DR26 cells were transfected with wildtype TβRII or mutated receptors. Following starvation cells were stimulated with TGF-β1 for different periods of time. Only R460C and, even more weakly R460H mutations mediated residual Smad phosphorylation, but none of the mutated receptors was capable of inducing ERK1/2 phosphorylation after TGF-β stimulation. (B) Quantification of phospho-Smad2 and ERK1/2 signals from Western blot after 40 minutes of stimulation. Relative pSmad2 and pERK intensities were obtained by normalizing to total Smad2. Figure: Horbelt et al. (2010).

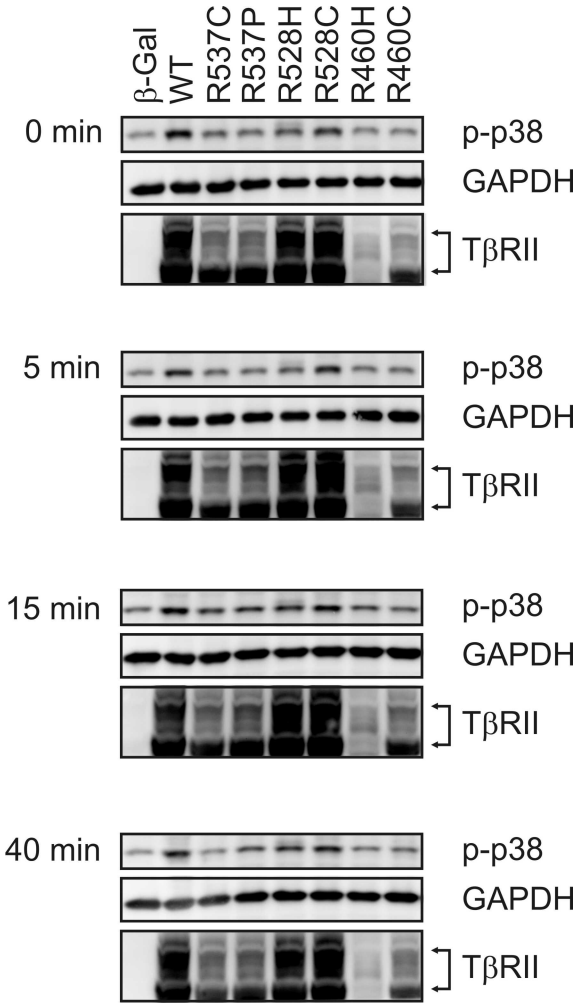

Fig. 24: Activation of the p38-MAPK pathway by TβRII mutations. HEK293T cells were transfected with wildtype or mutated TβRII. Cells were starved and stimulated with 250 pM TGF-β1 for 5 to 40 minutes. Overexpression of TβRII alone lead to activation of p38 in a ligand-independent manner. Levels of phosphorylated p38 (p-p38) seemed to correlate with the 95-kDa putative membrane form of the receptors rather than with their kinase activity.

Proliferation was expressed by the mitotic index which represents the proportion of cycling cells (S and G2 phase) in the total population (G0/G1, S, G2). Introduction of WT-TβRII into DR26 cells led to a reduced mitotic index as compared to control (β-Gal) cells whereas transfection with BMPR2 tended to promote proliferation (Fig. 25). R528C and R528H were incapable to induce proliferation arrest whereas R537C, R537P, R460H and R460C repressed proliferation to some extent with R537C and R460H being most effective in this regard.

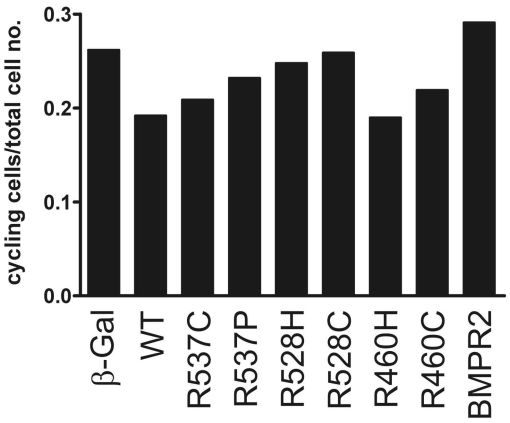

Fig. 25: Proliferation arrest induced by TβRII mutations. DR26 cells were transfected with wildtype or mutated TβRII. After 40 hours in growth medium cells were harvested, and their DNA content was determined by PI staining and flow cytometry. Relative populations in G0/G1, S or G2 phase containing 2n, $2 \leq n \leq 4$, and 4n DNA were determined from the histograms, and the proportion of cycling cells (G0/1, S) in the total populations was calculated.

4 Discussion: *TGFBR2* mutations in MFS related diseases

4.1 *TGFBR* mutations in MFS and related diseases

Mutations in the genes for TGF-β receptors I and II (*TGFBR1*, *TGFBR2*) have been found in persons with a range of clinical presentations (Loeys et al., 2006). At the mild end of the clinical spectrum, mutations at the arginine residue at position 460 of *TGFBR2* have been associated with familial thoracic aortic aneurysm/dissection (TAAD) with no or only mild and nonspecific skeletal manifestations (Hasham et al., 2003; Pannu et al., 2005). Several groups have identified *TGFBR2* mutations in persons with thoracic aortic aneurysm/dissection and skeletal features characteristic of classical Marfan syndrome but without ectopia lentis, which is an ocular finding with a high specificity for Marfan syndrome (Disabella et al., 2006; Mizuguchi et al., 2004; Singh et al., 2006). Loeys-Dietz syndrome represents the severe end of the spectrum. In addition to the previous findings, affected patients may display hypertelorism, bifid uvula, cleft palate, generalized arterial tortuosity with widespread vascular aneuryms and dissections (Loeys et al., 2005). A subset of patients additionally bypresents with features characteristic of the vascular type of Ehlers-Danlos syndrome such as vascular rupture, uterine, splenic, or intestinal rupture, translucent skin, and atrophic scars (Loeys et al., 2006). The latter presentation has been termed Loeys-Dietz syndrome type 2.

Therefore, although there has been debate as to whether isolated *TGFBR2*-associated TAAD and MFS type 2 exist as entities distinct from Loeys-Dietz syndrome, there clearly is a high degree of clinical heterogeneity in persons with mutations in *TGFBR2* (Attias et al., 2009). At the risk of oversimplification, one can say that the clinical features of TAAD represent a subset of the features of Marfan syndrome type 2, which in turn represent a subset of the features found in severe Loeys-Dietz syndrome (Fig. 26).

4.2 Differential expression of mutant TGF-β receptors

This study aimed to characterize the biochemical features of a series of mutations associated with MFS2, LDS, and TAAD by characterizing their signaling properties quantitatively in well established TGF-β signaling assays and correlating them to their clinical

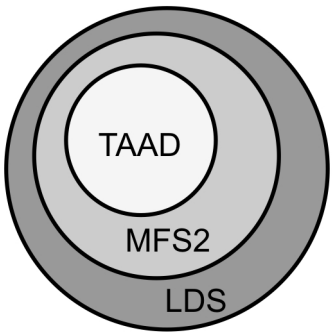

Fig. 26: Clinical manifestations of familial TAAD, MFS2 and LDS. TAAD is characterized by thoracic aortic aneurysm or dissection with or without mild and nonspecific skeletal findings. MFS2 is additionally characterized by skeletal findings typical of those found in classical MFS due to mutations in *FBN1* Robinson et al. (2006). Loeys-Dietz syndrome is characterized by all of these findings as well as additional dysmorphic features, generalized arterial tortuosity, and in some cases mild mental retardation.

phenotypes. In initial experiments the expression of mutated TβRII was evaluated by Western blotting.

Following translation into the rough endoplasmic reticulum both TβRI and TβRII translocate to the Golgi complex where the are glycosylated. TβRII undergoes N-linked glycolsyation at three sites, and at an undefined number of O-linked glycosylation sites (Lin et al., 1992, 1995). Glycosylated TβRII is sensitive to treatment with Endoglycosidase H (EndoH) before processing by Golgi α-mannosidase II. In gel electrophoresis TβRII migrates in two or more bands with an apparent molecular weight of 60-70 and 70-90 kDa, respectively. The smaller species is sensitive to EndoH and thus is regarded as the immature ER/Golgi form of TβRII, while the higher molecular weight variant represents the fully glycosylated and processed mature form which is present in the cell membrane and binds the ligands (Cheifetz et al., 1986; Wells et al., 1997).

In this study expression of all mutants was markedly reduced as compared to wildtype expression in total cell lysates. From the sum of all experiments it became apparent that both the unglycosylated ER form of the receptor and glycosylated mature receptors were less abundant with the strongest defects affecting Y336N and S449F and R537C. On the other hand, R528H/C was expressed at levels almost comparable to WT-TβRII in some experiments.

The reported half-life of EndoH sensitive TβRII is 30-35 minutes indicating that TβRII undergoes rapid folding and processing (Koli and Arteaga, 1997; Wells et al., 1997). In addition, the half-life of membrane TβRII is 2.5 hours (Centrella et al., 1996; Wells et al., 1997), which is longer than for instance the IL-2- or erythropoietin receptors (60 minutes and 45 minutes, respectively), but significantly shorter as compared to LDL- and transferrin receptors (11 hours and 20 hours, respectively) (Casciola et al., 1988; Duprez

and Dautry-Varsat, 1986; Klausner et al., 1983; Yoshimura et al., 1990). Half-life of the TβRI ER form was significantly longer than that for TβRII (3 hours), and even more dramatically for membrane TβRI (up to 12 hours) (Koli and Arteaga, 1997; Wells et al., 1997). Thus, due to its strongly increased turnover rates TβRII levels depend on efficient folding and rapid processing of newly synthesized receptors. It is likely that some of the mutations investigated in this study fail to translocate rapidly to and through the Golgi as a consequence of attenuated folding or misfolding (Pelham, 1989). Indeed, in some experiments the ratio between ER and membrane species, especially of R537C/P and R460H/C, indicated an accumulation of the ER form (Fig. 23 and Fig. 24).

The weakly expressed mutants Y336N and S449F were not included in the rest of this study. Instead, the in-depth analysis was focused on mutations of the conserved arginine residues R460, R528, and R537 which represent all MFS related disease phentotypes described above. Flow cytometric analysis of transmembrane TβRII revealed that except for R528H all receptors were expressed on the cell surface at levels of approximately 50% as compared to wildtype TβRII. R528H showed highly variable expression on the cell surface, which in some experiments was comparable to the wildtype. These findings complemented the Western blot analyses as they confirmed that decreased amounts of mature TβRII seen in mutant TβRII cell lysates corresponded to reduced levels of surface TβRII.

Taken together these data emphasize that the mutations that were characterized here strongly interfered with receptor expression. Since the reduction in mature TβRII in cell lysates and the reduced expression levels on the cell surface correlated, it seems likely that as a consequence of such mutations receptor folding and processing rather than trafficking of mature TβRII to the membrane is defective.

4.3 Internalization of mutant TGF-β receptors

Quantification of receptor internalization by flow cytometry is widely used on receptor tyrosine kinases and G-protein coupled receptors (Barak et al., 1994; Wang et al., 2005). In this study we used a refined experimental procedure to extend its applicability to TGF-β receptors, and thereby to complement immunocytochemical methods to determine internalization (Horbelt et al., 2010). Immunocytochemistry on fixed or on live cells provides a variety of options to visualize the endocytosis of surface receptors. By co-staining with antibodies for specific subcellular compartments in fixed and permeabilized cells the respective routes of internalization can be dissected. On the other hand it is possible to investigate the trajectories and internalization of single receptors on the cell membrane by microscopic single-molecule tracking (Zelman-Femiak et al., 2010). While these techniques generate detailed information on endocytic processes on individual cells,

data acquisition is limited to a few hundred cells and tends to suffer from time-consuming data evaluation and quantification. Flow cytometry on the other hand provides a means to interrgogate hundreds of thousands of cells in relatively short times, thereby leveling interindividual variations between cells of the same sample. In addition, quantification of fluorescent signals is straightforward since fluorescence intensities are recorded.

In order to apply flow cytometry on live cells for the quantification of TGF-β receptor internalization, the protocols used on other receptors and cell lines were adjusted. Most importantly, exclusion of apoptotic and necrotic cells as well as of cell aggregates were critical to improve experimental reproducibility. HEK293T cells are highly transfectable. They adhere to the culture surface rather loosely which allows for non-enzymatic detachment and dissociation which does not affect surface antigens. However, HEK293T cells are more sensitive as compared to other cells to harsh treatments and extensive periods on ice. As a consequence, an increasing number of these cells became permeabilized during the staining and internalization processes, leading to false-positive intracellular binding of antibodies. Furthermore, during preparation a population of cells appeared which was rather small (low FS) and granular (high SS). These cells were regarded non-viable and apoptotic and excluded from analysis by scatter gating (Shapiro, 1995). Lastly, aggregation of cells would contort the true surface fluorescence value. Cell aggregates were identified using their FS profiles and excluded from analysis. Reproducible results were obtained by combining these gates as described in the methods section (2.3.6.1).

The internalization of WT-TβRII as determined by flow cytometry fell in line with published results for constitutive endocytosis of TβRII. We observed 30-40% and 50-60% of wildtype TβRII being internalized after 15 and 45 minutes, respectively. The endocytosis rate which was determined from the linear part of the internalization curve, was 0.025 min^{-1}. Both values match those published for TβRII (Ehrlich et al., 2001).

In the presented experiments internalization of mutant receptors R537C, R537P, R528H, R528C, and R460C was comparable to the wildtype. These findings imply that the TβRII kinase activity is not per se a pre-requisite for constitutive internalization as was reported previously (Ehrlich et al., 2001). As reported, TβRII endocytosis is barely affected even by the absence of the entire kinase domain, and a I218-I219-L220 di-leucine motif upstream of the kinase domain was identified as the signal for constitutive internalization by clathrin vesicles. TβRII binds to adaptor protein-2 (AP2) (Yao et al., 2002). AP2 in in turn associates with PtdIns(4,5)P_2 in the plasma membrane and by binding to clathrin promotes the polymerization of triskelial clathrin to form the coat scaffold (Bonifacino and Lippincott-Schwartz, 2003). TGF-β receptors are recruited into coated membrane domains by binding of the β2 subunit of AP2 to the di-leucine motif (Ehrlich et al., 2001).

In contrast, the data presented here suggest that distinct structural alterations in the kinase may interfere with proper internalization as shown for R460H. Specifically, the

region around R460 is directly involved in substrate binding and positioning whereas R528 and R537 are at the backside of the lower kinase lobe (Fig. 8). An aspartic acid side chain (E456) four residues upstream of R460 at the C-terminal end of the α-helix F is highly conserved in protein kinase structures, and in cAMP-dependent protein kinase (PKA) it directly binds the P-2 arginine residue of a protein substrate (Kornev and Taylor, 2010). Although for TβRII the exact same interaction with the P-2 residue seems unlikely - none of the possible P-2 in the ALK5 GS-Box is an arginine - it is still likely that αF binds directly to the substrate or is involved in positioning the substrate as it is the case for PKA (Fig. 27). Of all mutations investigated in this study, R460 mutations may affect substrate interaction most directly, suggesting that binding of TβRI as the TβRII substrate is a prerequisite for efficient endocytosis of the receptor complex. Alternatively, mutations of R460 may alter the interaction of TβRII with receptor-binding proteins other than TβRI. Such proteins could be involved in the regulation of endocytosis.

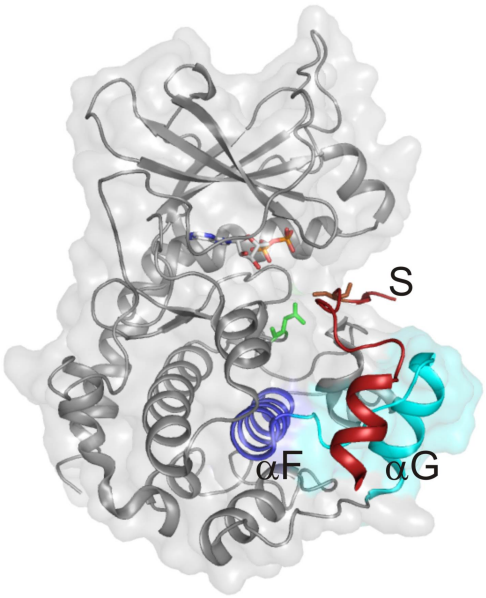

Fig. 27: Structure of the catalytic subunit of PKA . The catalytic subunit of PKA (grey) binds a substrate peptide (S; red) in the C-lobe the kinase domain. The catalytic Asp in PKA is depicted as sticks (green), the phosphorylation site Ser in the substrate as sticks (brown). ADP is bound by the N-lobe. α-helix F (blue) and αG (cyan) map close to the site of substrate interaction. Displacements of αF and of the loop connecting αF and αG (cyan) may directly interfere with substrate binding and positioning. Structure based on PDB 1JBP (Madhusudan et al., 1994).

In this context it seems highly promising to compare the differential interactomes not only of TβRII-R460 and WT-TβRII, but also to compare other mutants characterized in this study. It may be possible to identify potential alterations in associated proteins which then could be involved in the TGF-β pathway through mechanisms beyond

endocytosis. Proteomics assays with the cytoplasmic domain of TβRII , eventually including truncations or mutations have not been published so far. However, proteomics studies on the interactome of the cytoplasmic domain of WT-TβRII were performed in this work as a side project (7). A series of proteins, however, were shown to interact with TβRII, such as STRAP and TRIP-1 that negatively regulate TGF-β signaling (Chen et al., 1995; Datta et al., 1998; Datta and Moses, 2000). In these cases interaction appears to be dependend on TRII kinase activity but has not been mapped on TβRII. On the other hand, proteins associated with the TGF-β receptor complex facilitate Smad signalling, such as Dab2 (Hocevar et al., 2001), or induce non-Smad pathways, such as TRAF6 (Sorrentino et al., 2008; Yamashita et al., 2008). However, it has not been elucidated which of those components interact directly with specific parts of TβRI and/or TβRII.

4.4 TGF-β pathway activity of TβRII mutants

With respect to the fact that mutant receptor expression is significantly decreased in comparison to WT-TβRII, it was crucial to control expression of these mutants by titrating mutant and wildtype DNAs in the absence of endogenous TβRII background. In addition, DNA titration experiments were performed to explore a potential dominant negative effect of TβRII mutants.

Experiments to calibrate this setup revealed that linear reduction of wildtype receptor DNA did not as expected generate a linear decrease in reporter activity. Of note, the cellular response decreased only marginally, and as little as 25% of wildtype receptor DNA were sufficient to generate a response of about 75% as compared to 100% wildtype construct if empty vector, EGFP or, most importantly, the recceptor tyrosine kinase Ror2 were used as complement. Ror2 is a transmembrane receptor tyrosine kinase that was expressed under the same promoter (CMV) as the receptor contructs and served as an internal control showing that co-expression of an unrelated surface receptor does not interfere with TβRII signaling. This phenomenon was not considered in previous experiments which led to the conclusion that TGFBR2 mutations in MFS2 do not have a dominant negative effect (Mizuguchi et al., 2004). The dominant negative effect was further confirmed for the exemplary R528C mutation which repressed 3TP-luc activity and the induction of Smad2 phosphorylation of endogenous TβRII in HEK293T cells as compared to control transfectants.

In the experimental setup presented here the effect of a mutant dominant negative TβRII was identified by a linear decrease of the luciferase reporter signal if the proportion of WT-TβRII was reduced and the mutant receptor was increased concomitantly. This finding has to be taken into account for future experiments to identify a potential dominant negative effect of other TβRII mutations.

Co-transfection with mutant receptors repressed reporter gene activity resulting in a linear decrease. These results revealed that mutations of R537 and R528 exhibit dominant negative - rather than simply non-functional - effects on both reporters while being incapable of inducing any residual reporter activity if transfected in the absence of wildtype TβRII. Similar results were obtained for R460H.

In contrast, R460C was able to generate a significant response on both the 3TP and the $(CAGA)_{12}$ luciferase reporter. However, R460C was able to induce a significantly higher activity on the $(CAGA)_{12}$ reporter as compared to the 3TP reporter. This can be attributed to the different mode of activation of those reporters by TGF-β. Activation of the $(CAGA)_{12}$ reporter was shown to be exclusively dependent on activated Smad3/4 complexes in the nucleus whereas, due to the presence of three TPA response elements, the 3TP reporter can be co-activated to some extent by other pathways such as JNK or ERK-MAPK signaling (Carcamo et al., 1995; Dennler et al., 1998). It has not been directly shown so far that the $(CAGA)_{12}$ reporter can not be co-activated ERK signaling. Inhibition of ERK or stimulation of the ERK-MAPK pathway, however would not be an appropriate option to confirm this explanation. TGF-β and MAPK signaling pathways crosstalk in the cytoplasm, and it was shown that MAPK - by phosphorylating sites in the Smad linker - co-regulate Smad transcriptional activity (Guo and Wang, 2009). In addition, due to its pleiotropic functions, stimulation or inhibition of ERK is very likely to exhibit effects that would mask the true activation status of the $(CAGA)_{12}$ reporter. As to p38 MAPK and JNK, it was published that abrogation of TGF-β induced p38 or JNK activation did not affect the $(CAGA)_{12}$ response, which confirms that the $(CAGA)_{12}$ reporter is not co-activated by these kinases (Yamashita et al., 2008). The weaker dominant negative effect for R460C on $(CAGA)_{12}$-luc can therefore be explained by its residual siganling activity in the Smad pathway.

Taken together, a dominant negative effect on WT-TβRII signalling was documented for all TβRII mutants investigated. This effect was least pronounced for R460C, specifically on the $(CAGA)_{12}$ reporter. The apparent discrepancy in the R460C-induced responses on these two reporter genes could be explained if this mutation was capable of inducing Smad signaling but failed to mediate MAPK activation.

4.5 Dominant negative effect of mutant TβRII

The mechanistic basis for the observed dominant negative effect may be localized at the membrane for most mutations investigated in this study. All mutant receptors were shown to be expressed at significant levels at the cell surface. It seems likely that kinase-mutated TβRII homodimerizes with WT- or mutant TβRII similiar to WT-TβRII. As shown recently, the kinase domain of TβRII is dispensable for homodimerization (Recht-

man et al., 2009). Instead, a juxtamembrane site in TβRII is crucial in this regard. As, in addition, the ligand binding domain of the respective mutants is not altered, mutated TβRII is supposed to dimerize and to bind TGF-β and thereby to compete for ligand binding with WT-TβRII. Moreover mutant TβRII could compete with WT-TβRII for homodimerization, resulting in partly active homodimers. The kinase domain (residues 419-565) of TβRII, by contrast, was reported to be required for efficient heterooligomerization with TβRI (Rechtman et al., 2009). It is therefore possible that mutant TβRII exhibit a reduced tendency to hetero-oligomerize with TβRI. Since it cannot be predicted whether structural displacements induced by the mutations in this study alter the kinase structure sufficiently enough to interfere with hetero-oligomerization, it remains possible that co-expression of mutant TβRII competes with WT-TβRII for heterodimerization with TβRI as well. Furthermore, ligand-induced hetero-oligomerization was reported to be dependent on the juxtamembrane region of TβRII only and not on the kinase domain (Rechtman et al., 2009).

For the most part, mutations in TβRII investigated here did not interfere with constitutive receptor internalization and thus may not interfere with TGF-β signaling propagation at this step. By contrast, R460H TβRII displayed a significant defect in constitutive internalization. For this mutant, in addition to a suppressive function as suggested above, a dominant negative effect may be related to inefficient internalization as part of signaling propagation. However, the dominant negative effect of R460H was not more pronounced as compared to the rest of the mutations tested. This suggests that the effect of R460H as of the other mutations was dominated by competion for signaling components at the cell membrane.

4.6 Smad and MAPK signaling of TβRII mutants

To dissect the potential of TβRII mutations to activate Smad and MAPK signaling these receptors were introduced into WT-TβRII naive DR26 cells and tested in phosphoprotein assays. All mutated receptors except for R460C were inefficient in inducing Smad phosphorylation. Confirming results from luciferase reporter gene assays, R460C was able to mediate weak Smad2 phosphorylation which was about half the activity of WT-TβRII. By contrast, R460C like all other mutations investigated failed to induce ERK phosphorylation after TGF-β stimulation. This strongly supports the differential activation of the Smad-only $(CAGA)_{12}$ and the 3TP reporter which is co-activated by MAPK signaling.

TGF-β induced phosphorylation of p38 MAPK was investigated in HEK293T cells since no response at all was seen in DR26 cells. This may be explained by the fact that rather high expression of TβRII is required to activate p38. Alternatively, the effects of any transfection could mask the modest induction of pp38. Futhermore, DR26 cells may

not be capable to induce TGF-β induced p38 phosphorylation due to lack of sufficient levels of TRAF6 or TAK1 or other signaling components. Indeed, p38 phosphorylation has not been shown to be restored in DR26 cells with reconstituted TβRII (Sorrentino et al., 2008; Yamashita et al., 2008).

In HEK293T cells, however, overexpression of TβRII or any mutant was sufficient to induce pp38 as compared to β-Gal transfected cells. HEK293T cells were previously shown to endogenously respond to TGF-β by phosphorylation of p38 and thus seem to express sufficient amounts of the required co-factors like TRAF6 (Sorrentino et al., 2008). In the present study, overexpression of any WT or mutant TβRII lead to p38 phosphorylation even in the absence of ligand, and no further induction was observed following TGF-β stimulation. The amount of pp38 appeared to correlate with the expression levels of the respective receptors. It seems possible that all receptors investigated contribute to p38 activation. Assuming that the kinase in most TβRII mutations tested here is deficient in activating TβRI to the same extent as it was autokinase deficient, this finding would challenge the assumption that ALK5 kinase activity is crucial for p38 activation (Yamashita et al., 2008; Yu et al., 2002). However, it would fall in line with the notion of others who reported TGF-β induced p38 phosphorylation to be independent from ALK5 kinase activity (Sorrentino et al., 2008). Another explanation would be that TβRII is able to induce p38 activation in the absence of ligand if high levels of TβRII were sufficient to promote the formation of complexes with TβRI and thus to create platforms for TRAF6 association and activation by autoubiquitination. This scenario seems to be supported by some of the data presented by Sorrentino et al. (2008) and Yamashita et al. (2008). These results indicate that overexpression in HEK293T cells of either kinase deficient ALK5 or TβRII induced p38 phosphorylation or TRAF6 ubiquitination, respectively, in the absence of explicit stimulation with TGF-β.

It can only be speculated, though, on the functionality of TβRII mutations in endogenous TGF-β-p38 signaling. On the other hand p38 and TGF-β signaling were found to correlate in a mouse model for severe MFS (*Fbn1*-null, mgN/mgN). Primary cultures of aortic VSMC displayed accumulation of phospho-TAK1 and phospho-p38 in addition to phospho-Smad2 (Carta et al., 2009). Interestingly, these authors claimed to show p38 activation to be upstream of increased Smad signaling. Despite the fact that elevated TGF-β signaling in aortic tissues is a common phenotype in both classical MFS and in related diseases, it should be kept in mind that the origin of dysregulated TGF-β signaling may not be identical in *Fbn-1* mutant and *TGFBR2* mutant patients (Carta et al., 2009; Gomez et al., 2009; Loeys et al., 2005).

4.7 TGF-β induced cell cycle arrest

In epithelial cells TGF-β is a potent inducer of cell cycle arrest. In this study the growth inhibitory effect of mutant TβRII was assessed to complement the results from biochemical and signaling data by a physiological readout. In these cells TGF-β inhibits proliferation by two mechanisms. By induction of the cyclin dependent kinase (CDK-) inhibitors $p15^{Ink4B}$ and $p21^{Cip}$ TGF-β inactivates CDK2 and CDK4 (Massagué and Gomis, 2006). In parallel TGF-β signaling represses the transcription of mitogenic transcription factors such as c-Myc and inhibitors of differentiation transcription factors such as Id1, Id2, and Id3. Transcriptional activation of $p15^{Ink4B}$ and $p21^{Cip}$ as well as c-Myc and Id gene repression induced by TGF-β are Smad dependent responses (Chen et al., 2002; Gomis et al., 2006; Kang et al., 2003). In the present study proliferation arrest as a measure of Smad signaling activity in part - at least for mutations R460C, R528H, and R528C - reflected the results from direct signaling assays.

The limited effects of even WT-TβRII may be explained by the rather low transfection efficiency in DR26 cells and the fact that transfected cells can not be distinguished from non-transfected. However, these data have to be interpreted with caution as this assay could not be reproduced often enough to achieve the required reproducibility, nor was it performed with sample replicates. Thus, this specific assay will be reproduced in the future after optimization of the protocol.

4.8 Residual signaling activity by R460C

The TβRII cytoplasmic domain contains a constitutively active kinase domain and is autophosphorylated at serines, threonines and tyrosines (Lawler et al., 1997; Luo and Lodish, 1997). Activating autophosphorylation which occurs in cis (intramolecular autophosphorylation within the same polypeptide chain) and trans (intermolecular phosphorylation within the TβRII homodimer) promotes full activation of kinase activity and is a prerequisite for TβRII to efficiently mediate the TGF-β signal by transphosphorylating TβRI (Luo and Lodish, 1997; Wrana et al., 1994). The finding that all mutations of R460, R528 and R537 tested in this study were deficient in *in-vitro* autokinase assays with immunoprecipitated receptors suggests that these amino acid exchanges induce rearrangements in the TβRII kinase which renders it inactive. Of interest, even R460C, which showed residual signaling activity both in TGF-β reporter gene assays and in Smad phosphorylation assays, turned out to possess at best trace activity in this assay. This supports the assumption of a destabilizing effect of R460C which could possibly be compensated by a more favorable environment in cell-based assays where decreased receptor mobility in the membrane or associated proteins may stabilize both substrate interaction and kinase structure and enable weak but significant signaling activity of R460C.

R460 maps to the C-terminus α-helix F of the kinase domain which was identified as a major structural component in the eukaryotic kinase architecture. αF serves as a scaffold that establishes correct positioning of catalytic, substrate binding and substrate residues (Kornev et al., 2008). It has been suggested that mutations of R460 affecting the key C-lobe helices perturb *TGFBR2* signaling (Pannu et al., 2005).

The discrepancy between the effects of R460C and R460H found in the present study could be explained by analysis of structural consequences of these mutations (Fig. 28).

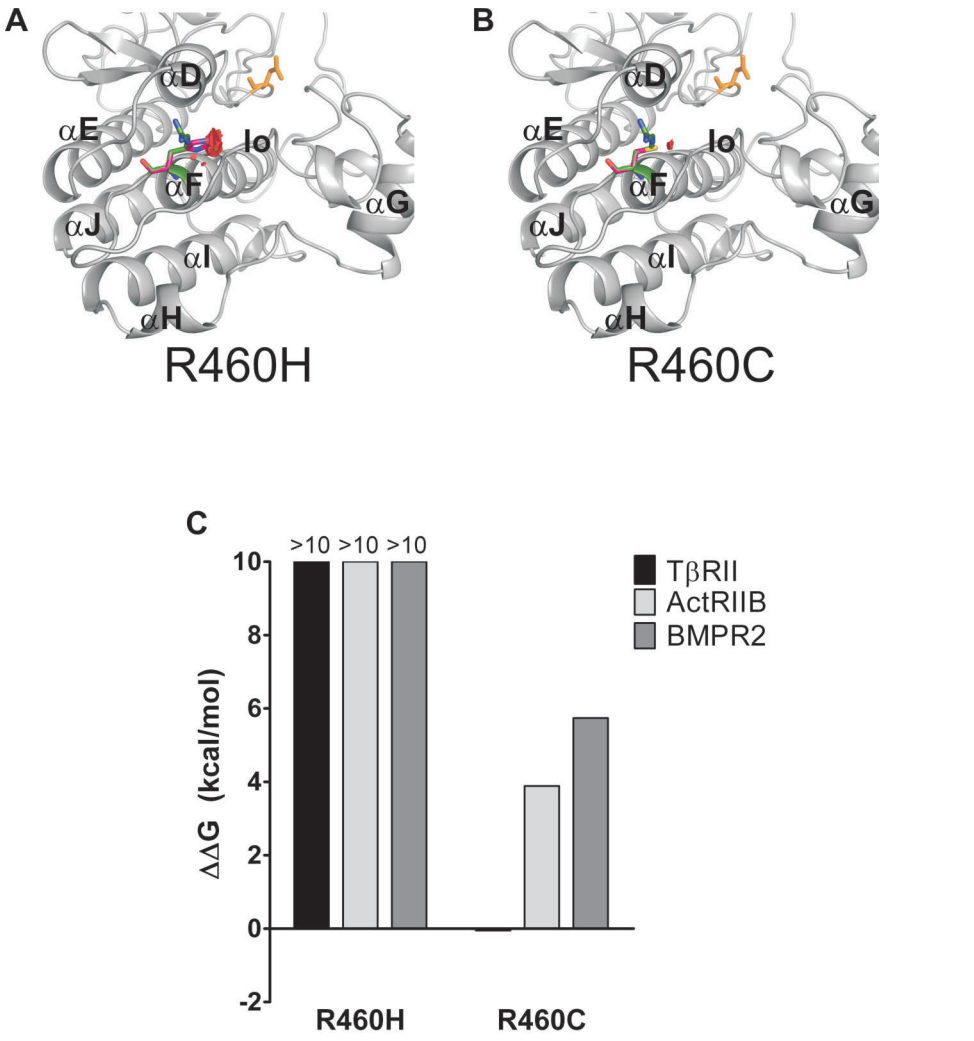

Fig. 28: TβRII kinase structure with mutants of R460. (A) R460 (green) is located in the substrate binding region at the C-terminal end of αF in TβRII. A histidine side chain (pink) in this position generates severe steric clashes (red discs) with the surrounding structure, especially the lobe preceding αG (lo) which will lead to displacements in the lower lobe of the kinase. (B) Cysteine fits in position 460 creating only minor steric incompatibilities. (C) Difference in free energy (ΔΔG) representing the change of protein stability induced by mutations of R460, in the structures of TβRII, ActRIIB, and BMPR2, respectively. Values were calculated using the Eris protein stability prediction server. ΔΔG<0: stabilizing, ΔΔG>0: destabilizing

The side chain of R460 in the modeled TβRII forms two H-bonds to backbone carbonyls in αD and a few residues downstream of αD (Fig. 8). A histidine side chain in this position is not able to form these H-bonds but creates steric clashes with the surrounding structure (Fig. 28A). This would induce structural displacements that propagate through the lower C-lobe and may not only disrupt the active kinase structure but also interfere with substrate binding. Mutation of this arginine to cysteine on the other hand abolishes intramolecular H-bonds of the arginine side chain which presumably leads to structural destabilization of this region (Fig. 28B). The unsaturated H-bonds are close to the solvent surface and thus can be substituted by water molecules. The small cysteine side chain, however, easily fits into that position probably without interfering with other structures (Fig. 28B).

The distinct consequences of the two mutations fell in line with the predicted change of protein stability induced by R460H or R460C mutations, respectively, calculated using the Eris protein stability prediction server (Yin et al., 2007). Histidine in position 460 has a strong destabilizing effect as reflected by a positive change in free energy (ΔΔG) in the structures of TβRII, ActRIIB as well as of BMPR2, while the destabilization induced by cysteine is less severe in ActRIIB and BMPR2, and even negligible in the model of TβRII (Fig. 28C).

Thus, while R460H may result in a distorted kinase structure entirely incapable of binding its substrate and/or to catalyze phosphotransfer, R460C might cause destabilization of the kinase structure which can be compensated to some extent by binding of the substrate or accessory proteins and thus may result in reduced but significant signaling activity.

The selective activation of Smad and ERK pathways by R460C that were apparent from reporter gene assays and from phosphoprotein Western blots may be explained by distinct effects on serine/threonine and tyrosine kinase activities in R460C. TGF-β superfamily receptor kinases belong to the tyrosine-kinase like family as suggested by sequence homology (Hanks and Hunter, 1995). Tyrosine kinases bind their peptide substrates further down in the C-lobe of the kinase. The substrate is positioned slightly further apart from the catalytic site which allows for accomodation of the larger tyrosine residue (Huse et al., 1999; Ubersax and Ferrell Jr, 2007). The kinase domain of TβRI exhibits structural similarities to tyrosin kinases and therefore is regarded as a dual-specificity kinase that is capable of catalyzing both serine/threonine and tyrosine phosphorylation (Huse et al., 1999). Moreover, TβRII was reported to autophoshorylate on tyrosines (Lawler et al., 1997). Activation of ERK, as desribed in the introduction, is accompanied by phosphorylation on serines, threonines, and tyrosines in TβRI, implicating that Tyr phosphorylation by either TβRI or TβRII might be crucial for ERK activation (Lee et al., 2007).

TβRII R460C might lack a significant tyrosine kinase activity and thus proved incapable to induce ERK activation. This finding may be explained by the fact that either minor displacements in the R460C kinase specifically impaired Tyr-kinase activity more strongly than Ser/Thr kinase function, or that the weak Tyr kinase activity of TβRII is reduced concomitantly with a general reduction of catalytic activity to undetectable levels.

4.9 Correlation of signaling activities with disease phenotypes

The mutations investigated in this study have been identified in persons reported to have TAAD, MFS2, and LDS (Tab. 1). While the lack of detailed and comprehensive clinical information in many of the published studies on these disorders makes a direct comparison of phenotypes difficult, published clinical evidence would suggest that mutations at R460 tend to be associated with milder phenotypes. R460H has been associated with TAAD, MFS2, and milder forms of LDS, and R460C has been described in individuals with TAAD and MFS2. On the other hand, R528C and R528H have both been found only in persons diagnosed with LDS. R537C has been described in a family and one unrelated individual with MFS2 as well as one person diagnosed with LDS1. The mutation R537P was found in a mother with MFS2 whose daughter had a typical facial phenotype of LDS1 (personal communication Eloisa Arbustini). It is tempting to speculate that different behavior of the mutations characterized in this work may be related to the different clinical phenotypes. Specifically, the mutation R460C had the most mild dominant negative effect and displayed significant residual TGF-β signaling activity on the Smad pathway which sets it apart from all other mutations, whereas failure to induce TGF-β induced ERK activation is a common feature in all mutations tested (Tab. 3).

Residual capability to induce Smad signaling thus could be sufficient to suppress the additional phenotypic defects which manifest in LDS and MFS2 whereas it may still be ineffective to prevent the development of aortic aneurysms seen in TAAD patients. This model was recently supported by the finding that R460C similiar to R460H and R528H in smooth muscle cells explanted from patients displayed severe defects in the expression of SMC contractile proteins in response to TGF-β (Inamoto et al., 2010). In addition tissue samples from affected patients showed reduced expression of those proteins. These authors suggest the contractile dysfunction as a consequence of impaired TGF-β signaling as the basis for the development of aortic aneurysms.

4.10 Paradoxal activation of TGF-β signaling

A series of studies reported paradoxical upregulation of TGF-β signaling in aortic tissues of patients with mutations in *TGFBR2* kinase domain as shown by increased levels of nuclear phosphorylated Smad, abundance of TGF-β and expression of TGF-β target genes (Gomez et al., 2009; Carta et al., 2009; Loeys et al., 2005). The basis of this observation, however, has not been elucidated to date. It was speculated that intrinsic features of those mutations such as altered receptor endocytosis or alternative pathways might promote TGF-β-Smad signaling in this scenario (Jones et al., 2008).

The quantitative biochemical and cell-based analyses in the present study do not support the assumption of a general cell-autonomous mechanism by which mutant variants of TβRII paradoxically induce elevated TGF-β activity, although the respective experiments were not designed to investigate the long term effects of TGFBR2 mutations on cellular networks related to TGF-β signaling. The most promising way to clarify the phenomenon of paradoxical activation of Smad signaling will therefore be to investigate intercellular communication in affected tissues in every detail, such as to identify the cells that secrete TGF-β and those responding to elevated levels of TGF-β. Further *ex-vivo* studies using patient tissues and cells, and, even more promisingly, mouse models for individual MFS related mutations hopefully will shed light on these important issues in the future.

4.11 Conclusions

The present study has documented that different *TGFBR2* mutations have distinct effects on protein stability and localization, receptor turnover, and signaling in the Smad and ERK pathways (Tab. 3). Many of the mutations demonstrated a striking dominant negative effect on Smad and ERK signaling. Characteristic cell biological differences between mutations associated with MFS2 and LDS did not emerge in the course of this study (Tab. 3). However, it is striking that the R460C mutation, which has been associated with TAAD rather than MFS2 or LDS, showed a quite distinct biochemical phenotype, in that of all tested TβRII mutants, only R460C possessed residual Smad signaling activity and only a minor degree of dominant negative effect on wildtype TβRII Smad signaling.

It appears possible that this residual Smad signaling activity is able to prevent the craniofacial and skeletal phenotypic manifestations characteristic of MFS2 and LDS, but that *TGFBR2* function is still sufficiently disturbed to cause defects in aortic homeostasis that lead to aortic dilatation and dissection (Fig. 29). On the other hand, it would appear that both near haploinsufficiency due to lack of expression of *TGFBR2* in the cell membrane (as seen with the mutations Y336N and S449F) or dominant negative effects of *TGFBR2* missense mutations on Smad and ERK signaling (as seen with the mutations

Tab. 3: Quantitative differences of the nine *TGFBR2* mutations studied in this work. One, two, or three vertical arrows indicate whether mild, moderate, or severe reductions in protein expression (Pr. Ex., including both immature forms in the ER and membrane-bound mature forms), receptor internalization (Rec.Int.), autokinase activity of the isolated mutant receptor (AK), activation of Smad signaling (Smad) and activation of ERK (ERK). A horizontal arrow was used if no change as compared to WT was observed. One, two, or three plus signs indicate whether there was a mild, moderate, or severe dominant negative effect (Dom.Neg.). n. d.: not done

Mutation	Pr. Ex.	Rec. Int.	AK.	Dom.Neg.	Smad	ERK
L308P	↓↓	n.d.	n.d.	n.d.	n.d.	n.d.
Y336N	↓↓↓	n.d.	n.d.	n.d.	n.d.	n.d.
S449F	↓↓↓	n.d.	n.d.	n.d.	n.d.	n.d.
R460C	↓	↓	↓↓↓	+	↓	↓↓↓
R460H	↓	↓↓↓	↓↓↓	++	↓↓↓	↓↓↓
R528C	↓	→	↓↓↓	++	↓↓↓	↓↓↓
R528H	↓	↓	↓↓↓	++	↓↓↓	↓↓↓
R537C	↓↓	↓	↓↓↓	++	↓↓↓	↓↓↓
R537P	↓	↓	↓↓↓	++	↓↓↓	↓↓↓

R528C, R528H, R537C, and R537P, and also R460H) lead to sufficiently severe defects in TGF-β signaling to predispose to the development of phenotypic defects not only in the aorta but also in the other organ systems typically affected by MFS2 and LDS. Alternatively, the fact that the clinical phenotypes of *TGFBR2* mutations that were barely expressed in this study and those that were dominant negative have not been diagnosed differentially may reflect chronic regulatory effects *in vivo*.

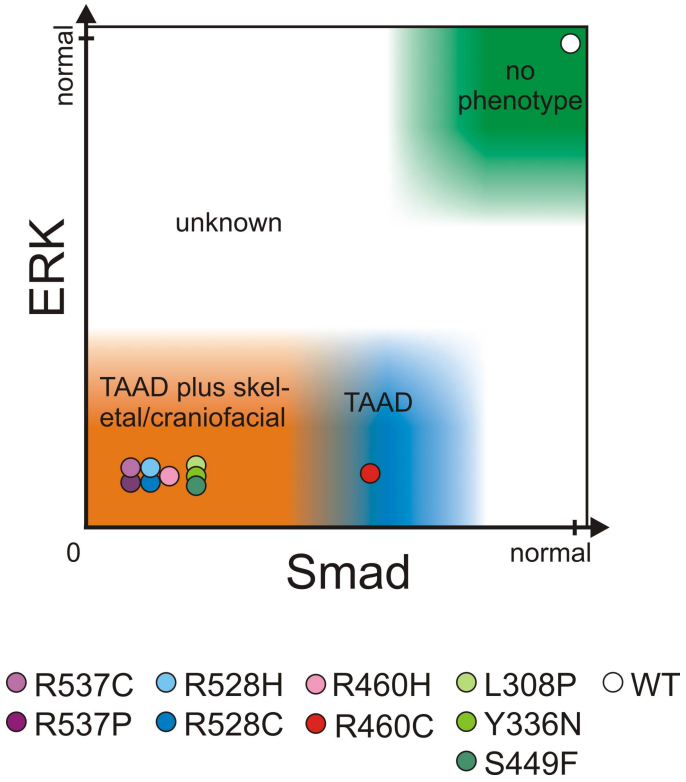

Fig. 29: Proposed model for the correlation of disease phenotypes with Smad and ERK signaling activities. TGF-β type II receptors carrying mutations associated with MFS related diseases display differential activities in TGF-β-Smad- and ERK signaling. Mutations are plotted according to their Smad- and ERK activities in the 2D plot. WT-TβRII promotes normal Smad and ERK signaling and no phenotype is observed (green shading). Most Mutations were shown to be inactive both on Smad and ERK signaling. These mutations are associated with clinically more severe phenotypes that include skeletal and craniofacial manifestations of MFS2 or LDS in addition to TAAD (orange shading) (Tab. 1). R460C, by contrast, was able to mediate reduced but significant activation of Smad signaling that was about 50% of WT Smad signaling. R460 C mutations tend to be associated with isolated TAAD with no or non-specific additional symptoms (shaded blue). From the data shown in this study not correlations can be drawn on certain ratios of Smad/ERK signaling (shaded white), nor can the exact boundaries between phenotypes be drawn in a quantitative manner (indicated by color fading).

5 Results: Antibodies against TβRII-B

5.1 Generation and selection of hybridoma clones

Mice were immunized with an ovalbumin-conjugated peptide KDEIICPSCNRTAHPLRH corresponding to the C-terminal portion of the human TβRII-B insert which is not conserved in mice (Phase I). After 3 immunizations (days 0, 21, 36) and 3 final boosts (week 6) lymphocytes were isolated from spleen cells and fused to Sp2/OAg 14 myeloma cells (Phase II). Hybrids were selectively expanded in HAT medium and supernatants were screened in ELISA with the free peptide immunogen as coating antigen (Phase III) for binding antibodies. Phase I to III were conducted by Eurogentec. Hybridoma clones were obtained from Eurogentec together with samples of their respective supernatants. A series of supernatants which had shown promising features in peptide ELISA (Tab. 4) were tested in ELISA with the extracellular domains (ECD) of TβRII, TβRII-B, or the immunogenic peptide as coating antigens, respectively (Fig. 30). Notably, except for clone 4D9 all supernatants generated signals not only for the TβRII-B peptide and ECD but also for the ECD of TβRII. Clone 4D9 was subjected to another round of limiting dilution subcloning, yielding one subclone (4D9-8) with even improved binding as compared to the parental 4D9 (Fig. 30).

Tab. 4: Hybridoma clones screening results. Relative signals from supernatants screened in ELISA using free peptide or no peptide (control) as coating antigens.

Clones	peptide	control
1B9	1,775	0,052
3H7	3,588	0,040
4B4	1,829	0,039
4D9	2,867	0,042
6A6	3,258	0,047
7C9	3,172	0,059
8E9	3,258	0,061

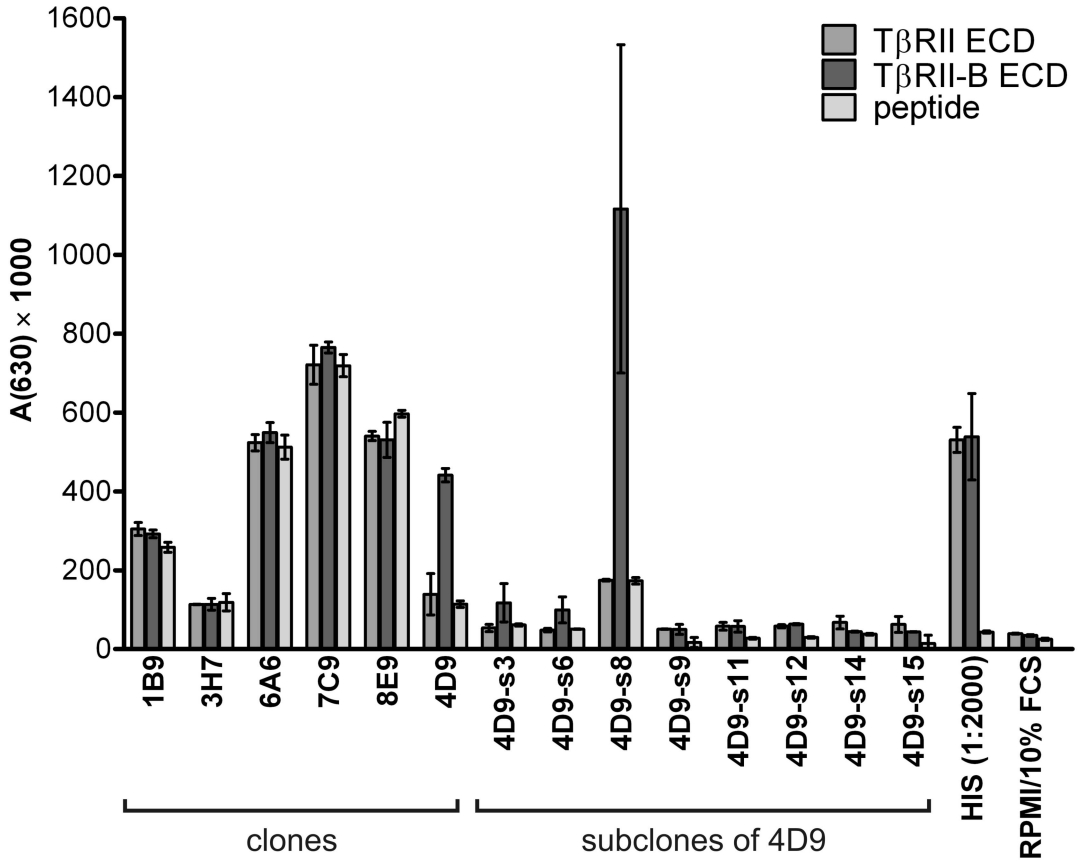

Fig. 30: Binding specificity of supernatants from hybridoma clones and subclones. Hybridoma supernatants of original clones and 4D9 subclones were tested in ELISA for binding to the HIS-tagged ECDs of TβRII, TβRII-B, and the TβRII-B specific peptide. α-HIS antibody and RPMI medium containing 10% FCS were used as positve and negative controls, respectively.

5.2 Purification and evaluation of monoclonal antibodies

For further large scale antibody production the conditions for cell expansion were optimized. Since the presence of FCS containing bovine immunoglobulins as an unwanted contaminant, cells were shifted stepwise to medium containing 5% FCS without negative effects on cell growth and antibody production. Lower amounts of FCS were not tolerated well, neither was replacement of RPMI/FCS by animal-free media that were supposed to enable growth of hybridoma cells in the absence of animal components (data not shown). The use of roller bottles to improve oxygen supply to batch cultures turned out to be unfavourable for the semi-adherent hybridoma cell lines. Consequently, cells of the 4D9-8 subclone (4D9-s8) were expanded in 175 ml cell culture flasks in RPMI containing 5% FCS. After 14 days of growth supernatants were harvested and purified by protein G-sepharose affintiy chromatography (Fig. 31A). Usually one to three fractions were pooled, concentrated and desalted in centrifugal concentrators yielding 500-1000 μg antibody per 100 ml supernatant. The content of contaminating bovine immunoglobulins was calculated below 20%. Enhanced concentration and specific binding of the purified 4D9 subclone 8 mAb was confirmed in ELISA. Dilutions of 1:100 to 1:1000 of the purified mAb (1mg/ml) resulted the same signals as undiluted supernatant (Fig. 32A). However, purified α-TβRII-B was shown to be somewhat less effective in binding to TβRII-B ECD as compared to a commercial mAb (R&D) that became available in the meantime (Fig. 32B). Of note, the supernatant of clone 4B4 produced a strong signal comparable to the 1:10 diluted 4D9-s8 mAb which had not been suggested by its intermediate performance in screening ELISAs (Tab. 4). Consequently, the 4B4 mAb was purified using the same strategy as 4D9-s8 (Fig. 31B), and both antibodies were tested in immunological applications.

5.3 Anti-TβRII-B mAbs 4D9-s8 and 4B4 in immunological applications

5.3.1 Anti-TβRII-B mAb in immunoprecipitation and Western blot

The 4D9-s8 and 4B4 antibodies were used to immunoprecipitate TβRII-B from lysates of L6 rat myoblasts stably expressing Dox-inducible TβRII or TβRII-B. L6 cells were shown to express endogenous TβRII but not TβRII-B Rotzer et al. (2001). Antibodies were incubated with the cell lysates for 12 hours and then precipitated with protein G-sepharose. Both receptors were bound by an α-HA antibody as expected (Fig. 33A). As

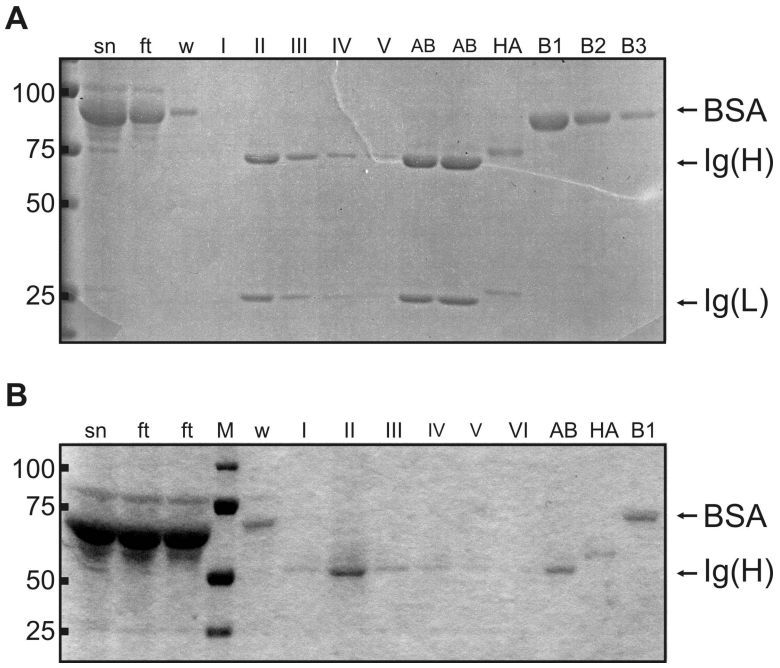

Fig. 31: Affintiy purification of TβRII-B antibodies. SDS-PAGE of chromatography fractions from 4D9-s8 (A) or 4B4 (B) purification. sn: original supernatant, ft: flow-through, M: molecular weight marker, w: wash fractions, I-VI: elution fractions, AB: purified antibodies, HA: α-HA antibody (Roche), B1: BSA (1 mg/ml), B2: BSA (0.5 mg/ml), B3: BSA (0.25 mg/ml), Ig(H): immunoglobulin heavy chains, Ig(L): immunoglobulin light chains; loading was 5 μl for purified antibodies, α-HA and BSA, and 10 μl for other samples.

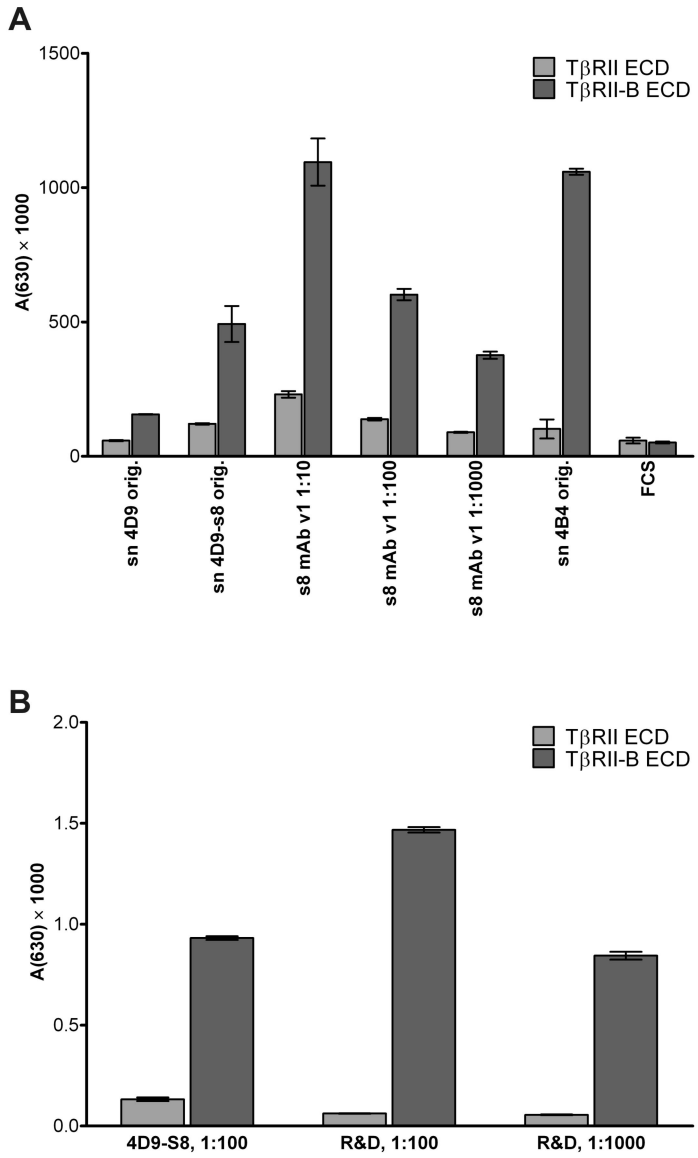

Fig. 32: Binding of purified α-TβRII-B mAb. (A) ELISA with affinity purified mAb from 4D9-s8 supernatants as compared to supernatants of the parental 4D9 clone, 4D9 subclone 8 (s8), and the supernatant from another clone (4B4). Plates were coated with the ECD of either receptor isoform. (B) Binding of 4D9-s8 as compared to a commerically available rabbit polyclonal TβRII-B antibody (R&D).

expected the 4B4 mAb precipitated TβRII-B but not TβRII. By contrast, the 4D9-s8 mAb did not precipitate detectable amounts of any receptor. (Fig. 33A).

Similiar results were obtained when both antibodies were used in SDS-PAGE Western blots directly. L6-TβRII-B cells were induced or not with Dox to express the receptor. The 4B4 mAb specifically recognized TβRII-B in induced cells resulting in the same pattern as a commercial antibody for TβRII-B (R&D) (Fig. 33B). Both antibodies detected a faint pattern also in non-induced cells. Since the position of these bands is the same as in the induced samples this could be attributed to leakiness of the Tet/CMV promoter in those cells rather than to unspecific binding endogenous TβRII. The 4D9-s8 mAb, however, did not detect any specific bands on Western blots (data not shown).

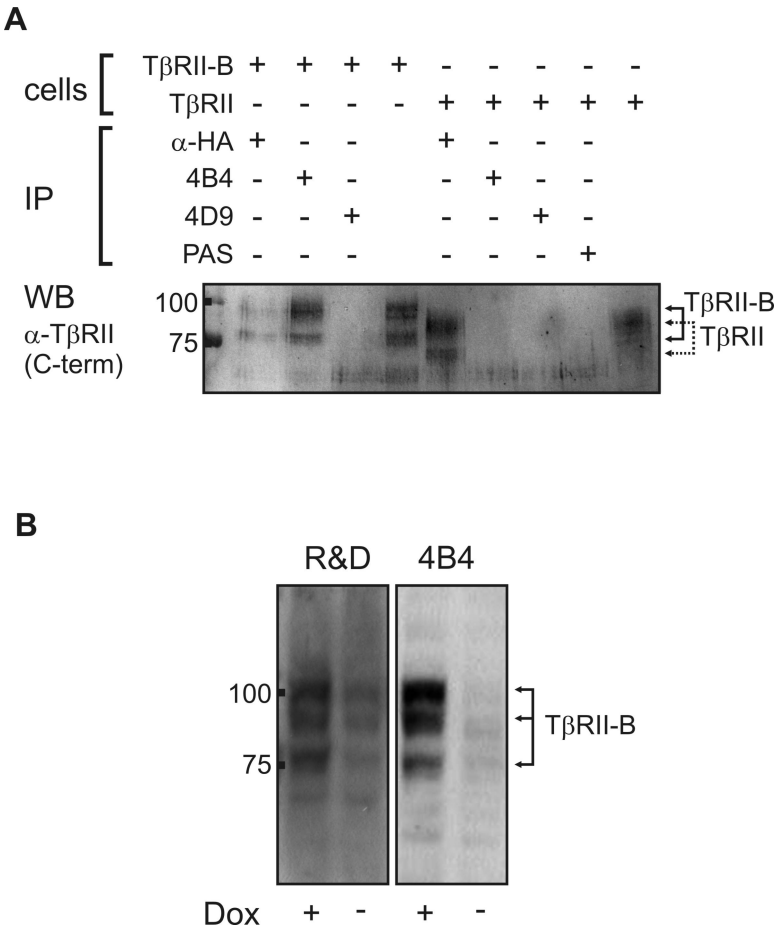

Fig. 33: Immunoprecipitation and Western blot with 4D9-s8 and 4B4 mAb. (A) Immunoprecipitation from stable L6 cells expressing HA-TβRII or HA-TβRII-B. Expression was induced by doxycyclin. Receptors were detected on Western blots by an antibody against the C-terminus TβRII which recognizes both isoforms. (B) Western blot after SDS-PAGE of Dox-induced or non-induced L6-TβRII-B cells. Left panel a commercially available α-TβRII-B (R&D). PAS:protein A-sepharose

5.3.2 Anti-TβRII-B in flow cytometry and immunocytochemistry

To test whether the α-TβRII-B antibodies recognize the receptor on the cell surface they were used in flow cytometry and immunocytochemistry.

For flow cytometry retrovirally transduced L6-HA-TβRII-B and L6-HA-TβRII were treated with Doxycyclin to induce receptor expression (2.3.1.1). Parental L6 cells were used as controls. Live cells were stained with either 4D9-s8 or 4B4 followed by staining with R-PE conjugated anti-mouse secondary antibodies. Cells carrying the inducible plasmid construct were identified by their constitutively expressed EGFP. An α-HA antibody detected both receptor variants on the surface of EGFP positive cells confirming that both receptors are expressed in their respective cell line (Fig. 34). The 4B4 antibody specifically stained TβRII-B isoform with no crossreactivity to TβRII. No signal could be detected with 4D9-s8 under various staining conditions (data not shown).

For immunocytochemistry C2C12 myoblast cells were transfected with Myc-tagged TβRII or TβRII-B. Receptors were stained on PFA fixed cells with either α-Myc-tag or 4B4 as primary antibodies followed by fluorescent secondary antibodies, or with a AF488-labelled 4B4 that was generated from purified 4B4. Both receptors were expressed in C2C12 cells as shown by Myc-staining (Fig. 35). TβRII-B transfected cells were stained by the unlabeled 4B4 at levels comparable to Myc-detection, whereas some unspecific staining in TβRII was observed at very long exposure. The latter was unspecific background staining of cells in general rather than cross reactivity with TβRII, since unspecific staining was observed on all cells, however, transfection efficiency usually was not 100% as shown in the other images of this panel. Staining with AF-488 labelled 4B4 resulted in specific staining of TβRII-B expressing cells. No cross reactivity and very low background staining even after extended exposure times was observed.

Taken together, the 4B4 antibody that was produced from hybridoma cells was proven to be applicable in a broad variety of immunological applications where it specifically recognized TβRII-B whether denatured or in lysis buffer, as well as on live and on PFA fixed cells (Tab. 5).

5.4 Inhibitory potential of anti-TβRII-B antibodies

5.4.1 Inhibition of TβRI:TβRII-B heterocomplex formation

The inhibitory potential of the 4B4 antibody was assessed in a set of assays. First, the antibody was used to interfere with TβRI:TβRII-B heterocomplex formation following TGF-β stimulation in receptor co-patching experiments. These experiments were performed by Maya Mouler Rechtman (Tel Aviv University, Israel). COS-7 cells were transfected with

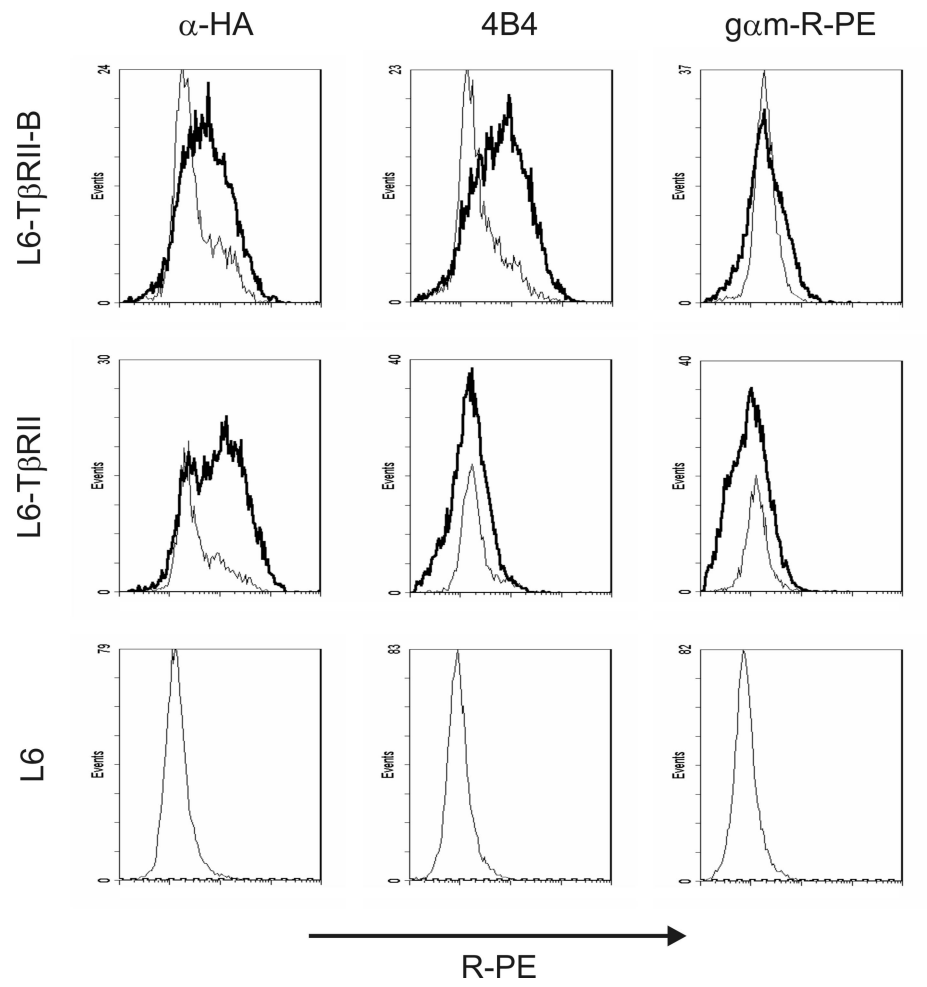

Fig. 34: Flow cytometry using the 4B4 mAb. Live L6-HA-TβRII-B and L6-HA-TβRII or parental L6 cells were stained with 4B4 or α-HA antibodies followed by R-PE anti-mouse secondary antibodies. L6 cells carrying the inducible expression plasmid for the respective receptors were identified by their constitutive EGFP expression. R-PE staining of EGFP positive cells was compared to negative cells. An α-HA antibody stained both isoforms on their respective cell lines. The 4B4 antibody only recognizes TβRII-B without any cross-reactivity to TβRII.

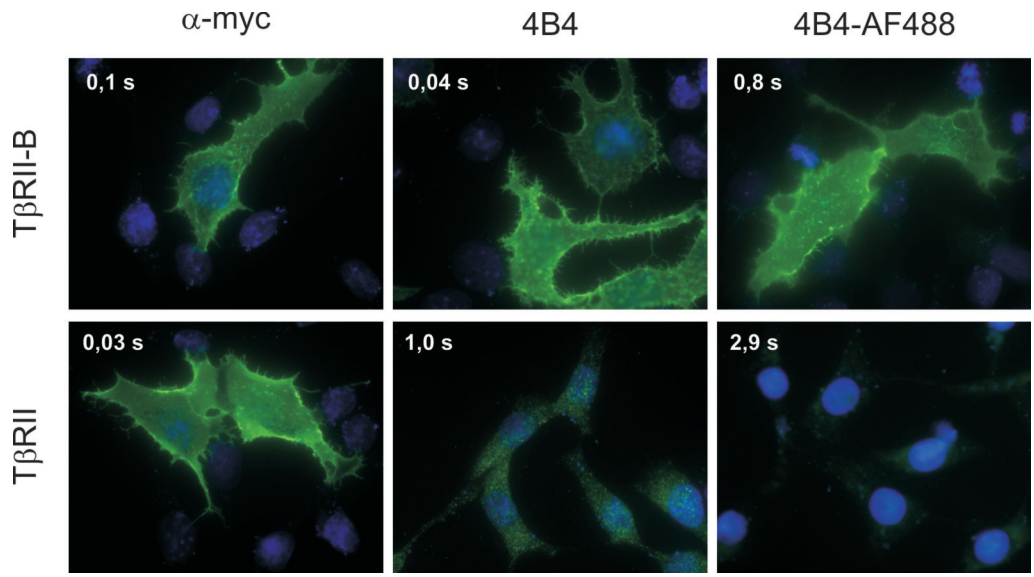

Fig. 35: Immunocytochemistry using the 4B4 mAb. C2C12 cells were transfected with Myc-TβRII or Myc-TβRII-B. Receptors on PFA fixed cells were stained with eiher α-Myc or 4B4 primary antobodies followed by secondary detection with gαm-AF488, or with a AF488-labelled 4B4. Expopsure times are given for each image.

HA-tagged TβRI and Myc-tagged TβRIIB. Both tags were stained with α-tag primary antibodies of rabiit and mouse origin, respectively, followed by detection with species-specific secondary antibodies. Patches on the cell surface was recorded by confocal laser microscopy and quantified in digital imaging analysis software. Co-localization of two patches of different colors was assumed if the centres of mass were closer than 0.2 μm. Stimulation with TGF-β1 or TGF-β2 induced the formation of TβRI:TβRII-B heterocomplexes (Fig. 36). Introduction of the 4B4 TβRII-B antibody interfered with TGF-β2 induced heterocomplex formation, but not if co-patching was induced by TGF-β1. A polyclonal antibody for TβRII-B which was generated previously in our lab reduced receptor co-patching in the same fashion, suggesting that targeting of TβRII-B by these antibodies interferes with binding of TGF-β2 to TβRII-B but not with binding of the TGF-β1 isoform.

5.4.2 Inhibition of Smad nuclear translocation

To test the existence of an inibitory effect of α-TβRII-B antibodies also on downstream events in the TGF-β pathway, the translocation of Smads in the nucleus as a consequence of TGF-β stimulation was visualized by immunocytochemistry. This assay was performed by Maya Mouler Rechtman (Tel Aviv University, Israel). Rat L6 cells which lack expression of the TGF-β type II-B and type III receptor were transfected with TβRII or TβRII-B. Following stimulation with TGF-β2 the cells were fixed, and the subcellular distribution

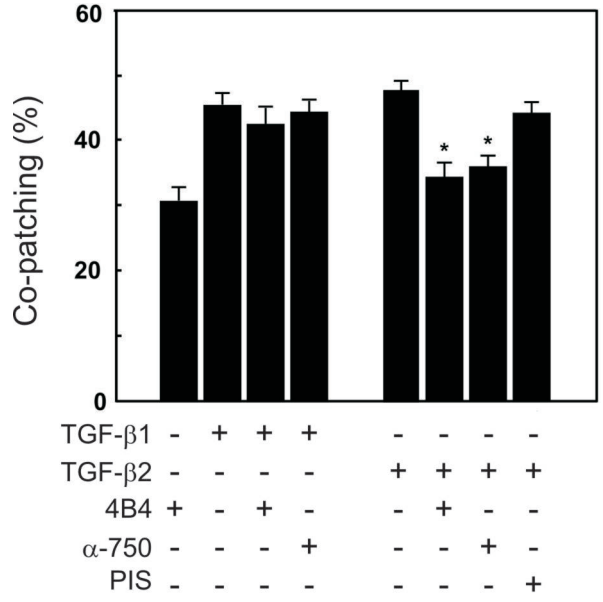

Fig. 36: Inhibition of TβRI:TβRII-B heterocomplex formation. COS-7 cells were transfected with extracellular tagged HA-TβRI and Myc-TβRII-B. rabbit HA-tag and mouse Myc-tag antibodies were recognized by AF-594 and AF-488 conjugated species-specific secondary antibodies, respectively. Red and green patches on the cell surface were recorded by confocal laser microscopy. Co-patching was defined as an overlapping of two patches if their centres of mass were closer than 0.2 μm. PIS: pre-immune serum. Figure: Maya Mouler Rechtman.

of Smad2/3 was visualized by immunocytochemistry (Fig. 37A). In TβRII transfected cells stimulation with TGF-β2 induced a weak increase in Smad nuclear localization, reflecting the fact that in the absence of TβRIII the regular isoform of TβRII is inefficient in binding TGF-β2 (Fig. 37B). By contrast, expression of TβRII-B in those cells dramatically enhanced the Smad2/3 response. As expected, signalling activity of TβRII in turn was not affected in the presence of the 4B4 α-TβRII-B antibody. By contrast, 4B4 significantly inhibited TGF-β2 induced signalling by TβRII-B.

5.4.3 Repression of Smad transcriptional activity

A TGF-β responsive luciferase reporter gene construct was used to quantify the inhibitory effect of the 4B4 antibody as at the level of transcriptional activity. L6 cells were transfected with TβRII-B and the Smad3/4 dependent $(CAGA)_{12}$ luciferase reporter. Stimulation with both TGF-β1 and TGF-β2 induced luciferase activity in a dose-dependent manner (Fig. 38). If the 4B4 antibody was present in the medium, the TGF-β1 induced response remained the same whereas the TGF-β2-TβRII-B signalling pathway was repressed by 40% and 25% for 20 pM and 50 pM stimulation with TGF-β2 (Fig. 38).

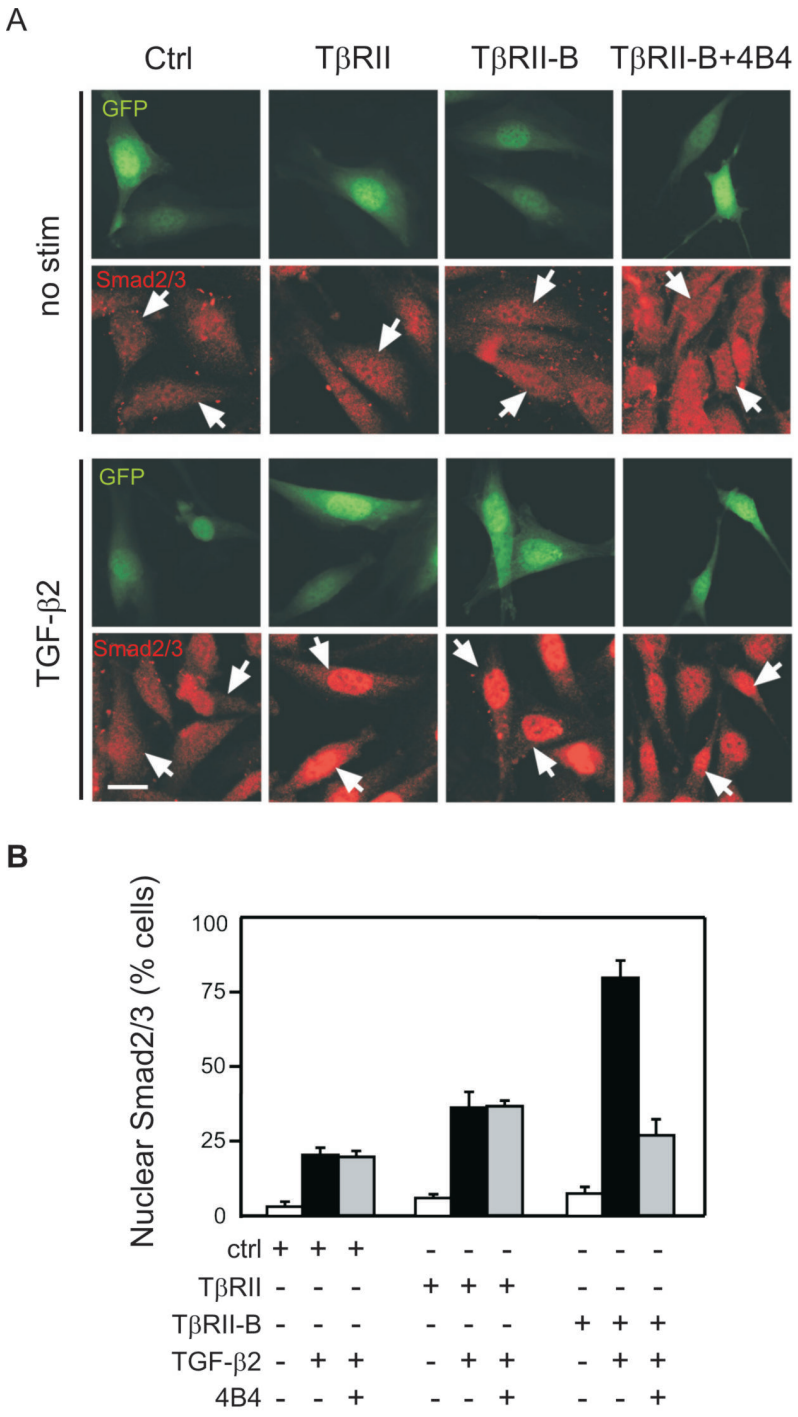

Fig. 37: Inhibition of Smad nuclear translokation in L6 cells. L6 rat myoblast cells lacking expression of TGF-β type II-B and type III receptors were transfected with extracellular tagged TβRII or TβRII-B. Control cells were transfected with β-Gal (A) Immunocytocheistry to visualize Smad subcellular distribution. Co-transfection with GFP identified cells expressing the respective receptors. (B) Smad nuclear translocation following TGF-β2 stimulation was quantified by the number of cells in which Smad2/3 were predominantly localized in the nucleus. Figure: Maya Mouler Rechtman.

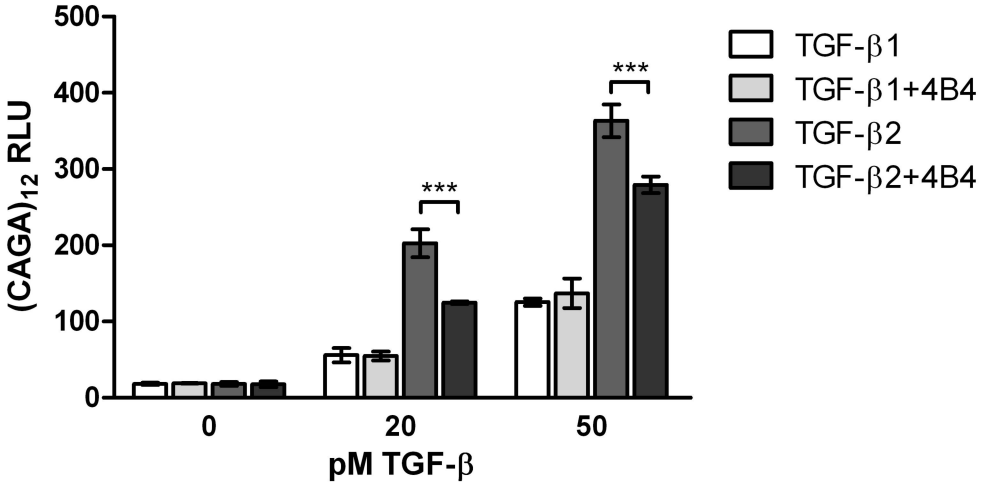

Fig. 38: Inhibition of TGF-β induced reporter gene activity. L6 cells were tranfected with TβRII-B together with $(CAGA)_{12}$ and renilla luciferase constructs. Cells were stimulated with or without 20 pM or 50 pM TGF-β1 or -2 for 24 hours in the presence or absence of 2000× molar excess of 4B4.

In conclusion, the 4B4 α-TβRII-B antibody could be shown to interfere with TGF-β2 induced signalling of TβRII-B. 4B4 interacted with TβRII-B to block activation of the TGF-β pathway at the very upstream level where it prevents recruitment of TβRI into the heterotetrameric signalling complex with TβRII-B following stimulation with TGF-β2. As a consequence, the downstream TGF-β-Smad pathway is repressed. The 4B4 antibody does not affect signalling by the TβRII isoform, nor does it repress signalling induced by TGF-β1. A summary of applications for 4D9-s8 and 4B4 antibodies is listed in Tab. 5.

Tab. 5: Antibody summary. Applicability of 4D9-s8 and 4B4 antibodies. performance +++: excellent, ++: good, +: fair, -: not applicable; n.d.: not determined; * data not shown

Application	4D9-s8	4B4	4B4-AF488
ELISA	++	+++	n.d.
Immunoprecipitation	-	++	n.d.
Western blot	-	+++	n.d.
Flow cytometry	-	+++	n.d.
Immunocytochemistry	+*	+++	+++
Pathway inhibition	-	++	n.d.

6 Discussion: Antibodies against TβRII-B

6.1 Antibodies against TβRII-B: previous approaches

The molecular basis of the exceptional signaling properties in TβRII-B remained obscure after their description nine years ago, neither was a specific function or role of this receptor identified. The generation of specific antibodies for TβRII-B was therefore a highly desired achievement that would enable more detailed exploration of TβRII-B. Such antibodies could be useful both as immunological tools to visualize the expression of TβRII-B in cells and tissues of normal or pathogenic origin. Moreover, antibodies that exhibit an inhibitory potential to specifically interfere with TβRII-B signaling would faciltiate the analysis of its functionality. Attempts were made in the past to establish such antibodies.

Polyclonal antibodies against the human-specific C-terminal portion of the TβRII-B insert (amino acids KDEI-LRH, serum α500) as well as the conserved N-terminal part (DVEM-KDEI, α750) were raised in rabbits (Fig. 4). The purified pAbs specifically recognized the extracellular domain of TβRII-B but not of TβRII in ELISA (Wittek, 2003). The α750 could be shown to react with TβRII-B in Western blots, immunoprecipitations and in flow cytometric assays (Scheich, 2003). However, none of the purified antibodies exhibited an inhibitory effect on TβRII-B signaling in 3TP-luc reporter and Smad phosphorylation assays (Scheich, 2003; Wittek, 2003).

Subsequently, the production of mouse monoclonal antibodies turned out to be problematic. Mice that were immunized with the N-terminal peptide which is conserved in mice and human (Fig. 4) failed to generate specific antibodies for this peptide. Instead, four mice developed antibodies for ovalbumin which was used as a carrier for the insert peptide (Wittek, 2003). It appears that the peptide was non-immunogenic in mice due to the presence of the respective antigen in mouse TβRII-B. For this reason the C-terminal sequence of the insert was used for immunization in this study.

6.2 Purification and evaluation of TβRII-B mAbs

A series of hybridoma clone supernatants obtained from Eurogentec displayed variable affinities and specificities in ELISA with the ECDs of TβRII, TβRII-B, or the free peptide as coating antigens. Of seven supernatants tested only two displayed resonable specificity

for TβRII-B. The results from these ELISA do not fully mirror the screening results obtained by Eurogentec. Some clones which displayed the strongest binding in the screens exhibited strong but unspecific binding in our hands. This discrepancy may be explained by the fact that screening assays were done with empty wells as controls by Eurogentec and did not include negative protein controls. High binding to the ECDs of TβRII, TβRII-B, and the peptide to the same extent supposedly was due to a more general affninty to proteins .

Hybridoma cells corresponding to two promising supernatants were expanded, and subcloned in one case. Antibodies purified from these two hybridoma supernatants, 4B4 and 4D9-s8, were purified by protein G affinity chromatography and reacted with the ECD of TβRII-B in a specific and highly affine manner as measured by ELISA. The 4B4 α-TβRII-B mAb generated strong and specific signals in Western blots and immunoprecipitations, showing that it recognizes its target both in a denatured and native conformation. Furthermore, the 4B4 mAb was applicable in flow cytometry on live cells, as well as in immunocytochemical stainings on PFA fixed cells which emphasized its broad applicability. Moreover, a FITC-conjugated variant of the 4B4 displayed specificity and high affinty on fixed cells and is thus applicable for direct labeling of TβRII-B.

The fact that the 4B4 mAb recognized its target under denaturing conditions as well as in the native form and even after PFA fixation suggested that the peptide sequence sequence KDEI-LRH which was used for immunization was not part of a secondary structure in native TβRII-B and thus did not change its conformation during denaturation.

Taken together, the 4B4 α-TβRII-B mAb provides a versatile immunological tool to specifically visualize expression, localization and dynamics of TβRII-B.

6.3 Inhibitory potential of TβRII-B mAbs

The potential of the α-TβRII-B mAb to interfere with TβRII-B mediated signaling was confirmed in assyas that monitor several steps in the TGF-β signaling pathway. TGF-β1- and TGF-β2-induced hetero-oligomerization of TβRII-B and TβRI was determined by immunofluorescence co-patching studies on COS-7 cells. The 4B4 α -TβRII-B mAb interfered with co-patching induced by TGF-β2 but not by TGF-β1. Luciferase reporter gene assays in L6 cells which were transfected with TβRII-B confirmed the specific inhibition of TGF-β2 induced signaling by TβRII-B in the presence of the 4B4 mAb, while signal activation by TGF-β1 was not affected. These data documented the inhibitory potential of the α-TβRII-B mAb at two stages which are far upstream and at the downstream end of the TGF-β pathway, respectively.

COS-7 cells express both TβRII-B and TβRIII and thus are able to respond to TGF-β1 and TGF-β2 (Rotzer et al., 2001). Responsiveness to TGF-β1 can be established by binding

of TGF-β1 to TβRII or TβRII-B. On the contrary, due to the low affinity of TβRII for TGF-β2, binding of TGF-β2 requires either presence of TβRII-B or contribution of TβRIII, the latter binding and presenting TGF-β2 to TβRII (López-Casillas et al., 1993; Rotzer et al., 2001). TβRII-B was demonstrated to bind TGF-β1 and TGF-β2 in the absence of TβRIII. TβRIII, however, was shown to co-immunoprecipitated in with TGF-β2-bound TβRII-B, indicating that TβRIII, if present, could contribute to binding of TGF-β2 to TβRII-B (Rotzer et al., 2001). The relatively strong repression of TGF-β2 stimulated recruitment of TβRI by 4B4 observed in the present study could suggest that in COS-7 cells the contribution binding of TGF-β2 to TβRII-B to signaling is more crucial than the contribution of TβRIII.

L6 cells on the other hand lack endogenous expression of TβRII-B and TβRIII. TGF-β2 signaling in these cells therefore is strongly dependent on TβRII-B (Rotzer et al., 2001). This is supported by the finding that in L6 cells quantitative assays to measure Smad2/3 nuclear translocation revealed a much stronger responsiveness to TGF-β2 if TβRII-B was introduced as compared to TβRII. In addition, these assays demonstrated a specific interaction of the 4B4 mAb with TβRII-B resulting in repression of Smad nuclear accumulation while signaling by TβRII was not affected.

Thus, the 4B4 α-TβRII-B mAb generated in this study has demonstrated its potential to inhibit TGF-β2-TβRII-B signaling with high specificity. Importantly, the antibody does not interfere TGF-β1 induced signaling of TβRII-B. It will be used in the future to scrutinize the functional roles of TGF-β2 induced signaling by TβRII-B. For further optimization of this mAb - eventually with regard to potential clinical applicability - it may be worth to generate Fab fragments of 4B4. Single Fab fragments of appoximately 50 kDa are significantly smaller as compared to the 150 kDa immunoglobulin and are widely used diagnostics and therapy. Fab fragments of 4B4 would represent the first ligand-specific extracellular inhibitors for TGF-β receptors.

6.4 Implications for binding of TGF-β to TβRII-B

The results described above have documented the specific interference of an antibody targeting the TβRII-B insert peptide with TGF-β2 induced receptor complex formation and signaling activation. This observation could be explained by the scenario that binding of the antibody to the C-terminal part of the TβRII-B insert prevents binding of TGF-β2 to TβRII-B and/or the recruitment of TβRI in an active signaling complex. At the same time, binding of TGF-β1 was not affected by antibody binding. This supports the assumption that binding of TGF-β2 occurs by interactions distinct from, or in addition to, binding sites of TGF-β1 to TβRII and TβRII-B.

High affinity binding of TGF-β1 and TGF-β3 to TβRII is mediated by mainly polar interactions between TβRII and the fingertips of TGF-β1/3 as described in the introduction (Fig. 3). The very N-terminus of TβRII was shown to be dispensable for binding of TGF-β1 to TβRII (Pepin et al., 1996). Both crystallographic and NMR solution structures of TβRII suggest the N-terminal about 20 residues do not adopt an ordered structure which is why they are not represented in any of the crystallographic structures (Groppe et al., 2008; Hart et al., 2002; Radaev et al., 2010). NMR solution structures include a only few more upstream residues (Deep et al., 2003).

However, this does not preclude that in TβRII-B the insert is involved in binding of TGF-β2 to the receptors. The peptide sequence of TβRII-B comprises about 20 residues upstream of the published TβRII structures - depending on the respective study - and an additional 25 amino acids contributed by the TβRII-B insert. These 45 amino acids constitute a peptide chain of significant dimensions as compared to the receptor signaling complex and might well contact either TGF-β or TβRI through (Fig. 39).

For this reason in the present study an *in-silico* analyses of the N-terminal portion of TβRII-B were performed using the PredictProtein web server (Rost et al., 2004) and the PSIPRED Protein Structure Prediction server (Jones, 1999). In the N-terminal portion of the insert an α-helical structure (DVEM-AQKD; Fig. 4) was predicted with intermediate reliability by PSIPRED (Appendix B.1). More importantly, from local sequence information a protein-protein interaction site was predicted for the C-terminal portion of the insert (PSCN-TAHP; Appendix B.2). Of note, the 4B4 α-TβRII-B mAb which efficiently inhibited TGF-β2 signaling through TβRII-B in the present study was raised against a peptide comprising this part of the insert. This sequence may be involved in binding of TβRII-B to TGF-β2 and thereby confer TβRII-B with reasonable affinity for TGF-β2 by tethering TGF-β2 to TβRII to compensate for its reduced affinity at the TGF-β2 fingertips epitope. On the other hand, one study did not report an increased affinity of TβRII-B for TGF-β2 as compared to TβRII (del Re et al., 2004). However, these results were obtained by surface plasmon resonance assays (using soluble Fc-fused ECD of TβRII-B and TβRII) which does not reconstitute environment of the cell membrane, and in cell-based assays in which presence of TRIII potentially masked receptor specific binding.

Alternatively , the C-terminal insert sequence may increase affinity of TβRII-B to TβRI leading to the establishment of pre-formed complexes of TβRI and TβRII-B. Notably, the contribution of such complexes to TGF-β2 binding and signaling in the absence of TβRIII was suggested by a series of reports (del Re et al., 2004; Radaev et al., 2010; Rodriguez et al., 1995).

The existence of pre-formed TβRI:TβRII-B complexes in the absence of ligand has not been determined to date, and this possibility may be the most promising mechanism to be explored. Moreover, TβRII was found in hetero-oligomers with TβRI at low but

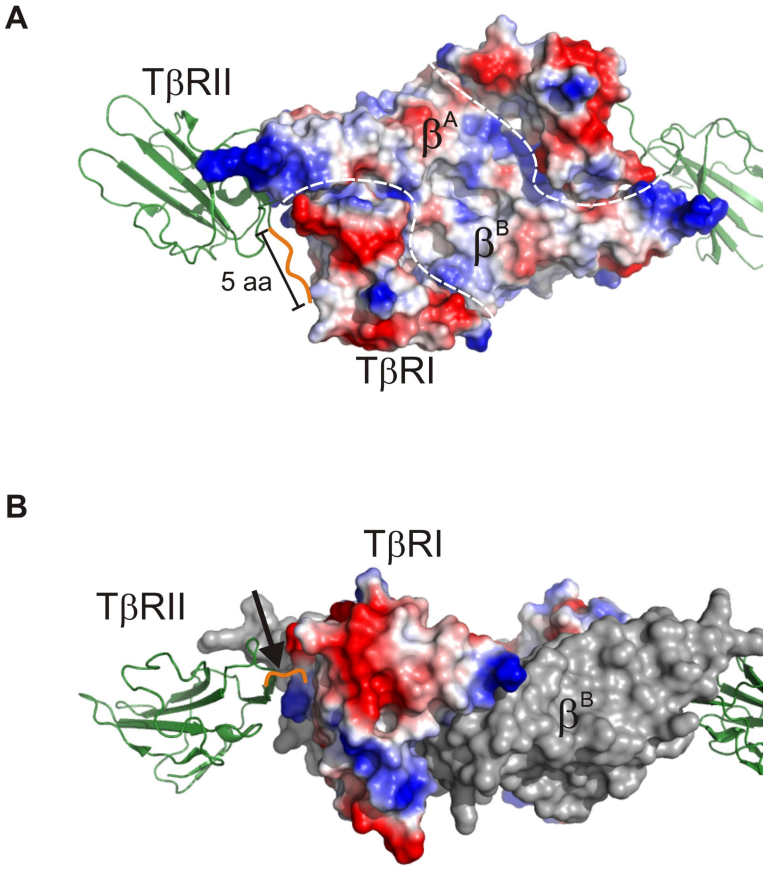

Fig. 39: Spatial dimensions in the TGF-β receptor signaling complex.
(A) Top view of the TGF-β receptor signaling complex comprising TGF-β1 monomers A (β^A) and B (β^B), TβRI and TβRII (green cartoon). Crystal structure of TβRII start with Ala21 at the N-terminus of TβRII. The N-terminal stretch of five amino acids (Ala21 and downstream) are shown in orange for size reference. TGF-β 1 and TβRI surfaces are depicted with their vacuum electrostatics potential (red - negative, blue - positive). The TβRII-B ECD comprises an additional 45 amino acids upstream of the depicted N-terminus of TβRII. These residues constitute a peptide chain of significant length as compared to the signaling complex that could well promote interaction with either the ligand or TβRI. (B) Side view showing TGF-β1 (grey), TβRI (surface electrostatics potential), and TβRII (green cartoon). The N-terminal five amino acids in TβRII are highlighted in orange (arrow). Images were generated with PyMOL based on PDB 3KFD (Radaev et al., 2010).

detectable levels also in the absence of TGF-β (Wells et al., 1999). In this regard it should be considered that increased affinity of TβRII-B to TβRI may not be sufficient to promote pre-formed complexes in the absence of ligand to the same extent as it was documented for BMP receptors (Gilboa et al., 2000). Instead, residual direct affintiy of TβRII-B for TGF-β2 and an increased tendency to recruit TβRI may act synergistically to form active receptor signaling complexes, potentially involving induced-fit conformational changes in the TβRII-B insert sequence.

In this work - through the generation of a TβRII-B specific inhibitory monoclonal antibody - the involvement of the TβRII-B specific insert region in TGF-β2 induced signaling was clearly demonstrated. It will be highly rewarding to confirm the role of the insert by mutagensis approaches scanning the insert sequence in TβRII-B.

7 Side Project: The TβRII interactome

To identify novel proteins involved in the modulation of TGF-β signaling we screened for proteins interacting with the cytoplasmic domain of the TGF-beta type II receptor and characterized the impact of candidates on the TGF-β pathway.

Experimental work for this project experiments was carried out mainly by two students, Sandra Schmidt and Manuel Bauer, who did their diploma projects under my supervision.

Using GST-pulldown assays followed by 2D-BAC-gel electrophoresis and mass spectrometry about 90 proteins were identified. In addition to established interactors of the receptor signaling complex, components of other signaling pathways, the ubiquitin system, metabolism, vesicle transport as well transcriptional and translational control were found. These experiments were carried out by Manuel Bauer and performed in collaboration with Albert Sickmann (University of Würzburg) (Bauer, 2005). Interaction with the type II receptor cytoplasmic domain could be confirmed by co-immunoprecipitations for a set of those proteins, and effects on TGF-β signaling were evaluated.

Specifically, the role of one interacting protein, Fas-associated factor 1 (FAF1), which was known before as a player in apoptotic signaling pathways, was characterized in further detail. These experiments were carried out for the most part by Sandra Schmidt (Schmidt, 2007).

FAF1 is a 74-kDa adaptor protein that was first shown to associate with the Fas receptor complex. Following overexpression FAF1 was shown to augment Fas induced apoptosis or to promote Fas-independent apoptosis depending on the cell type. FAF1 contains an N-terminal ubiquitin associated (UBA) domain that was shown to bind to mono- and K48-linked di-ubiquitin (Fig. 40) (Song et al., 2009). The UBA domain is followed by two ubiquitin-homology domains that share sequence homology with ubiquitin. At the C-terminus of FAF1 a UBX domain which revealed homology to ubiquitin based on the structure was shown to interact with the N-terminus of valosin-containing protein (p97/VCP). VCP is a proteasome-associated chaperone which cooperates with proteasomes, and the interaction of FAF1 and VCP was shown to inhibit proteasomal degradation. Experiments to elucidate the role of FAF1 in TGF-β signal transduction were carried out by Sandra Schmidt.

We could confirm by co-immunoprecipitation that FAF1 interacts with the putative membrane form of TβRII and co-localizes with TβRII at the membrane (Schmidt, 2007). Overexpression of FAF1 repressed TGF-β induced $(CAGA)_{12}$ luciferase reporter gene

activity but not BMP2-induced responses on a BMP-responsive element (BRE) luciferase reporter (Fig. 41 and 42). Conversely, downregultation of FAF1 by shRNA constructs enhanced responsiveness for TGF-β (Fig. 43) (Schmidt, 2007). Although the mechanism by which FAF1 specifically represses TGF-β signaling will be subject to detailed investigation in the future, it can be assumed that the interference occurs outside the nucleus (Schmidt, 2007) and does not involve regulation of TβRII surface expression or internalization (Fig. 44).

Work on this project is ongoing.

Fig. 40: FAF1 domain structure. UBA - ubiquitin binding domain, UB - ubiquitin-homologue domains, P - CK2 phosphorylation sites, UBX - domain structurally homologous to ubiquitin, CAF - chromatin assembly factor p150 subunit homologous domain

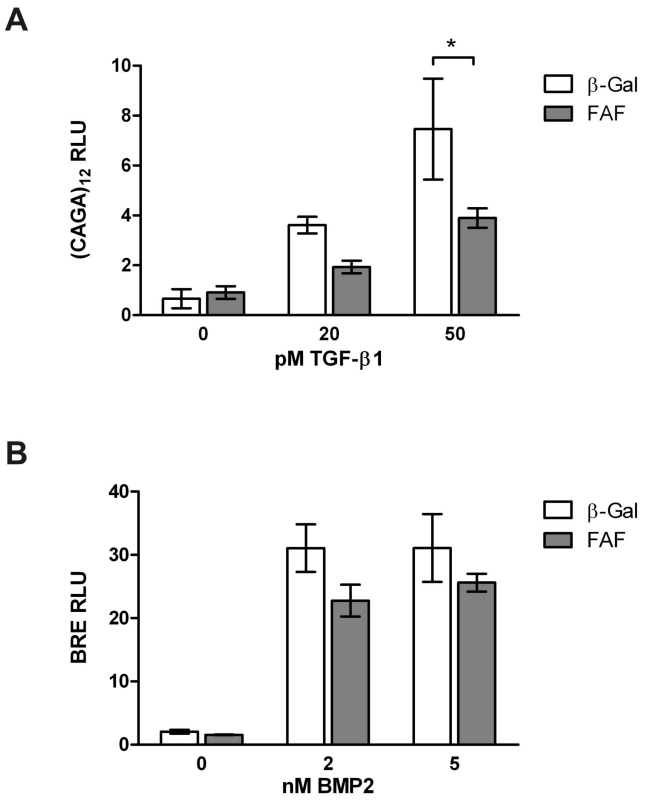

Fig. 41: Overexpression of FAF1 represses TGF-β signaling. C2C12 cells were transfected with TGF-β responsive $(CAGA)_{12}$ (A) or BMP-inducible BMP response element (BRE) (B) luciferase reporter constructs and either FAF1 or control (β-Gal). Cells were stimulated with increasing amounts of TGF-β or BMP. Experiments were performed by Sandra Schmidt.

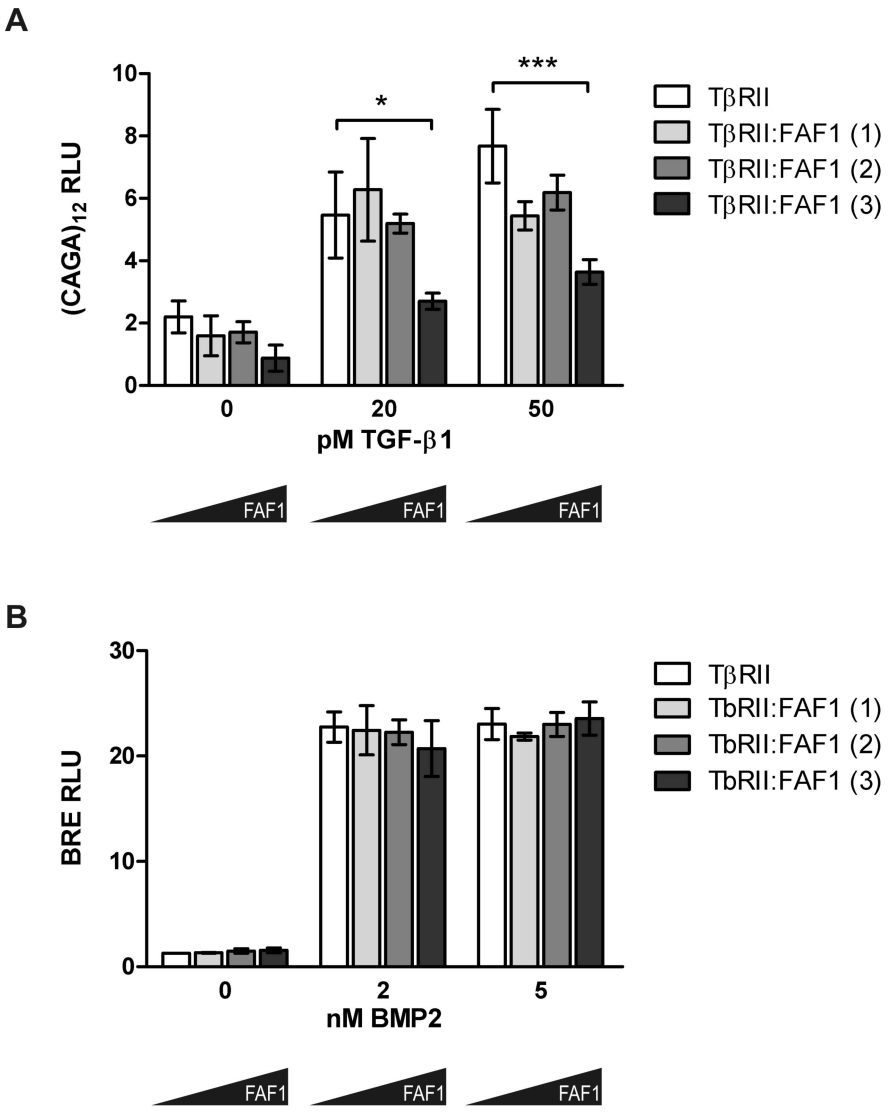

Fig. 42: Overexpression of FAF1 represses TβRII signaling. C2C12 cells were transfected with TGF-β responsive $(CAGA)_{12}$ (A) or BMP-inducible BMP response element (BRE) (B) luciferase reporter constructs, and co-transfected with TβRII and increasing amounts of FAF1. Cells were stimulated with increasing concentrations of TGF-β or BMP. Asterisks indicate statistical significance (Two-way ANOVA followed by Bonferroni's post test for multiple comparisons): $p \leq 0.05$ (*), $p \leq 0.01$ (**), $p \leq 0.001$ (***). Experiments were performed by Sandra Schmidt.

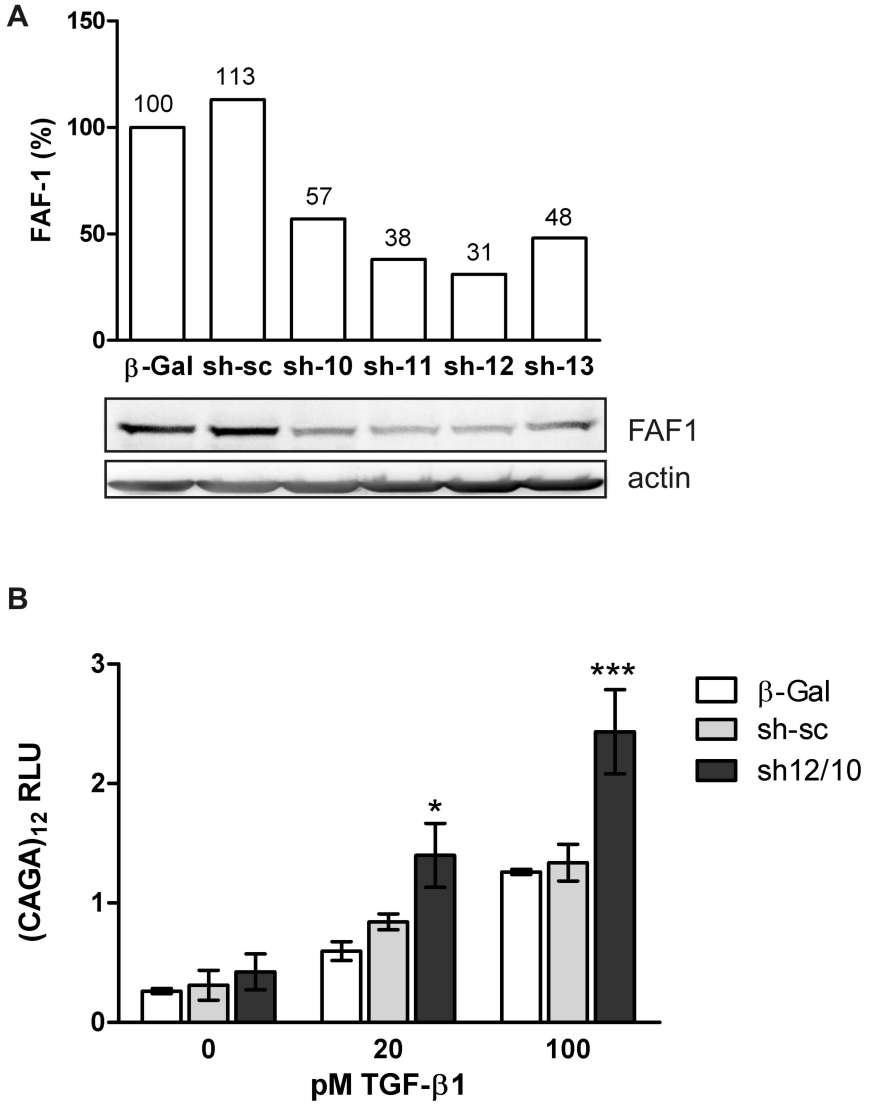

Fig. 43: Knockdown of FAF1 enhances TGF-β responsiveness. (A) C2C12 cells were transfected with small hairpin (sh-) RNA constructs (sh-10 - sh-13) for FAF1 or scrambled shRNA (sh-sc) or control plasmid (β-Gal) 48 hours post-transfection the amount of FAF1 protein was determined by Western blotting. (B) Cells were co-transfected with FAF1 specific shRNAs sh-12 and sh-10 and $(CAGA)_{12}$-luc reporter constructs and stimulated with TGF-β48 hours post-transfection. Asterisks indicate statistical significance (Two-way ANOVA followed by Bonferroni's post test for multiple comparisons): $p \leq 0.05$ (*), $p \leq 0.01$ (**), $p \leq 0.001$ (***). Experiments were performed by Sandra Schmidt.

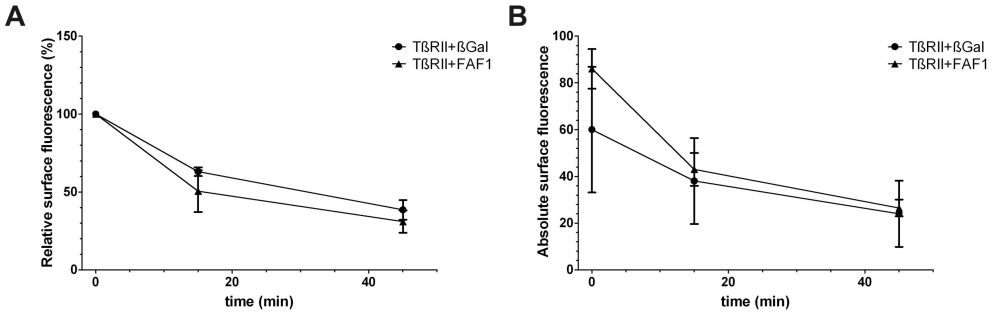

Fig. 44: TβRII surface levels are not affected by FAF1 overexpression. HEK293T cells were co-transfected with HA-tagged TβRII and FAF1 or β-Gal controls. (A) Internalization of TβRII was determined by flow cytometry and given as fractions of TβRII internalized (B). Absolute amounts of surface TβRII.

Bibliography

Adam, P. J., Regan, C. P., Hautmann, M. B., and Owens, G. K. (2000). Positive- and negative-acting Kruppel-like transcription factors bind a transforming growth factor beta control element required for expression of the smooth muscle cell differentiation marker SM22alpha in vivo. *J Biol Chem*, 275(48):37798–37806.

Alarcón, C., Zaromytidou, A.-I., Xi, Q., Gao, S., Yu, J., Fujisawa, S., Barlas, A., Miller, A. N., Manova-Todorova, K., Macias, M. J., Sapkota, G., Pan, D., and Massagué, J. (2009). Nuclear CDKs drive Smad transcriptional activation and turnover in BMP and TGF-beta pathways. *Cell*, 139(4):757–769.

Allendorph, G. P., Vale, W. W., and Choe, S. (2006). Structure of the ternary signaling complex of a TGF-beta superfamily member. *Proc Natl Acad Sci U S A*, 103(20):7643–7648.

Annes, J. P., Munger, J. S., and Rifkin, D. B. (2003). Making sense of latent TGFbeta activation. *J Cell Sci*, 116(Pt 2):217–224.

Arnold, K., Bordoli, L., Kopp, J., and Schwede, T. (2006). The SWISS-MODEL workspace: a web-based environment for protein structure homology modelling. *Bioinformatics*, 22(2):195–201.

Attias, D., Stheneur, C., Roy, C., Collod-Béroud, G., Detaint, D., Faivre, L., Delrue, M.-A., Cohen, L., Francannet, C., Béroud, C., Claustres, M., Iserin, F., Kien, P. K. V., Lacombe, D., Le Merrer, M., Lyonnet, S., Odent, S., Plauchu, H., Rio, M., Rossi, A., Sidi, D., Steg, P. G., Ravaud, P., Boileau, C., and Jondeau, G. (2009). Comparison of clinical presentations and outcomes between patients with TGFBR2 and FBN1 mutations in Marfan syndrome and related disorders. *Circulation*, 120(25):2541–2549.

Bakin, A. V., Tomlinson, A. K., Bhowmick, N. A., Moses, H. L., and Arteaga, C. L. (2000). Phosphatidylinositol 3-kinase function is required for transforming growth factor beta-mediated epithelial to mesenchymal transition and cell migration. *J Biol Chem*, 275(47):36803–36810.

Barak, L. S., Tiberi, M., Freedman, N. J., Kwatra, M. M., Lefkowitz, R. J., and Caron, M. G. (1994). A highly conserved tyrosine residue in G protein-coupled receptors is

required for agonist-mediated beta 2-adrenergic receptor sequestration. *J Biol Chem*, 269(4):2790–2795.

Batut, J., Howell, M., and Hill, C. S. (2007). Kinesin-mediated transport of Smad2 is required for signaling in response to TGF-beta ligands. *Dev Cell*, 12(2):261–274.

Bauer, M. (2005). Identifikation von TGF-beta typ II Rezeptor-assoziierten Proteinen. Master's thesis, Freie Universität Berlin.

Boesen, C. C., Radaev, S., Motyka, S. A., Patamawenu, A., and Sun, P. D. (2002). The 1.1 Å crystal structure of human TGF-beta type II receptor ligand binding domain. *Structure*, 10(7):913–919.

Bonifacino, J. S. and Lippincott-Schwartz, J. (2003). Coat proteins: shaping membrane transport. *Nat Rev Mol Cell Biol*, 4(5):409–414.

Borders, C. L., Broadwater, J. A., Bekeny, P. A., Salmon, J. E., Lee, A. S., Eldridge, A. M., and Pett, V. B. (1994). A structural role for arginine in proteins: multiple hydrogen bonds to backbone carbonyl oxygens. *Protein Sci*, 3(4):541–548.

Carcamo, J., Zentella, A., and Massagué, J. (1995). Disruption of transforming growth factor beta signaling by a mutation that prevents transphosphorylation within the receptor complex. *Mol Cell Biol*, 15(3):1573–1581.

Carta, L., Smaldone, S., Zilberberg, L., Loch, D., Dietz, H. C., Rifkin, D. B., and Ramirez, F. (2009). p38 MAPK is an early determinant of promiscuous Smad2/3 signaling in the aortas of Fibrillin-1 (Fbn1)-null mice. *J Biol Chem*, 284(9):5630–5636.

Casciola, L. A., van der Westhuyzen, D. R., Gevers, W., and Coetzee, G. A. (1988). Low density lipoprotein receptor degradation is influenced by a mediator protein(s) with a rapid turnover rate, but is unaffected by receptor up- or down-regulation. *J Lipid Res*, 29(11):1481–1489.

Centrella, M., Ji, C., Casinghino, S., and McCarthy, T. L. (1996). Rapid flux in transforming growth factor-beta receptors on bone cells. *J Biol Chem*, 271(31):18616–18622.

Chacko, B. M., Qin, B., Correia, J. J., Lam, S. S., de Caestecker, M. P., and Lin, K. (2001). The L3 loop and C-terminal phosphorylation jointly define Smad protein trimerization. *Nat Struct Biol*, 8(3):248–253.

Chakraborti, S., Mandal, M., Das, S., Mandal, A., and Chakraborti, T. (2003). Regulation of matrix metalloproteinases: an overview. *Mol Cell Biochem*, 253(1-2):269–285.

Chaudhry, S. S., Cain, S. A., Morgan, A., Dallas, S. L., Shuttleworth, C. A., and Kielty, C. M. (2007). Fibrillin-1 regulates the bioavailability of TGFbeta1. *J Cell Biol*, 176(3):355–367.

Cheifetz, S., Hernandez, H., Laiho, M., ten Dijke, P., Iwata, K. K., and Massagué, J. (1990). Distinct transforming growth factor-beta (TGF-beta) receptor subsets as determinants of cellular responsiveness to three TGF-beta isoforms. *J Biol Chem*, 265(33):20533–20538.

Cheifetz, S., Like, B., and Massagué, J. (1986). Cellular distribution of type I and type II receptors for transforming growth factor-beta. *J Biol Chem*, 261(21):9972–9978.

Chen, C.-R., Kang, Y., Siegel, P. M., and Massagué, J. (2002). E2F4/5 and p107 as Smad cofactors linking the TGFbeta receptor to c-myc repression. *Cell*, 110(1):19–32.

Chen, R. H., Miettinen, P. J., Maruoka, E. M., Choy, L., and Derynck, R. (1995). A WD-domain protein that is associated with and phosphorylated by the type II TGF-beta receptor. *Nature*, 377(6549):548–552.

Chen, W., Kirkbride, K. C., How, T., Nelson, C. D., Mo, J., Frederick, J. P., Wang, X.-F., Lefkowitz, R. J., and Blobe, G. C. (2003). Beta-arrestin 2 mediates endocytosis of type III TGF-beta receptor and down-regulation of its signaling. *Science (80-)*, 301(5638):1394–1397.

Chen, Y., Budd, R. C., Kelm, R. J., Sobel, B. E., and Schneider, D. J. (2006). Augmentation of proliferation of vascular smooth muscle cells by plasminogen activator inhibitor type 1. *Arterioscler Thromb Vasc Biol*, 26(8):1777–1783.

Chen, Y.-G. (2009). Endocytic regulation of TGF-beta signaling. *Cell Res*, 19(1):58–70.

Chen, Y. G., Hata, A., Lo, R. S., Wotton, D., Shi, Y., Pavletich, N., and Massagué, J. (1998). Determinants of specificity in TGF-beta signal transduction. *Genes Dev*, 12(14):2144–2152.

Collod, G., Babron, M. C., Jondeau, G., Coulon, M., Weissenbach, J., Dubourg, O., Bourdarias, J. P., Bonaïti-Pellié, C., Junien, C., and Boileau, C. (1994). A second locus for marfan syndrome maps to chromosome 3p24.2-p25. *Nat Genet*, 8(3):264–268.

Conery, A. R., Cao, Y., Thompson, E. A., Townsend, C. M., Ko, T. C., and Luo, K. (2004). Akt interacts directly with Smad3 to regulate the sensitivity to TGF-beta induced apoptosis. *Nat Cell Biol*, 6(4):366–372.

Crawford, S. E., Stellmach, V., Murphy-Ullrich, J. E., Ribeiro, S. M., Lawler, J., Hynes, R. O., Boivin, G. P., and Bouck, N. (1998). Thrombospondin-1 is a major activator of TGF-beta1 in vivo. *Cell*, 93(7):1159–1170.

Crescenzo, G. D., Hinck, C. S., Shu, Z., niga, J. Z., Yang, J., Tang, Y., Baardsnes, J., Mendoza, V., Sun, L., López-Casillas, F., O'Connor-McCourt, M., and Hinck, A. P. (2006). Three key residues underlie the differential affinity of the TGFbeta isoforms for the TGFbeta type II receptor. *J Mol Biol*, 355(1):47–62.

Daly, A. C., Randall, R. A., and Hill, C. S. (2008). Transforming growth factor beta-induced Smad1/5 phosphorylation in epithelial cells is mediated by novel receptor complexes and is essential for anchorage-independent growth. *Mol Cell Biol*, 28(22):6889–6902.

Daopin, S., Piez, K. A., Ogawa, Y., and Davies, D. R. (1992). Crystal structure of transforming growth factor-beta 2: an unusual fold for the superfamily. *Science (80-)*, 257(5068):369–373.

Datta, P. K., Chytil, A., Gorska, A. E., and Moses, H. L. (1998). Identification of strap, a novel wd domain protein in transforming growth factor-beta signaling. *J Biol Chem*, 273(52):34671–34674.

Datta, P. K. and Moses, H. L. (2000). Strap and smad7 synergize in the inhibition of transforming growth factor beta signaling. *Mol Cell Biol*, 20(9):3157–3167.

Deep, S., Walker, K. P., Shu, Z., and Hinck, A. P. (2003). Solution structure and backbone dynamics of the TGFbeta type II receptor extracellular domain. *Biochemistry*, 42(34):10126–10139.

del Re, E., Babitt, J. L., Pirani, A., Schneyer, A. L., and Lin, H. Y. (2004). In the absence of type III receptor, the transforming growth factor (tgf)-beta type II-B receptor requires the type I receptor to bind TGF-beta2. *J Biol Chem*, 279(21):22765–22772.

Dennler, S., Itoh, S., Vivien, D., ten Dijke, P., Huet, S., and Gauthier, J. M. (1998). Direct binding of Smad3 and Smad4 to critical TGF beta-inducible elements in the promoter of human plasminogen activator inhibitor-type 1 gene. *EMBO J*, 17(11):3091–3100.

Derynck, R. and Miyazono, K. (2007). *The TGF-beta Family*. Cold Spring Harbor Laboratory Press.

Derynck, R. and Zhang, Y. E. (2003). Smad-dependent and Smad-independent pathways in TGF-beta family signalling. *Nature*, 425(6958):577–584.

Di Guglielmo, G. M., Le Roy, C., Goodfellow, A. F., and Wrana, J. L. (2003). Distinct endocytic pathways regulate TGF-beta receptor signalling and turnover. *Nat Cell Biol*, 5(5):410–421.

Dietz, H. C., Cutting, G. R., Pyeritz, R. E., Maslen, C. L., Sakai, L. Y., Corson, G. M., Puffenberger, E. G., Hamosh, A., Nanthakumar, E. J., and Curristin, S. M. (1991). Marfan syndrome caused by a recurrent de novo missense mutation in the fibrillin gene. *Nature*, 352(6333):337–339.

Disabella, E., Grasso, M., Marziliano, N., Ansaldi, S., Lucchelli, C., Porcu, E., Tagliani, M., Pilotto, A., Diegoli, M., Lanzarini, L., Malattia, C., Pelliccia, A., Ficcadenti, A., Gabrielli,

O., and Arbustini, E. (2006). Two novel and one known mutation of the TGFBR2 gene in marfan syndrome not associated with FBN1 gene defects. *Eur J Hum Genet*, 14(1):34–38.

Duprez, V. and Dautry-Varsat, A. (1986). Receptor-mediated endocytosis of interleukin 2 in a human tumor T cell line. Degradation of interleukin 2 and evidence for the absence of recycling of interleukin receptors. *J Biol Chem*, 261(33):15450–15454.

Ehrlich, M., Shmuely, A., and Henis, Y. (2001). A single internalization signal from the di-leucine family is critical for constitutive endocytosis of the type II TGF-(beta) receptor. *J Cell Sci*, 114(9):1777–1786.

El-Hamamsy, I. and Yacoub, M. H. (2009). Cellular and molecular mechanisms of thoracic aortic aneurysms. *Nat Rev Cardiol*, 6(12):771–786.

Engelman, J. A., Luo, J., and Cantley, L. C. (2006). The evolution of phosphatidylinositol 3-kinases as regulators of growth and metabolism. *Nat Rev Genet*, 7(8):606–619.

Engh, R. A. and Bossemeyer, D. (2001). The protein kinase activity modulation sites: mechanisms for cellular regulation - targets for therapeutic intervention. *Adv Enzyme Regul*, 41:121–149.

Faivre, L., Collod-Beroud, G., Loeys, B. L., Child, A., Binquet, C., Gautier, E., Callewaert, B., Arbustini, E., Mayer, K., Arslan-Kirchner, M., Kiotsekoglou, A., Comeglio, P., Marziliano, N., Dietz, H. C., Halliday, D., Beroud, C., Bonithon-Kopp, C., Claustres, M., Muti, C., Plauchu, H., Robinson, P. N., Adès, L. C., Biggin, A., Benetts, B., Brett, M., Holman, K. J., Backer, J. D., Coucke, P., Francke, U., Paepe, A. D., Jondeau, G., and Boileau, C. (2007). Effect of mutation type and location on clinical outcome in 1,013 probands with Marfan syndrome or related phenotypes and FBN1 mutations: an international study. *Am J Hum Genet*, 81(3):454–466.

Feng, X. H. and Derynck, R. (1997). A kinase subdomain of transforming growth factor-beta (TGF-beta) type I receptor determines the TGF-beta intracellular signaling specificity. *EMBO J*, 16(13):3912–3923.

Fuller, S. A., Takahashi, M., and Hurrell, J. G. (2001). Cloning of hybridoma cell lines by limiting dilution. *Curr Protoc Mol Biol*, Chapter 11:Unit11.8.

Furuhashi, M., Yagi, K., Yamamoto, H., Furukawa, Y., Shimada, S., Nakamura, Y., Kikuchi, A., Miyazono, K., and Kato, M. (2001). Axin facilitates Smad3 activation in the transforming growth factor beta signaling pathway. *Mol Cell Biol*, 21(15):5132–5141.

Gao, S., Alarcón, C., Sapkota, G., Rahman, S., Chen, P.-Y., Goerner, N., Macias, M. J., Erdjument-Bromage, H., Tempst, P., and Massagué, J. (2009). Ubiquitin ligase Nedd4L targets activated Smad2/3 to limit TGF-beta signaling. *Mol Cell*, 36(3):457–468.

Garamszegi, N., Doré, J. J., Penheiter, S. G., Edens, M., Yao, D., and Leof, E. B. (2001). Transforming growth factor beta receptor signaling and endocytosis are linked through a COOH terminal activation motif in the type I receptor. *Mol Biol Cell*, 12(9):2881–2893.

García-Alvarez, J., Ramirez, R., Checa, M., Nuttall, R. K., Sampieri, C. L., Edwards, D. R., Selman, M., and Pardo, A. (2006). Tissue inhibitor of metalloproteinase-3 is up-regulated by transforming growth factor-beta1 in vitro and expressed in fibroblastic foci in vivo in idiopathic pulmonary fibrosis. *Exp Lung Res*, 32(5):201–214.

Gerthoffer, W. T. and Singer, C. A. (2002). Secretory functions of smooth muscle: cytokines and growth factors. *Mol Interv*, 2(7):447–456.

Gilboa, L., Nohe, A., Geissendörfer, T., Sebald, W., Henis, Y. I., and Knaus, P. (2000). Bone morphogenetic protein receptor complexes on the surface of live cells: a new oligomerization mode for serine/threonine kinase receptors. *Mol Biol Cell*, 11(3):1023–1035.

Gomez, D., Zen, A. A. H., Borges, L. F., Philippe, M., Gutierrez, P. S., Jondeau, G., Michel, J.-B., and Vranckx, R. (2009). Syndromic and non-syndromic aneurysms of the human ascending aorta share activation of the Smad2 pathway. *J Pathol*, 218(1):131–142.

Gomis, R. R., Alarcón, C., Nadal, C., Poznak, C. V., and Massagué, J. (2006). C/EBPbeta at the core of the TGFbeta cytostatic response and its evasion in metastatic breast cancer cells. *Cancer Cell*, 10(3):203–214.

Gordon, K. J. and Blobe, G. C. (2008). Role of transforming growth factor-beta superfamily signaling pathways in human disease. *Biochim Biophys Acta*, 1782(4):197–228.

Goumans, M.-J., Liu, Z., and ten Dijke, P. (2009). TGF-beta signaling in vascular biology and dysfunction. *Cell Res*, 19(1):116–127.

Goumans, M. J., Valdimarsdottir, G., Itoh, S., Lebrin, F., Larsson, J., Mummery, C., Karlsson, S., and ten Dijke, P. (2003). Activin receptor-like kinase (ALK)1 is an antagonistic mediator of lateral TGFbeta/ALK5 signaling. *Mol Cell*, 12(4):817–828.

Grady, W. M., Myeroff, L. L., Swinler, S. E., Rajput, A., Thiagalingam, S., Lutterbaugh, J. D., Neumann, A., Brattain, M. G., Chang, J., Kim, S. J., Kinzler, K. W., Vogelstein, B., Willson, J. K., and Markowitz, S. (1999). Mutational inactivation of transforming growth factor beta receptor type II in microsatellite stable colon cancers. *Cancer Res*, 59(2):320–324.

Greenwald, J., Fischer, W. H., Vale, W. W., and Choe, S. (1999). Three-finger toxin fold for the extracellular ligand-binding domain of the type II activin receptor serine kinase. *Nat Struct Biol*, 6(1):18–22.

Gregory, K. E., Ono, R. N., Charbonneau, N. L., Kuo, C.-L., Keene, D. R., Bächinger, H. P., and Sakai, L. Y. (2005). The prodomain of BMP-7 targets the BMP-7 complex to the extracellular matrix. *J Biol Chem*, 280(30):27970–27980.

Groppe, J., Hinck, C. S., Samavarchi-Tehrani, P., Zubieta, C., Schuermann, J. P., Taylor, A. B., Schwarz, P. M., Wrana, J. L., and Hinck, A. P. (2008). Cooperative assembly of TGF-beta superfamily signaling complexes is mediated by two disparate mechanisms and distinct modes of receptor binding. *Mol Cell*, 29(2):157–168.

Guex, N. and Peitsch, M. C. (1997). SWISS-MODEL and the Swiss-PdbViewer: an environment for comparative protein modeling. *Electrophoresis*, 18(15):2714–2723.

Guo, X. and Wang, X.-F. (2009). Signaling cross-talk between TGF-beta/BMP and other pathways. *Cell Res*, 19(1):71–88.

Habashi, J. P., Judge, D. P., Holm, T. M., Cohn, R. D., Loeys, B. L., Cooper, T. K., Myers, L., Klein, E. C., Liu, G., Calvi, C., Podowski, M., Neptune, E. R., Halushka, M. K., Bedja, D., Gabrielson, K., Rifkin, D. B., Carta, L., Ramirez, F., Huso, D. L., and Dietz, H. C. (2006). Losartan, an AT1 antagonist, prevents aortic aneurysm in a mouse model of Marfan syndrome. *Science (80-)*, 312(5770):117–121.

Han, S., Loulakis, P., Griffor, M., and Xie, Z. (2007). Crystal structure of activin receptor type IIB kinase domain from human at 2.0 Ångstrom resolution. *Protein Sci*, 16(10):2272–7.

Hanks, S. and Hunter, T. (1995). Protein kinases 6. the eukaryotic protein kinase superfamily: kinase (catalytic) domain structure and classification. *FASEB J*, 9(8):576–596.

Hart, P. J., Deep, S., Taylor, A. B., Shu, Z., Hinck, C. S., and Hinck, A. P. (2002). Crystal structure of the human TbetaR2 ectodomain–TGF-beta3 complex. *Nat Struct Biol*, 9(3):203–208.

Hasham, S. N., Willing, M. C., Guo, D.-c., Muilenburg, A., He, R., Tran, V. T., Scherer, S. E., Shete, S. S., and Milewicz, D. M. (2003). Mapping a locus for familial thoracic aortic aneurysms and dissections (TAAD2) to 3p24-25. *Circulation*, 107(25):3184–3190.

Hautmann, M. B., Madsen, C. S., and Owens, G. K. (1997). A transforming growth factor beta (TGFbeta) control element drives TGFbeta-induced stimulation of smooth muscle alpha-actin gene expression in concert with two CArG elements. *J Biol Chem*, 272(16):10948–10956.

Hayashi, H., Abdollah, S., Qiu, Y., Cai, J., Xu, Y. Y., Grinnell, B. W., Richardson, M. A., Topper, J. N., Gimbrone, M. A., Wrana, J. L., and Falb, D. (1997). The MAD-related

protein Smad7 associates with the TGFbeta receptor and functions as an antagonist of TGFbeta signaling. *Cell*, 89(7):1165–1173.

Hayes, S., Chawla, A., and Corvera, S. (2002). TGFbeta receptor internalization into EEA1-enriched early endosomes: role in signaling to Smad2. *J Cell Biol*, 158(7):1239–1249.

Hinck, A. P., Archer, S. J., Qian, S. W., Roberts, A. B., Sporn, M. B., Weatherbee, J. A., Tsang, M. L., Lucas, R., Zhang, B. L., Wenker, J., and Torchia, D. A. (1996). Transforming growth factor beta 1: three-dimensional structure in solution and comparison with the X-ray structure of transforming growth factor beta 2. *Biochemistry*, 35(26):8517–8534.

Hirai, R. and Fijita, T. (1996). A human transforming growth factor-beta type II receptor that contains an insertion in the extracellular domain. *Exp Cell Res*, 223(1):135–141.

Hocevar, B. A., Smine, A., Xu, X. X., and Howe, P. H. (2001). The adaptor molecule Disabled-2 links the transforming growth factor beta receptors to the Smad pathway. *EMBO J*, 20(11):2789–2801.

Hoover, L. L. and Kubalak, S. W. (2008). Holding their own: The noncanonical roles of Smad proteins. *Sci Signal*, 1(46):pe48–pe48.

Horbelt, D., Guo, G., Robinson, P. N., and Knaus, P. (2010). Quantitative analysis of TGFBR2 mutations in Marfan syndrome related disorders suggests correlation between phenotypic severity and Smad signaling activity. *J Cell Sci*, accepted manuscript.

Huse, M., Chen, Y.-G., Massagué, J., and Kuriyan, J. (1999). Crystal structure of the cytoplasmic domain of the type I TGF beta receptor in complex with FKBP12. *Cell*, 96(3):425–436.

Huse, M., Muir, T. W., Xu, L., Chen, Y.-G., Kuriyan, J., and Massagué, J. (2001). The TGFbeta receptor activation process :: An inhibitor- to substrate-binding switch. *Mol Cell*, 8(3):671–682.

Ignotz, R. A. and Massagué, J. (1986). Transforming growth factor-beta stimulates the expression of fibronectin and collagen and their incorporation into the extracellular matrix. *J Biol Chem*, 261(9):4337–4345.

Inamoto, S., Kwartler, C. S., Lafont, A. L., Liang, Y. Y., Fadulu, V. T., Duraisamy, S., Willing, M., Estrera, A., Safi, H., Hannibal, M. C., Carey, J., Wiktorowicz, J., Tan, F. K., Feng, X.-H., Pannu, H., and Milewicz, D. M. (2010). TGFBR2 mutations alter smooth muscle cell phenotype and predispose to thoracic aortic aneurysms and dissections. *Cardiovasc Res*.

Inman, G. J., Nicolás, F. J., and Hill, C. S. (2002). Nucleocytoplasmic shuttling of Smads 2, 3, and 4 permits sensing of TGF-beta receptor activity. *Mol Cell*, 10(2):283–294.

Isogai, Z., Ono, R. N., Ushiro, S., Keene, D. R., Chen, Y., Mazzieri, R., Charbonneau, N. L., Reinhardt, D. P., Rifkin, D. B., and Sakai, L. Y. (2003). Latent transforming growth factor beta-binding protein 1 interacts with fibrillin and is a microfibril-associated protein. *J Biol Chem*, 278(4):2750–2757.

Itoh, F., Divecha, N., Brocks, L., Oomen, L., Janssen, H., Calafat, J., Itoh, S., and ten Dijke Pt, P. (2002). The FYVE domain in Smad anchor for receptor activation (SARA) is sufficient for localization of SARA in early endosomes and regulates TGF-beta/Smad signalling. *Genes Cells*, 7(3):321–331.

Itoh, S., Thorikay, M., Kowanetz, M., Moustakas, A., Itoh, F., Heldin, C.-H., and ten Dijke, P. (2003). Elucidation of Smad requirement in transforming growth factor-beta type I receptor-induced responses. *J Biol Chem*, 278(6):3751–3761.

Jones, D. T. (1999). Protein secondary structure prediction based on position-specific scoring matrices. *J Mol Biol*, 292(2):195–202.

Jones, J. A., Spinale, F. G., and Ikonomidis, J. S. (2008). Transforming growth factor-beta signaling in thoracic aortic aneurysm development: A paradox in pathogenesis. *J Vasc Res*, 46(2):119–137.

Judge, D. P. and Dietz, H. C. (2005). Marfan's syndrome. *Lancet*, 366(9501):1965–1976.

Kaartinen, V., Voncken, J. W., Shuler, C., Warburton, D., Bu, D., Heisterkamp, N., and Groffen, J. (1995). Abnormal lung development and cleft palate in mice lacking TGF-beta 3 indicates defects of epithelial-mesenchymal interaction. *Nat Genet*, 11(4):415–421.

Kähäri, V. M., Olsen, D. R., Rhudy, R. W., Carrillo, P., Chen, Y. Q., and Uitto, J. (1992). Transforming growth factor-beta up-regulates elastin gene expression in human skin fibroblasts. Evidence for post-transcriptional modulation. *Lab Invest*, 66(5):580–588.

Kang, J. S., Liu, C., and Derynck, R. (2009). New regulatory mechanisms of TGF-beta receptor function. *Trends Cell Biol*, 19(8):385–394.

Kang, Y., Chen, C.-R., and Massagué, J. (2003). A self-enabling TGFbeta response coupled to stress signaling: Smad engages stress response factor ATF3 for Id1 repression in epithelial cells. *Mol Cell*, 11(4):915–926.

Kavsak, P., Rasmussen, R. K., Causing, C. G., Bonni, S., Zhu, H., Thomsen, G. H., and Wrana, J. L. (2000). Smad7 binds to Smurf2 to form an E3 ubiquitin ligase that targets the TGF beta receptor for degradation. *Mol Cell*, 6(6):1365–1375.

Kim, E.-S., Kim, M.-S., and Moon, A. (2004). TGF-beta-induced upregulation of MMP-2 and MMP-9 depends on p38 MAPK, but not ERK signaling in MCF10A human breast epithelial cells. *Int J Oncol*, 25(5):1375–1382.

Klausner, R. D., Renswoude, J. V., Ashwell, G., Kempf, C., Schechter, A. N., Dean, A., and Bridges, K. R. (1983). Receptor-mediated endocytosis of transferrin in K562 cells. *J Biol Chem*, 258(8):4715–4724.

Knighton, D. R., Zheng, J. H., Eyck, L. F. T., Xuong, N. H., Taylor, S. S., and Sowadski, J. M. (1991). Structure of a peptide inhibitor bound to the catalytic subunit of cyclic adenosine monophosphate-dependent protein kinase. *Science (80-)*, 253(5018):414–420.

Koli, K. M. and Arteaga, C. L. (1997). Processing of the transforming growth factor beta type i and ii receptors. biosynthesis and ligand-induced regulation. *J Biol Chem*, 272(10):6423–6427.

Komuro, A., Imamura, T., Saitoh, M., Yoshida, Y., Yamori, T., Miyazono, K., and Miyazawa, K. (2004). Negative regulation of transforming growth factor-beta (TGF-beta) signaling by WW domain-containing protein 1 (WWP1). *Oncogene*, 23(41):6914–6923.

Kornev, A. P. and Taylor, S. S. (2010). Defining the conserved internal architecture of a protein kinase. *Biochim Biophys Acta*, 1804(3):440–444.

Kornev, A. P., Taylor, S. S., and Eyck, L. F. T. (2008). A helix scaffold for the assembly of active protein kinases. *Proc Natl Acad Sci U S A*, 105(38):14377–14382.

Krishnaveni, M. S., Hansen, J. L., Seeger, W., Morty, R. E., Sheikh, S. P., and Eickelberg, O. (2006). Constitutive homo- and hetero-oligomerization of TbetaRII-B, an alternatively spliced variant of the mouse TGF-beta type II receptor. *Biochem Biophys Res Commun*, 351(3):651–657.

Kucich, U., Rosenbloom, J. C., Abrams, W. R., and Rosenbloom, J. (2002). Transforming growth factor-beta stabilizes elastin mRNA by a pathway requiring active Smads, protein kinase C-delta, and p38. *Am J Respir Cell Mol Biol*, 26(2):183–188.

Kulkarni, A. B., Huh, C. G., Becker, D., Geiser, A., Lyght, M., Flanders, K. C., Roberts, A. B., Sporn, M. B., Ward, J. M., and Karlsson, S. (1993). Transforming growth factor beta 1 null mutation in mice causes excessive inflammatory response and early death. *Proc Natl Acad Sci U S A*, 90(2):770–774.

Kurisaki, A., Kose, S., Yoneda, Y., Heldin, C. H., and Moustakas, A. (2001). Transforming growth factor-beta induces nuclear import of Smad3 in an importin-beta1 and Ran-dependent manner. *Mol Biol Cell*, 12(4):1079–1091.

Kurisaki, A., Kurisaki, K., Kowanetz, M., Sugino, H., Yoneda, Y., Heldin, C.-H., and Moustakas, A. (2006). The mechanism of nuclear export of Smad3 involves exportin 4 and Ran. *Mol Cell Biol*, 26(4):1318–1332.

Kwak, H.-J., Park, M.-J., Cho, H., Park, C.-M., Moon, S.-I., Lee, H.-C., Park, I.-C., Kim, M.-S., Rhee, C. H., and Hong, S.-I. (2006). Transforming growth factor-beta1 induces tissue inhibitor of metalloproteinase-1 expression via activation of extracellular signal-regulated kinase and Sp1 in human fibrosarcoma cells. *Mol Cancer Res*, 4(3):209–220.

Laiho, M., Saksela, O., and Keski-Oja, J. (1986). Transforming growth factor beta alters plasminogen activator activity in human skin fibroblasts. *Exp Cell Res*, 164(2):399–407.

Lamouille, S. and Derynck, R. (2007). Cell size and invasion in TGF-beta-induced epithelial to mesenchymal transition is regulated by activation of the mTOR pathway. *J Cell Biol*, 178(3):437–451.

Larsson, J., Goumans, M. J., Sjöstrand, L. J., van Rooijen, M. A., Ward, D., Levéen, P., Xu, X., ten Dijke, P., Mummery, C. L., and Karlsson, S. (2001). Abnormal angiogenesis but intact hematopoietic potential in TGF-beta type I receptor-deficient mice. *EMBO J*, 20(7):1663–1673.

Law, C., Bunyan, D., Castle, B., Day, L., Simpson, I., Westwood, G., and Keeton, B. (2006). Clinical features in a family with an R460H mutation in transforming growth factor beta receptor 2 gene. *J Med Genet*, 43(12):908–916.

Lawler, S., Feng, X.-H., Chen, R.-H., Maruoka, E. M., Turck, C. W., Griswold-Prenner, I., and Derynck, R. (1997). The type II transforming growth factor-beta receptor autophosphorylates not only on serine and threonine but also on tyrosine residues. *J Biol Chem*, 272(23):14850–14859.

Lebrin, F., Goumans, M.-J., Jonker, L., Carvalho, R. L. C., Valdimarsdottir, G., Thorikay, M., Mummery, C., Arthur, H. M., and Dijke, P. t. (2004). Endoglin promotes endothelial cell proliferation and TGF-beta/ALK1 signal transduction. *EMBO J*, 23(20):4018–4028–4018–4028.

Lee, M. K., Pardoux, C., Hall, M. C., Lee, P. S., Warburton, D., Qing, J., Smith, S. M., and Derynck, R. (2007). TGF-beta activates Erk MAP kinase signalling through direct phosphorylation of ShcA. *EMBO J*, 26(17):3957–3967.

LeMaire, S. A., Pannu, H., Tran-Fadulu, V., Carter, S. A., Coselli, J. S., and Milewicz, D. M. (2007). Severe aortic and arterial aneurysms associated with a TGFBR2 mutation. *Nat Clin Pract Cardiovasc Med*, 4(3):167–171.

Lijnen, H. R. (2001). Plasmin and matrix metalloproteinases in vascular remodeling. *Thromb Haemost*, 86(1):324–333.

Lin, H. Y., Moustakas, A., Knaus, P., Wells, R. G., Henis, Y. I., and Lodish, H. F. (1995). The soluble exoplasmic domain of the type ii transforming growth factor (TGF)-beta receptor. a heterogeneously glycosylated protein with high affinity and selectivity for TGF-beta ligands. *J Biol Chem*, 270(6):2747–2754.

Lin, H. Y., Wang, X.-F., Ng-Eaton, E., Weinberg, R. A., and Lodish, H. F. (1992). Expression cloning of the TGF-beta type II receptor, a functional transmembrane serine/threonine kinase. *Cell*, 68(4):775–785.

Lin, X., Duan, X., Liang, Y.-Y., Su, Y., Wrighton, K. H., Long, J., Hu, M., C, Davis, i. M., Wang, J., Brunicardi, F. C., Shi, Y., Chen, Y.-G., Meng, A., and Feng, X.-H. (2006). PPM1A functions as a Smad phosphatase to terminate TGFbeta signaling. *Cell*, 125(5):915–928.

Lin, X., Liang, M., and Feng, X. H. (2000). Smurf2 is a ubiquitin E3 ligase mediating proteasome-dependent degradation of Smad2 in transforming growth factor-beta signaling. *J Biol Chem*, 275(47):36818–36822.

Lingwood, D. and Simons, K. (2010). Lipid rafts as a membrane-organizing principle. *Science (80-)*, 327(5961):46–50.

Liu, C., Xu, P., Lamouille, S., Xu, J., and Derynck, R. (2009). TACE-mediated ectodomain shedding of the type i TGF-beta receptor downregulates TGF-beta signaling. *Mol Cell*, 35(1):26–36.

Livak, K. J. and Schmittgen, T. D. (2001). Analysis of relative gene expression data using real-time quantitative PCR and the 2(-Delta Delta C(T)) method. *Methods*, 25(4):402–408.

Lo, R. S. and Massagué, J. (1999). Ubiquitin-dependent degradation of TGF-beta-activated Smad2. *Nat Cell Biol*, 1(8):472–478.

Loeys, B. L., Chen, J., Neptune, E. R., Judge, D. P., Podowski, M., Holm, T., Meyers, J., Leitch, C. C., Katsanis, N., Sharifi, N., Xu, F. L., Myers, L. A., Spevak, P. J., Cameron, D. E., Backer, J. D., Hellemans, J., Chen, Y., Davis, E. C., Webb, C. L., Kress, W., Coucke, P., Rifkin, D. B., De Paepe, A. M., and Dietz, H. C. (2005). A syndrome of altered cardiovascular, craniofacial, neurocognitive and skeletal development caused by mutations in TGFBR1 or TGFBR2. *Nat Genet*, 37(3):275–281.

Loeys, B. L., Schwarze, U., Holm, T., Callewaert, B. L., Thomas, G. H., Pannu, H., De Backer, J. F., Oswald, G. L., Symoens, S., Manouvrier, S., Roberts, A. E., Faravelli, F., Greco, M. A., Pyeritz, R. E., Milewicz, D. M., Coucke, P. J., Cameron, D. E., Braverman,

A. C., Byers, P. H., De Paepe, A. M., and Dietz, H. C. (2006). Aneurysm syndromes caused by mutations in the TGF-beta receptor. *N Engl J Med*, 355(8):788–798.

Lohse, M. J., Benovic, J. L., Codina, J., Caron, M. G., and Lefkowitz, R. J. (1990). beta-Arrestin: a protein that regulates beta-adrenergic receptor function. *Science (80-)*, 248(4962):1547–1550.

López-Casillas, F., Wrana, J. L., and Massagué, J. (1993). Betaglycan presents ligand to the TGF beta signaling receptor. *Cell*, 73(7):1435–1444.

Luo, K. and Lodish, H. F. (1997). Positive and negative regulation of type II TGF-beta receptor signal transduction by autophosphorylation on multiple serine residues. *EMBO J*, 16(8):1970–1981.

Luttrell, L. M. and Lefkowitz, R. J. (2002). The role of beta-arrestins in the termination and transduction of G-protein-coupled receptor signals. *J Cell Sci*, 115(Pt 3):455–465.

Lutz, M. (2002). *Effects of nerve growth factor on TGF-beta/Smad signal transduction in PC12 cells*. PhD thesis, Universtiät Würzburg.

Macia, E., Ehrlich, M., Massol, R., Boucrot, E., Brunner, C., and Kirchhausen, T. (2006). Dynasore, a cell-permeable inhibitor of dynamin. *Dev Cell*, 10(6):839–850.

Macías-Silva, M., Abdollah, S., Hoodless, P. A., Pirone, R., Attisano, L., and Wrana, J. L. (1996). MADR2 is a substrate of the TGFbeta receptor and its phosphorylation is required for nuclear accumulation and signaling. *Cell*, 87(7):1215–1224.

Madhusudan, Trafny, E. A., Xuong, N. H., Adams, J. A., Eyck, L. F. T., Taylor, S. S., and Sowadski, J. M. (1994). cAMP-dependent protein kinase: crystallographic insights into substrate recognition and phosphotransfer. *Protein Sci*, 3(2):176–187.

Marfan, A. B. (1896). Un cas de deformation congenitale des quarte membres plus prononcee aux extremites caracterisee par l´allongement des os avec un certain degre d´amincissement. *Bull Mem Soc Med Hop*, 13:220–226.

Massagué, J. and Gomis, R. R. (2006). The logic of TGFbeta signaling. *FEBS Lett*, 580(12):2811–2820.

Massagué, J. and Kelly, B. (1986). Internalization of transforming growth factor-beta and its receptor in BALB/c 3T3 fibroblasts. *J Cell Physiol*, 128(2):216–222.

Mátyás, G., Arnold, E., Carrel, T., Baumgartner, D., Boileau, C., Berger, W., and Steinmann, B. (2006). Identification and in silico analyses of novel TGFBR1 and TGFBR2 mutations in Marfan syndrome-related disorders. *Hum Mutat*, 27(8):760–769.

McDonald, P. H. and Lefkowitz, R. J. (2001). Beta-Arrestins: new roles in regulating heptahelical receptors' functions. *Cell Signal*, 13(10):683–689.

Milewicz, D. M., Guo, D.-C., Tran-Fadulu, V., Lafont, A. L., Papke, C. L., Inamoto, S., Kwartler, C. S., and Pannu, H. (2008). Genetic basis of thoracic aortic aneurysms and dissections: focus on smooth muscle cell contractile dysfunction. *Annu Rev Genomics Hum Genet*, 9:283–302.

Mitchell, H., Choudhury, A., Pagano, R. E., and Leof, E. B. (2004). Ligand-dependent and -independent transforming growth factor-beta receptor recycling regulated by clathrin-mediated endocytosis and Rab11. *Mol Biol Cell*, 15(9):4166–4178.

Mittl, P. R., Priestle, J. P., Cox, D. A., McMaster, G., Cerletti, N., and Grütter, M. G. (1996). The crystal structure of TGF-beta 3 and comparison to TGF-beta 2: implications for receptor binding. *Protein Sci*, 5(7):1261–1271.

Miyazawa, K., Shinozaki, M., Hara, T., Furuya, T., and Miyazono, K. (2002). Two major Smad pathways in TGF-beta superfamily signalling. *Genes Cells*, 7(12):1191–1204.

Mizuguchi, T., Collod-Béroud, G., Akiyama, T., Abifadel, M., Harada, N., Morisaki, T., Allard, D., Varret, M., Claustres, M., Morisaki, H., Ihara, M., Kinoshita, A., Yoshiura, K.-i., Junien, C., Kajii, T., Jondeau, G., Ohta, T., Kishino, T., Furukawa, Y., Nakamura, Y., Niikawa, N., Boileau, C., and Matsumoto, N. (2004). Heterozygous TGFBR2 mutations in marfan syndrome. *Nat Genet*, 36(8):855–860.

Moussad, E. E. and Brigstock, D. R. (2000). Connective tissue growth factor: what's in a name? *Mol Genet Metab*, 71(1-2):276–292.

Moustakas, A. and Heldin, C.-H. (2005). Non-Smad TGF-beta signals. *J Cell Sci*, 118(16):3573–3584.

Moustakas, A. and Heldin, C.-H. (2009). The regulation of TGFbeta signal transduction. *Development*, 136(22):3699–3714.

Nakao, A., Afrakhte, M., Morén, A., Nakayama, T., Christian, J. L., Heuchel, R., Itoh, S., Kawabata, M., Heldin, N. E., Heldin, C. H., and ten Dijke, P. (1997). Identification of Smad7, a TGFbeta-inducible antagonist of TGF-beta signalling. *Nature*, 389(6651):631–635.

Neptune, E. R., Frischmeyer, P. A., Arking, D. E., Myers, L., Bunton, T. E., Gayraud, B., Ramirez, F., Sakai, L. Y., and Dietz, H. C. (2003). Dysregulation of TGF-beta activation contributes to pathogenesis in Marfan syndrome. *Nat Genet*, 33(3):407–411.

Nickel, J., Sebald, W., Groppe, J. C., and Mueller, T. D. (2009). Intricacies of BMP receptor assembly. *Cytokine Growth Factor Rev*, 20(5-6):367–377.

Nunes, I., Gleizes, P. E., Metz, C. N., and Rifkin, D. B. (1997). Latent transforming growth factor-beta binding protein domains involved in activation and transglutaminase-dependent cross-linking of latent transforming growth factor-beta. *J Cell Biol*, 136(5):1151–1163.

Oshima, M., Oshima, H., and Taketo, M. M. (1996). TGF-beta receptor type II deficiency results in defects of yolk sac hematopoiesis and vasculogenesis. *Dev Biol*, 179(1):297–302.

Owens, G. K., Geisterfer, A. A., Yang, Y. W., and Komoriya, A. (1988). Transforming growth factor-beta-induced growth inhibition and cellular hypertrophy in cultured vascular smooth muscle cells. *J Cell Biol*, 107(2):771–780.

Owens, G. K., Kumar, M. S., and Wamhoff, B. R. (2004). Molecular regulation of vascular smooth muscle cell differentiation in development and disease. *Physiol Rev*, 84(3):767–801.

Padua, D. and Massagué, J. (2009). Roles of TGFbeta in metastasis. *Cell Res*, 19(1):89–102.

Paepe, A. D., Devereux, R. B., Dietz, H. C., Hennekam, R. C., and Pyeritz, R. E. (1996). Revised diagnostic criteria for the Marfan syndrome. *Am J Med Genet*, 62(4):417–426.

Pannu, H., Fadulu, V. T., Chang, J., Lafont, A., Hasham, S. N., Sparks, E., Giampietro, P. F., Zaleski, C., Estrera, A. L., Safi, H. J., Shete, S., Willing, M. C., Raman, C., and Milewicz, D. M. (2005). Mutations in transforming growth factor-beta receptor type II cause familial thoracic aortic aneurysms and dissections. *Circulation*, 112(4):513–520.

Pardali, E., Goumans, M.-J., and Dijke, P. T. (2010). Signaling by members of the TGF-beta family in vascular morphogenesis and disease. *Trends Cell Biol*.

Parker, W. L., Finnson, K. W., Soe-Lin, H., Knaus, P., and Philip, A. (2007). Expression and function of TbetaRII-B, a variant of the type II TGF-beta receptor, in human chondrocytes. *Osteoarthritis Cartilage*, 15(4):442–453.

Pelham, H. R. (1989). Control of protein exit from the endoplasmic reticulum. *Annu Rev Cell Biol*, 5:1–23.

Penheiter, S. G., Mitchell, H., Garamszegi, N., Edens, M., Doré, J. J. E., and Leof, E. B. (2002). Internalization-dependent and -independent requirements for transforming growth factor beta receptor signaling via the Smad pathway. *Mol Cell Biol*, 22(13):4750–4759.

Pepin, M. C., Beauchemin, M., Plamondon, J., and O'Connor-McCourt, M. D. (1996). Scanning-deletion analysis of the extracellular domain of the TGF-beta receptor type II. *Biochem Biophys Res Commun*, 220(2):289–293.

Pereira, L., Andrikopoulos, K., Tian, J., Lee, S. Y., Keene, D. R., Ono, R., Reinhardt, D. P., Sakai, L. Y., Biery, N. J., Bunton, T., Dietz, H. C., and Ramirez, F. (1997). Targetting of the gene encoding fibrillin-1 recapitulates the vascular aspect of marfan syndrome. *Nat Genet*, 17(2):218–222.

Pfaffl, M. W. (2001). A new mathematical model for relative quantification in real-time RT-PCR. *Nucleic Acids Res*, 29(9):e45–e45.

Pierreux, C. E., Nicolás, F. J., and Hill, C. S. (2000). Transforming growth factor beta-independent shuttling of Smad4 between the cytoplasm and nucleus. *Mol Cell Biol*, 20(23):9041–9054.

Pitcher, J. A., Freedman, N. J., and Lefkowitz, R. J. (1998). G protein-coupled receptor kinases. *Annu Rev Biochem*, 67:653–692.

Proetzel, G., Pawlowski, S. A., Wiles, M. V., Yin, M., Boivin, G. P., Howles, P. N., Ding, J., Ferguson, M. W., and Doetschman, T. (1995). Transforming growth factor-beta 3 is required for secondary palate fusion. *Nat Genet*, 11(4):409–414.

Qiu, T., Wu, X., Zhang, F., Clemens, T. L., Wan, M., and Cao, X. (2010). TGF-beta type II receptor phosphorylates PTH receptor to integrate bone remodelling signalling. *Nat Cell Biol*, 12(3):224–234.

Radaev, S., Zou, Z., Huang, T., Lafer, E. M., Hinck, A. P., and Sun, P. D. (2010). Ternary complex of transforming growth factor-beta1 reveals isoform-specific ligand recognition and receptor recruitment in the superfamily. *J Biol Chem*, 285(19):14806–14814.

Ramirez, F. and Dietz, H. C. (2007). Fibrillin-rich microfibrils: Structural determinants of morphogenetic and homeostatic events. *J Cell Physiol*, 213(2):326–330.

Ramirez, F. and Dietz, H. C. (2009). Extracellular microfibrils in vertebrate development and disease processes. *J Biol Chem*, 284(22):14677–14681.

Ramos-DeSimone, N., Hahn-Dantona, E., Sipley, J., Nagase, H., French, D. L., and Quigley, J. P. (1999). Activation of matrix metalloproteinase-9 (MMP-9) via a converging plasmin/stromelysin-1 cascade enhances tumor cell invasion. *J Biol Chem*, 274(19):13066–13076.

Razani, B., Zhang, X. L., Bitzer, M., von Gersdorff, G., Böttinger, E. P., and Lisanti, M. P. (2001). Caveolin-1 regulates transforming growth factor (TGF)-beta/SMAD signaling through an interaction with the TGF-beta type I receptor. *J Biol Chem*, 276(9):6727–6738.

Rechtman, M. M., Nakaryakov, A., Shapira, K. E., Ehrlich, M., and Henis, Y. I. (2009). Different domains regulate homomeric and heteromeric complex formation among type I and type II transforming growth factor-beta receptors. *J Biol Chem*, 284(12):7843–7852.

Remy, I., Montmarquette, A., and Michnick, S. W. (2004). PKB/Akt modulates TGF-beta signalling through a direct interaction with Smad3. *Nat Cell Biol*, 6(4):358–365.

Rensen, S. S. M., Doevendans, P. A. F. M., and van Eys, G. J. J. M. (2007). Regulation and characteristics of vascular smooth muscle cell phenotypic diversity. *Neth Heart J*, 15(3):100–108.

Robinson, P. N., Arteaga-Solis, E., Baldock, C., Collod-Beroud, G., Booms, P., De Paepe, A., Dietz, H. C., Guo, G., Handford, P. A., Judge, D. P., Kielty, C. M., Loeys, B., Milewicz, D. M., Ney, A., Ramirez, F., Reinhardt, D. P., Tiedemann, K., Whiteman, P., and Godfrey, M. (2006). The molecular genetics of Marfan syndrome and related disorders. *J Med Genet*, 43(10):769–787.

Rodriguez, C., Chen, F., Weinberg, R. A., and Lodish, H. F. (1995). Cooperative binding of transforming growth factor (TGF)-beta 2 to the types I and II TGF-beta receptors. *J Biol Chem*, 270(27):15919–15922.

Rodríguez-Vita, J., Sánchez-López, E., Esteban, V., Rupérez, M., Egido, J., and Ruiz-Ortega, M. (2005). Angiotensin II activates the Smad pathway in vascular smooth muscle cells by a transforming growth factor-beta-independent mechanism. *Circulation*, 111(19):2509–2517.

Ross, S. and Hill, C. S. (2008). How the Smads regulate transcription. *Int J Biochem Cell Biol*, 40(3):383–408.

Rossi, P., Karsenty, G., Roberts, A. B., Roche, N. S., Sporn, M. B., and de Crombrugghe, B. (1988). A nuclear factor 1 binding site mediates the transcriptional activation of a type I collagen promoter by transforming growth factor-beta. *Cell*, 52(3):405–414.

Rossignol, P., Luttun, A., Martin-Ventura, J. L., Lupu, F., Carmeliet, P., Collen, D., Anglès-Cano, E., and Lijnen, H. R. (2006). Plasminogen activation: a mediator of vascular smooth muscle cell apoptosis in atherosclerotic plaques. *J Thromb Haemost*, 4(3):664–670.

Rost, B., Yachdav, G., and Liu, J. (2004). The predictprotein server. *Nucleic Acids Res*, 32(Web Server issue):W321–W326.

Rotzer, D., Roth, M., Lutz, M., Lindemann, D., Sebald, W., and Knaus, P. (2001). Type III TGF-beta receptor-independent signalling of TGF-beta2 via TbetaRII-B, an alternatively spliced TGF-beta type II receptor. *EMBO J*, 20(3):480–490.

Roy, C. L. and Wrana, J. L. (2005). Clathrin- and non-clathrin-mediated endocytic regulation of cell signalling. *Nat Rev Mol Cell Biol*, 6(2):112–126.

Runyan, C. E., Schnaper, H. W., and Poncelet, A.-C. (2005). The role of internalization in transforming growth factor beta1-induced Smad2 association with Smad anchor for receptor activation (SARA) and Smad2-dependent signaling in human mesangial cells. *J Biol Chem*, 280(9):8300–8308.

Saharinen, J., Taipale, J., and Keski-Oja, J. (1996). Association of the small latent transforming growth factor-beta with an eight cysteine repeat of its binding protein LTBP-1. *EMBO J*, 15(2):245–253.

Sambrook, J. (2001). *Molecular Cloning: A Laboratory Manual, Third Edition*. Cold Spring Harbor Laboratory Press.

Sanford, L. P., Ormsby, I., de Groot, A. C. G., Sariola, H., Friedman, R., Boivin, G. P., Cardell, E. L., and Doetschman, T. (1997). TGFbeta2 knockout mice have multiple developmental defects that are non-overlapping with other TGFbeta knockout phenotypes. *Development*, 124(13):2659–2670.

Scheich, F. (2003). Untersuchung zur Expression und Signaltransduktion des TGFß typ IIB-Rezeptors. Master's thesis, Universität Würzburg.

Schlunegger, M. P. and Grütter, M. G. (1992). An unusual feature revealed by the crystal structure at 2.2 A resolution of human transforming growth factor-beta 2. *Nature*, 358(6385):430–434.

Schmidt, S. (2007). Einfluss des Transforming Growth Factor-beta Receptor type II assoziierten Proteins Fas-associated Factor 1 auf die kontextspezifische Signaltransduktion von TGF-beta. Master's thesis, Freie Universität Berlin.

Schmierer, B. and Hill, C. S. (2005). Kinetic analysis of Smad nucleocytoplasmic shuttling reveals a mechanism for transforming growth factor beta-dependent nuclear accumulation of Smads. *Mol Cell Biol*, 25(22):9845–9858.

Schmierer, B. and Hill, C. S. (2007). TGFbeta-SMAD signal transduction: molecular specificity and functional flexibility. *Nat Rev Mol Cell Biol*, 8(12):970–982.

Schmierer, B., Tournier, A. L., Bates, P. A., and Hill, C. S. (2008). Mathematical modeling identifies Smad nucleocytoplasmic shuttling as a dynamic signal-interpreting system. *Proc Natl Acad Sci U S A*, 105(18):6608–6613.

Schwede, T., Kopp, J., Guex, N., and Peitsch, M. C. (2003). SWISS-MODEL: An automated protein homology-modeling server. *Nucleic Acids Res*, 31(13):3381–3385.

Seay, U., Sedding, D., Krick, S., Hecker, M., Seeger, W., and Eickelberg, O. (2005). Transforming growth factor-beta-dependent growth inhibition in primary vascular smooth muscle cells is p38-dependent. *J Pharmacol Exp Ther*, 315(3):1005–1012.

Sengle, G., Charbonneau, N. L., Ono, R. N., Sasaki, T., Alvarez, J., Keene, D. R., Bächinger, H. P., and Sakai, L. Y. (2008). Targeting of bone morphogenetic protein growth factor complexes to fibrillin. *J Biol Chem*, 283(20):13874–13888.

Seo, S. R., Lallemand, F., Ferrand, N., Pessah, M., L'Hoste, S., Camonis, J., and Atfi, A. (2004). The novel E3 ubiquitin ligase Tiul1 associates with TGIF to target Smad2 for degradation. *EMBO J*, 23(19):3780–3792.

Shapiro, H. M. (1995). *Practical flow cytometry*. John Wiley and Sons.

Sheppard, D. (2005). Integrin-mediated activation of latent transforming growth factor beta. *Cancer Metastasis Rev*, 24(3):395–402.

Shi, Y. and Massagué, J. (2003). Mechanisms of TGF-beta signaling from cell membrane to the nucleus. *Cell*, 113(6):685–700.

Shim, J.-H., Xiao, C., Paschal, A. E., Bailey, S. T., Rao, P., Hayden, M. S., Lee, K.-Y., Bussey, C., Steckel, M., Tanaka, N., Yamada, G., Akira, S., Matsumoto, K., and Ghosh, S. (2005). TAK1, but not TAB1 or TAB2, plays an essential role in multiple signaling pathways in vivo. *Genes Dev*, 19(22):2668–2681.

Shull, M. M., Ormsby, I., Kier, A. B., Pawlowski, S., Diebold, R. J., Yin, M., Allen, R., Sidman, C., Proetzel, G., and Calvin, D. (1992). Targeted disruption of the mouse transforming growth factor-beta 1 gene results in multifocal inflammatory disease. *Nature*, 359(6397):693–699.

Siegel, P. M. and Massagué, J. (2003). Cytostatic and apoptotic actions of TGF-beta in homeostasis and cancer. *Nat Rev Cancer*, 3(11):807–821.

Sigismund, S., Argenzio, E., Tosoni, D., Cavallaro, E., Polo, S., and Fiore, P. P. D. (2008). Clathrin-mediated internalization is essential for sustained EGFR signaling but dispensable for degradation. *Dev Cell*, 15(2):209–219.

Simon, P. (2003). Q-gene: processing quantitative real-time RT-PCR data. *Bioinformatics*, 19(11):1439–1440.

Simonsson, M., Kanduri, M., Grönroos, E., Heldin, C.-H., and Ericsson, J. (2006). The DNA binding activities of Smad2 and Smad3 are regulated by coactivator-mediated acetylation. *J Biol Chem*, 281(52):39870–39880.

Singh, K. K., Rommel, K., Mishra, A., Karck, M., Haverich, A., Schmidtke, J., and Arslan-Kirchner, M. (2006). TGFBR1 and TGFBR2 mutations in patients with features of Marfan syndrome and Loeys-Dietz syndrome. *Hum Mutat*, 27(8):770–777.

Sinha, S., Hoofnagle, M. H., Kingston, P. A., McCanna, M. E., and Owens, G. K. (2004). Transforming growth factor-beta1 signaling contributes to development of smooth muscle cells from embryonic stem cells. *Am J Physiol Cell Physiol*, 287(6):C1560–C1568.

Sirard, C., Kim, S., Mirtsos, C., Tadich, P., Hoodless, P. A., Itié, A., Maxson, R., Wrana, J. L., and Mak, T. W. (2000). Targeted disruption in murine cells reveals variable requirement for Smad4 in transforming growth factor beta-related signaling. *J Biol Chem*, 275(3):2063–2070.

Song, B., Estrada, K. D., and Lyons, K. M. (2009). Smad signaling in skeletal development and regeneration. *Cytokine Growth Factor Rev*, 20(5-6):379–388.

Sorrentino, A., Thakur, N., Grimsby, S., Marcusson, A., von Bulow, V., Schuster, N., Zhang, S., Heldin, C.-H., and Landström, M. (2008). The type I TGF-beta receptor engages TRAF6 to activate TAK1 in a receptor kinase-independent manner. *Nat Cell Biol*, 10(10):1199–1207.

Souchelnytskyi, S., Dijke, P. t., Miyazono, K., and Heldin, C. H. (1996). Phosphorylation of ser165 in TGF-beta type i receptor modulates TGF-beta1-induced cellular responses. *EMBO J*, 15(22):6231–6240–6231–6240.

Sun, P. D. and Davies, D. R. (1995). The cystine-knot growth-factor superfamily. *Annu Rev Biophys Biomol Struct*, 24:269–291.

Suzuki, A., Shioda, N., Maeda, T., Tada, M., and Ueno, N. (1994). Cloning of an isoform of mouse TGF-beta type II receptor gene. *FEBS Lett*, 355(1):19–22.

Takekawa, M., Tatebayashi, K., Itoh, F., Adachi, M., Imai, K., and Saito, H. (2002). Smad-dependent GADD45beta expression mediates delayed activation of p38 MAP kinase by TGF-beta. *EMBO J*, 21(23):6473–6482.

ten Dijke, P. and Arthur, H. M. (2007). Extracellular control of TGFbeta signalling in vascular development and disease. *Nat Rev Mol Cell Biol*, 8(11):857–869.

Thompson, R. W., Geraghty, P. J., and Lee, J. K. (2002). Abdominal aortic aneurysms: basic mechanisms and clinical implications. *Curr Probl Surg*, 39(2):110–230.

Tsukazaki, T., Chiang, T. A., Davison, A. F., Attisano, L., and Wrana, J. L. (1998). SARA, a FYVE domain protein that recruits Smad2 to the TGFbeta receptor. *Cell*, 95(6):779–791.

Tu, A. W. and Luo, K. (2007). Acetylation of Smad2 by the co-activator p300 regulates activin and transforming growth factor beta response. *J Biol Chem*, 282(29):21187–21196.

Ubersax, J. A. and Ferrell Jr, J. E. (2007). Mechanisms of specificity in protein phosphorylation. *Nat Rev Mol Cell Biol*, 8(7):530–541.

Urness, L. D., Sorensen, L. K., and Li, D. Y. (2000). Arteriovenous malformations in mice lacking activin receptor-like kinase-1. *Nat Genet*, 26(3):328–331.

Varelas, X., Sakuma, R., Samavarchi-Tehrani, P., Peerani, R., Rao, B. M., Dembowy, J., Yaffe, M. B., Zandstra, P. W., and Wrana, J. L. (2008). TAZ controls Smad nucleocytoplasmic shuttling and regulates human embryonic stem-cell self-renewal. *Nat Cell Biol*, 10(7):837–848.

Varga, J. and Jimenez, S. A. (1986). Stimulation of normal human fibroblast collagen production and processing by transforming growth factor-beta. *Biochem Biophys Res Commun*, 138(2):974–980.

Verrecchia, F. and Mauviel, A. (2002). Transforming growth factor-beta signaling through the Smad pathway: role in extracellular matrix gene expression and regulation. *J Invest Dermatol*, 118(2):211–215.

Verrecchia, F. and Mauviel, A. (2007). Transforming growth factor-beta and fibrosis. *World J Gastroenterol*, 13(22):3056–3062.

Vieira, A. V., Lamaze, C., and Schmid, S. L. (1996). Control of EGF receptor signaling by clathrin-mediated endocytosis. *Science (80-)*, 274(5295):2086–2089.

Vilar, J. M. G., Jansen, R., and Sander, C. (2006). Signal processing in the TGF-beta superfamily ligand-receptor network. *PLoS Comput Biol*, 2(1):e3–e3.

Wang, Q., Villeneuve, G., and Wang, Z. (2005). Control of epidermal growth factor receptor endocytosis by receptor dimerization, rather than receptor kinase activation. *EMBO Rep*, 6(10):942–948.

Watanabe, M., Masuyama, N., Fukuda, M., and Nishida, E. (2000). Regulation of intracellular dynamics of Smad4 by its leucine-rich nuclear export signal. *EMBO Rep*, 1(2):176–182.

Watkins, S. J., Jonker, L., and Arthur, H. M. (2006). A direct interaction between TGFbeta activated kinase 1 and the TGFbeta type II receptor: implications for TGFbeta signalling and cardiac hypertrophy. *Cardiovasc Res*, 69(2):432–439.

Weber, D., Kotzsch, A., Nickel, J., Harth, S., Seher, A., Mueller, U., Sebald, W., and Mueller, T. D. (2007). A silent H-bond can be mutationally activated for high-affinity interaction of BMP-2 and activin type IIB receptor. *BMC Struct Biol*, 7:6.

Wells, R. G., Gilboa, L., Sun, Y., Liu, X., Henis, Y. I., and Lodish, H. F. (1999). Transforming growth factor-beta induces formation of a dithiothreitol-resistant type I/type II receptor complex in live cells. *J Biol Chem*, 274(9):5716–5722.

Wells, R. G., Yankelev, H., Lin, H. Y., and Lodish, H. F. (1997). Biosynthesis of the type I and type II TGF-beta receptors. Implications for complex formation. *J Biol Chem*, 272(17):11444–11451.

Wenzel, S., Taimor, G., Piper, H. M., and Schlüter, K. D. (2001). Redox-sensitive intermediates mediate angiotensin ii-induced p38 MAP kinase activation, AP-1 binding activity, and TGF-beta expression in adult ventricular cardiomyocytes. *FASEB J*, 15(12):2291–2293.

Wersto, R. P., Chrest, F. J., Leary, J. F., Morris, C., Stetler-Stevenson, M. A., and Gabrielson, E. (2001). Doublet discrimination in DNA cell-cycle analysis. *Cytometry*, 46(5):296–306.

Wieser, R., Attisano, L., Wrana, J. L., and Massagué, J. (1993). Signaling activity of transforming growth factor beta type II receptors lacking specific domains in the cytoplasmic region. *Mol Cell Biol*, 13(12):7239–7247.

Wilkes, M. C., Mitchell, H., Penheiter, S. G., Doré, J. J., Suzuki, K., Edens, M., Sharma, D. K., Pagano, R. E., and Leof, E. B. (2005). Transforming growth factor-beta activation of phosphatidylinositol 3-kinase is independent of Smad2 and Smad3 and regulates fibroblast responses via p21-activated kinase-2. *Cancer Res*, 65(22):10431–10440.

Wittek, B. (2003). Charakterisierung poly- und monoklonaler Antikörper gegen den TGF-ß rezeptor TßRIIB. Master's thesis, Universität Würzburg.

Wrana, J. L., Attisano, L., Cárcamo, J., Zentella, A., Doody, J., Laiho, M., Wang, X. F., and Massagué, J. (1992). TGF beta signals through a heteromeric protein kinase receptor complex. *Cell*, 71(6):1003–1014.

Wrana, J. L., Attisano, L., Wieser, R., Ventura, F., and Massagué, J. (1994). Mechanism of activation of the TGF-beta receptor. *Nature*, 370(6488):341–347.

Wrighton, K. H. and Feng, X.-H. (2008). To (TGF)beta or not to (TGF)beta: Fine-tuning of Smad signaling via post-translational modifications. *Cell Signal*, 20(9):1579–1591.

Wrighton, K. H., Lin, X., and Feng, X.-H. (2009a). Phospho-control of TGF-beta superfamily signaling. *Cell Res*, 19(1):8–20.

Wrighton, K. H., Lin, X., Yu, P. B., and Feng, X.-H. (2009b). Transforming growth factor beta can stimulate Smad1 phosphorylation independently of bone morphogenic protein receptors. *J Biol Chem*, 284(15):9755–9763.

Wu, G., Chen, Y. G., Ozdamar, B., Gyuricza, C. A., Chong, P. A., Wrana, J. L., Massagué, J., and Shi, Y. (2000). Structural basis of Smad2 recognition by the Smad anchor for receptor activation. *Science (80-)*, 287(5450):92–97.

Wu, J. W., Hu, M., Chai, J., Seoane, J., Huse, M., Li, C., Rigotti, D. J., Kyin, S., Muir, T. W., Fairman, R., Massagué, J., and Shi, Y. (2001). Crystal structure of a phosphorylated Smad2. recognition of phosphoserine by the MH2 domain and insights on smad function in TGF-beta signaling. *Mol Cell*, 8(6):1277–1289.

Wu, M. Y. and Hill, C. S. (2009). TGF-beta superfamily signaling in embryonic development and homeostasis. *Dev Cell*, 16(3):329–343.

Xiao, Z., Latek, R., and Lodish, H. F. (2003). An extended bipartite nuclear localization signal in Smad4 is required for its nuclear import and transcriptional activity. *Oncogene*, 22(7):1057–1069.

Xiao, Z., Liu, X., Henis, Y. I., and Lodish, H. F. (2000a). A distinct nuclear localization signal in the N terminus of Smad 3 determines its ligand-induced nuclear translocation. *Proc Natl Acad Sci U S A*, 97(14):7853–7858.

Xiao, Z., Liu, X., and Lodish, H. F. (2000b). Importin beta mediates nuclear translocation of Smad 3. *J Biol Chem*, 275(31):23425–23428.

Xu, L., Alarcón, C., Cöl, S., and Massagué, J. (2003). Distinct domain utilization by Smad3 and Smad4 for nucleoporin interaction and nuclear import. *J Biol Chem*, 278(43):42569–42577.

Xu, L., Kang, Y., Cöl, S., and Massagué, J. (2002). Smad2 nucleocytoplasmic shuttling by nucleoporins CAN/Nup214 and Nup153 feeds TGFbeta signaling complexes in the cytoplasm and nucleus. *Mol Cell*, 10(2):271–282.

Yamashita, M., Fatyol, K., Jin, C., Wang, X., Liu, Z., and Zhang, Y. E. (2008). TRAF6 mediates Smad-independent activation of JNK and p38 by TGF-beta. *Mol Cell*, 31(6):918–924.

Yan, C. and Boyd, D. D. (2007). Regulation of matrix metalloproteinase gene expression. *J Cell Physiol*, 211(1):19–26.

Yang, Z., Eton, D., Zheng, F., Livingstone, A. S., and Yu, H. (2005). Effect of tissue plasminogen activator on vascular smooth muscle cells. *J Vasc Surg*, 42(3):532–538.

Yao, D., Ehrlich, M., Henis, Y. I., and Leof, E. B. (2002). Transforming growth factor-beta receptors interact with AP2 by direct binding to beta2 subunit. *Mol Biol Cell*, 13(11):4001–4012.

Yi, J. Y., Shin, I., and Arteaga, C. L. (2005). Type I transforming growth factor beta receptor binds to and activates phosphatidylinositol 3-kinase. *J Biol Chem*, 280(11):10870–10876.

Yin, S., Ding, F., and Dokholyan, N. V. (2007). Eris: an automated estimator of protein stability. *Nat Methods*, 4(6):466–467.

Yoshimura, A., D'Andrea, A. D., and Lodish, H. F. (1990). Friend spleen focus-forming virus glycoprotein gp55 interacts with the erythropoietin receptor in the endoplasmic reticulum and affects receptor metabolism. *Proc Natl Acad Sci U S A*, 87(11):4139–4143.

Yu, L., Hébert, M. C., and Zhang, Y. E. (2002). TGF-beta receptor-activated p38 MAP kinase mediates smad-independent TGF-beta responses. *EMBO J*, 21(14):3749–3759.

Zelman-Femiak, M., Wang, K., Gromova, K., Knaus, P., and Harms, G. (2010). Covalent quantum dot receptor linkage via the acyl carrier protein for single-molecule tracking, internalization, and trafficking studies. *Biotechniques*, 49(2):574–579.

Zhang, Y., Chang, C., Gehling, D. J., Hemmati-Brivanlou, A., and Derynck, R. (2001). Regulation of smad degradation and activity by Smurf2, an E3 ubiquitin ligase. *Proc Natl Acad Sci U S A*, 98(3):974–979.

Zhang, Y. E. (2009). Non-Smad pathways in TGF-beta signaling. *Cell Res*, 19(1):128–139.

Zhou, Y., Poczatek, M. H., Berecek, K. H., and Murphy-Ullrich, J. E. (2006). Thrombospondin 1 mediates angiotensin II induction of TGF-beta activation by cardiac and renal cells under both high and low glucose conditions. *Biochem Biophys Res Commun*, 339(2):633–641.

Zhou, Y., Scolavino, S., Funderburk, S. F., Ficociello, L. F., Zhang, X., and Klibanski, A. (2004). Receptor internalization-independent activation of Smad2 in activin signaling. *Mol Endocrinol*, 18(7):1818–1826.

Zhu, H., Kavsak, P., Abdollah, S., Wrana, J. L., and Thomsen, G. H. (1999). A SMAD ubiquitin ligase targets the BMP pathway and affects embryonic pattern formation. *Nature*, 400(6745):687–693.

Zi, Z. and Klipp, E. (2007). Constraint-based modeling and kinetic analysis of the Smad dependent TGF-beta signaling pathway. *PLoS ONE*, 2(9):e936–e936.

Zúñiga, J. E., Groppe, J. C., Cui, Y., Hinck, C. S., Contreras-Shannon, V., Pakhomova, O. N., Yang, J., Tang, Y., Mendoza, V., López-Casillas, F., Sun, L., and Hinck, A. P. (2005). Assembly of TbetaRI:TbetaRII:TGFbeta ternary complex in vitro with receptor extracellular domains is cooperative and isoform-dependent. *J Mol Biol*, 354(5):1052–1068.

Abbreviations

APS - Ammonium persulfate
ATP - Adenosine triphosphate
BSA - Bovine serum albumin
cDNA - complementary DNA
DEPC - Diethylpyrocarbonate
dH_2O - desalted water
DMEM - Dulbecco's modified Eagle's medium
DNA - Deoxyribonucleic acid
DNase - Deoxyribonuclease
dNTPs - Deoxyribonucleotide triphoshate mix
ECD - Extracellular domain
EDTA - Ethylenediaminetetraacetic acid
ELISA - Enzyme-linked immunosorbent assay
EMEM - Eagle's minimal essential medium
FCS - Fetal calf serum
FS - Forward scatter
g - G-force
GAPDH - Glyceraldehyde 3-phosphate dehydrogenase
GTP - Guanosine triphosphate
h - Hours
HEPES - 4-(2-hydroxyethyl)-1-piperazineethanesulfonic acid
HRP - Horseraddish peroxidase
kDa - Kilodalton
mAb - Monoclonal antibody
MAPK - Mitogen-activated protein kinase
MAPKK - MAPK kinase
MAPKKK- MAPKK kinase
MeOH - Methanol
min - Minutes
MMLV - Moloney murine leukemia virus
MP-H_2O - Millipore-purified water
mRNA - messenger RNA

NV - [any DNA base][any DNA base but thymidine]
pAb - Polyclonal antibody
PBS - Phosphate-buffered saline
PBS-T - PBS-Tween20
PCR - Polymerase chain reaction
PI - Propidium iodide
PMSF - phenylmethylsulfonyl fluoride
PVDF - Polyvinylidene fluoride
qPCR - Quantitative PCR
RNA - Ribonucleic acid
RNase - Ribonuclease
RPMI - Roswell Park Memorial Institute medium
RT-PCR - Reverse transcriptase PCR
RT - Room temperature
s - Seconds
SD - Standard deviation
SDS - Sodium dodecyl sulfate
SDS-PAGE - SDS polyacrylamide gel electrophoresis
SE - Standard error
sMP-H_2O - sterile Millipore-purified water
SS - Side scatter
TAB - TAK1-binding protein
TAK-1 - TGF-beta-activated kinase 1
TBS - Tris-buffered saline
TBS-T - TBS-Tween20
TEMED - Tetramethylethylenediamine
TMB - Tetramethylbenzidine
TRAF6 - TNF receptor associated factor (TRAF) family protein 6
WT - Wildtype

Amino acids nomenclature

A - Ala, Alanine
C - Cys, Cysteine
D - Asp, Aspartic acid
E - Glu, Glutamic acid
F - Phe, Phenylalanine
G - Gly, Glycine
H - His, Histidine
I - Ile, Isoleucine
K - Lys, Lysine
L - Leu, Leucine
M - Met, Methionine
N - Asn, Asparagine
P - Pro, Proline
Q - Gln, Glutamine
R - Arg, Arginine
S - Ser, Serine
T - Thr, Threonine
V - Val, Valine
W - Trp, Tryptophane
Y - Tyr, Tyrosine

A Nucleotide sequences and plasmid charts

A.1 Plasmid charts

HA-TβRII

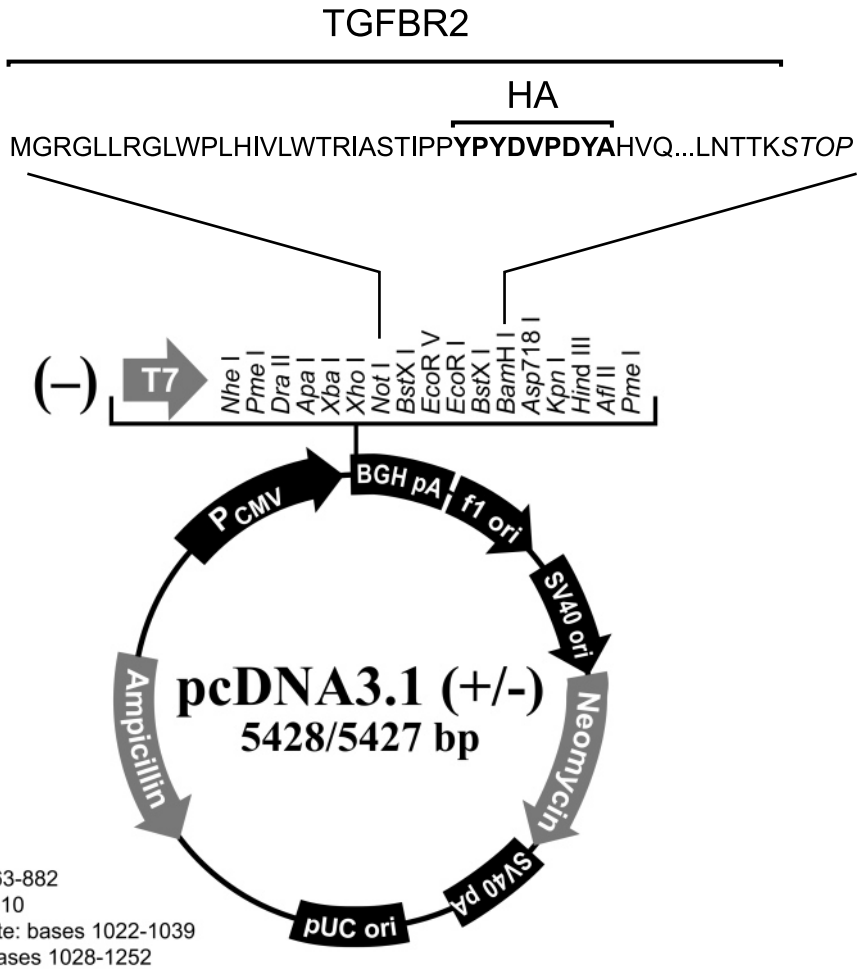

Comments for pcDNA3.1 (+)
5428 nucleotides

CMV promoter: bases 232-819
T7 promoter/priming site: bases 863-882
Multiple cloning site: bases 895-1010
pcDNA3.1/BGH reverse priming site: bases 1022-1039
BGH polyadenylation sequence: bases 1028-1252
f1 origin: bases 1298-1726
SV40 early promoter and origin: bases 1731-2074
Neomycin resistance gene (ORF): bases 2136-2930
SV40 early polyadenylation signal: bases 3104-3234
pUC origin: bases 3617-4287 (complementary strand)
Ampicillin resistance gene (*bla*): bases 4432-5428 (complementary strand)
ORF: bases 4432-5292 (complementary strand)
Ribosome binding site: bases 5300-5304 (complementary strand)
bla promoter (P3): bases 5327-5333 (complementary strand)

TβRII-Flag

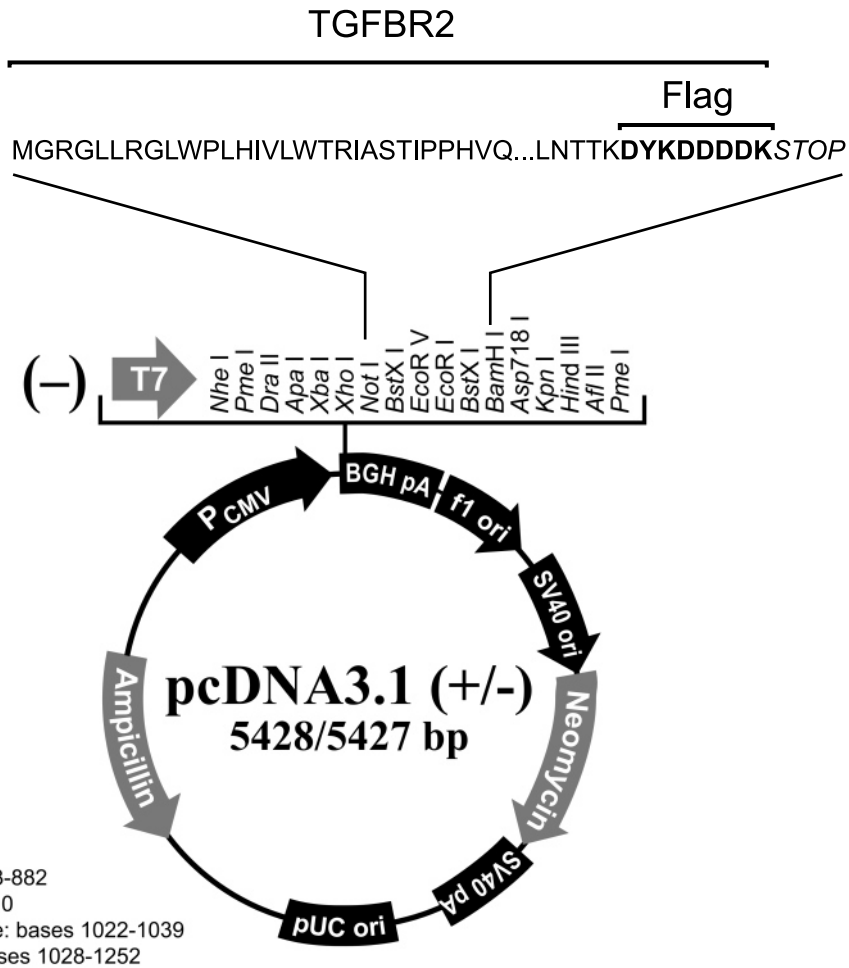

Comments for pcDNA3.1 (+)
5428 nucleotides

CMV promoter: bases 232-819
T7 promoter/priming site: bases 863-882
Multiple cloning site: bases 895-1010
pcDNA3.1/BGH reverse priming site: bases 1022-1039
BGH polyadenylation sequence: bases 1028-1252
f1 origin: bases 1298-1726
SV40 early promoter and origin: bases 1731-2074
Neomycin resistance gene (ORF): bases 2136-2930
SV40 early polyadenylation signal: bases 3104-3234
pUC origin: bases 3617-4287 (complementary strand)
Ampicillin resistance gene (*bla*): bases 4432-5428 (complementary strand)
ORF: bases 4432-5292 (complementary strand)
Ribosome binding site: bases 5300-5304 (complementary strand)
bla promoter (P3): bases 5327-5333 (complementary strand)

A.2 Mutagenesis primer sequences

Tab. 6: TβRII mutagenesis primers. Oligonucleotide primer sequences for site-directed mutagenesis using the GeneTailor site directed mutagenesis kit (Invitrogen). Nucleotides at the site of mutation are underlined.

Mutation		Primer sequence 5′→3′
R537P	forward	CAGTGTGTGGCAGAACCCTTCAGTGAGCT
	reverse	GTTCTGCCACACACACTGGGCTGTGAGACGG
R537C	forward	CCCAGTGTGTGGCAGAATGCTTCAGTGAG
	reverse	TTCTGCCACACACTGGGCTGTGAGACGGGCC
R528H	forward	CACGACCCAGAGGCCCATCTCACAGCCCA
	reverse	GGGCCTCTGGGTCGTGGTCCCAGCACTCAGTC
R528C	forward	CCACGACCCAGAGGCCTGTCTCACAGCCCA
	reverse	GGCCTCTGGGTCGTGGTCCCAGCACTCAGTCA
R460H	forward	CTGGGAAATGACATCTCACTGTAATGCAGTG
	reverse	GAGATGTCATTTCCCAGAGCACCAGAGCCAT
R460C	forward	CTGGGAAATGACATCTTGCTGTAATGCAGT
	reverse	AGATGTCATTTCCCAGAGCACCAGAGCCAT
L308P	forward	AACATACTCCAGTTCCCGACGGCTGAGGA
	reverse	GGAACTGGAGTATGTTCTCATGCTTCAGATTG
Y336N	forward	GGGCAACCTACAGGAGAACCTGACGCGGCA
	reverse	CTCCTGTAGGTTGCCCTTGGCGTGGAAGGCGG
S449F	forward	CAGACCGATGTCTACTTCATGGCTCTGGTG
	reverse	AGTAGACATCGGTCTGCTTGAAGGACTCAAC

A.3 qPCR Primer sequences

Tab. 7: Primers used in quantitative PCR. Oligonucleotide primers used in SYBR green qPCR for human TβRII and for hypoxanthine phosphoribosyltransferase (HPRT) as reference gene.

Gene		Primer sequence 5′→3′
TβRII	forward	CTAACCTGCTGCCTGTGTGA
	reverse	TCGGTCTGCTTGAAGGACTC
HPRT	forward	TGCTCGAGATGTGATGAAGG
	reverse	TCCCCTGTTGACTGGTCATT

B *In-silico* analysis results for the TβRII-B insert

B.1 Results from PSIPRED

Results for psipred job 59513

Output for PSIPRED predictions

Psipred Residue Predictions

Conf: Confidence 0 =low 9 =high
Pred: Predicted secondary structure H =helix E =strand C =coil
AA: Target sequence

```
# PSIPRED HFORMAT (PSIPRED V2.6 by David Jones)
Conf: 976433135756674202686023023010022200188853788 7
Pred: CCCCCCCHHHHHHHHHEEEEECCCCCCCCEECHHHHCCEEEECCCCC
  AA: IPPHVQKSDVEMEAQKDEIICPSCNRTAHPLRHINNDMIVTDNNGA
```

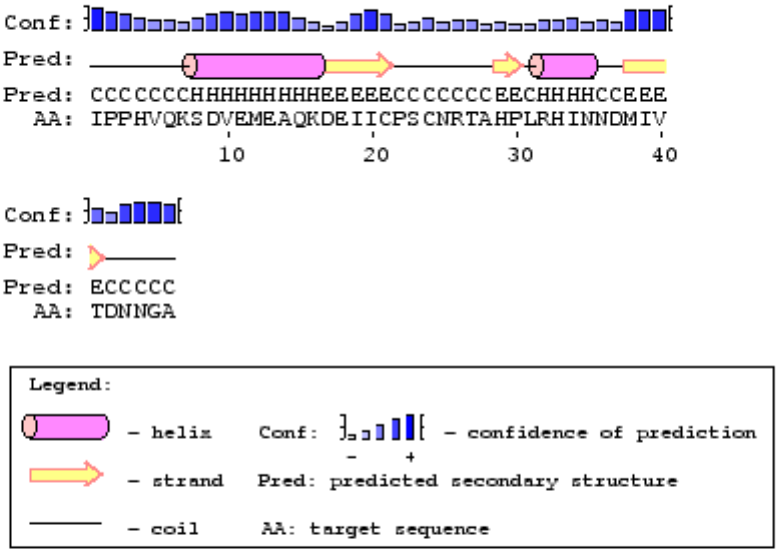

B.2 Results from PredictProtein

PROF predictions

TOP - BOTTOM - PROF

Bottom - Summary - Details - PredictProtein

PROF predictions for query (*name_unk*)

Contents:

SYNOPSIS of prediction for query (*name_unk*)

- **PROFsec summary** overall your protein can be classified as:
  mixed given the following classes:
  - 'all-alpha': %H > 45% AND %E < 5%
  - 'all-beta': %H < 5% AND %E > 45%
  - 'alpha-beta': %H > 30% AND %E > 20%
  - 'mixed': all others

- **Predicted secondary structure composition for your protein:**

sec str type	H	E	L
% in protein	9.21	28.95	61.84

- **Predicted solvent accessibility composition (core/surface ratio) for your protein:**
  Classes used:
  - e: residues exposed with more than 16% of their surface
  - b: all other residues.
- The subsets are for the fractions of residues predicted at higher levels of reliability, i.e. accuracy. This set covers 44% of all residues.

accessib type	b	e		sub...:	accessib type	b	e
% in protein	31.58	68.42		...set:	% in subset	35.29	64.71

HEADER information

- **About your protein:**

protid	query
protname	name_unk
protnres	152
protnali	10
protnchn	1
protnfar	4

- **About the alignment used:**

ali_orig	/nfs/data5/users/ppuser/server/work/predh_165450.hsspPsiFil

- **Residue composition for your protein:**

%A: 4.0	%C: 9.2	%D: 7.9	%E: 7.2	%F: 4.6
%G: 1.3	%H: 3.3	%I: 7.9	%K: 8.6	%L: 3.3
%M: 3.3	%N: 7.2	%P: 6.6	%Q: 3.3	%R: 2.6
%S: 7.9	%T: 4.6	%V: 5.9	%W: 0.7	%Y: 0.7

- **About the PROF methods used:**

prof_fpar	acc=/nfs/data5/users/ppuser/server/pub/prof/net/PROFboth_best.par
prof_nnet	acc=6

- **Please quote:**
  1. PROF: B Rost & C Sander (1993) J Mol Biol, 232:584-599
  2. PROFhtm: B Rost, P Fariselli & R Casadio (1996) Prot Science, 7:1704-1718

- **Copyright & Contact:**

  - Burkhard Rost, CUBIC NYC / LION Heidelberg
  - Email: rost@columbia.edu
  - WWW: http://cubic.bioc.columbia.edu
  - Fax: +1-212-305 3773

- **ABBREVIATIONS used:**

AA :	amino acid sequence
OBS_sec:	observed secondary structure: H=helix, E=extended (sheet), blank=other (loop)
PROF_sec:	PROF predicted secondary structure: H=helix, E=extended (sheet), blank=other (loop) PROF = PROF: Profile network prediction HeiDelberg
Rel_sec:	reliability index for PROFsec prediction (0=low to 9=high) Note: for the brief presentation strong predictions marked by '*'
SUB_sec:	subset of the PROFsec prediction, for all residues with an expected average accuracy > 82% (tables in header) NOTE: for this subset the following symbols are used: L: is loop (for which above ' ' is used) .: means that no prediction is made for this residue, as the reliability is: Rel < 5
pH_sec:	'probability' for assigning helix (1=high, 0=low)
pE_sec:	'probability' for assigning strand (1=high, 0=low)
pL_sec:	'probability' for assigning neither helix, nor strand (1=high, 0=low)
Q2_acc:	observerd relative solvent accessibility (acc) in 2 states: b = 0-16%, e = 16-100%.
P_2_acc:	PROF predicted relative solvent accessibility (acc) in 2 states: b = 0-16%, e = 16-100%.
Q3_acc:	observerd relative solvent accessibility (acc) in 3 states: b = 0-9%, i = 9-36%, e = 36-100%.
P_3_acc:	PROF predicted relative solvent accessibility (acc) in 3 states: b = 0-9%, i = 9-36%, e = 36-100%.
OBS_acc:	observed relative solvent accessibility (acc) in 10 states: a value of n (=0-9) corresponds to a relative acc. of between n*n % and (n+1)*(n+1) % (e.g. for n=4: 16-25%).
PROF_acc:	PROF predicted relative solvent accessibility (acc) in 10 states: a value of n (=0-9) corresponds to a relative acc. of between n*n % and (n+1)*(n+1) % (e.g. for n=4: 16-25%).
Rel_acc:	reliability index for PROFacc prediction (0=low to 9=high) Note: for the brief presentation strong predictions marked by '*'
SUB_acc:	subset of the PROFacc prediction, for all residues with an expected average correlation > 0.69 (tables in header) NOTE: for this subset the following symbols are used: I: is intermediate (for which above ' ' is used) .: means that no prediction is made for this residue, as the reliability is: Rel < 4
ali_orig:	input file
prof_fpar:	name of parameter file, used [w]
prof_nnet:	number of networks used for prediction [d]
prof_skip:	note: sequence stretches with less than 9 are not predicted, the symbol '*' is used!

BODY with predictions for query (*name_unk*)

PROF results (normal)

```
          ....,....10...,....20...,....30...,....40...,....50...,....60...,....70...,....80...,....90...,....100..,....110..,....120..,....130..,....140..,....150
AA        IPPHVQKSDVEMEAQKDEIICPSCNRTAHPLRHINNDMIVTDNNGAVKFPQLCKFCDVRFSTCDNQKSCMSNCSITSICEKPQEVCVAVWRKNDENITLETVCHDPKLPYHDFILEDAASPKCIMKEKKKPGETFFMCSCSSDECNDNIIFS
OBS_sec
PROF_sec                   HHHHHHH             EEEE       HHHHHHH                   EEEE     EEEEEEEEE    EEEEEEE          EEEE     EEEEEE      EEEEEE        EEEE
Rel_sec   98744235533133655011023015688753125531664687620211220001120332567640002440233212876057877862688615765520667641123651578861577411587742687505764013402418
SUB_sec   LLL....LL.....LLL.......LLLLLL...LL..EE.LLLL................LLLL.............LLL.EEEEEEE.LLLL.EEEEE..LLLL.....EE.LLLLL.EEE...LLLL..EEEE.LLL.........L

O_3_acc   bbbbbbbbbbbbbbbbbbbbbbbbbbbbbbbbbbbbbbbbbbbbbbbbbbbbbbbbbbbbbbbbbbbbbbbbbbbbbbbbbbbbbbbbbbbbbbbbbbbbbbbbbbbbbbbbbbbbbbbbbbbbbbbbbbbbbbbbbbbbbbbbbbbbbb
P_3_acc   eeee ee e e eeeeeee beebeeee e e  eee      eeb bebeebbe be e  ebeeee b  eb bbbbbeeee bbbbbb  eeee  b b b   e eb  bbb   eeeeb beeeeeee  bbbbbb eeeb e b be
Rel_acc   54731450407183393641483348641103103343010284102433444703425023373431401350413254664077977602789721605140208032005370225226505337889620646733234320112038
SUB_acc   eee..ee.e.e.e..e.ee.be..eeee.......e.....ee...e..ebbe..e.e....e.e..b...b.b...beeee.bbbbbb..eeee..b.b.b...e.....b.b...e..eb.b..eeeee..bbbb....e........e
```

PROF results (detail)

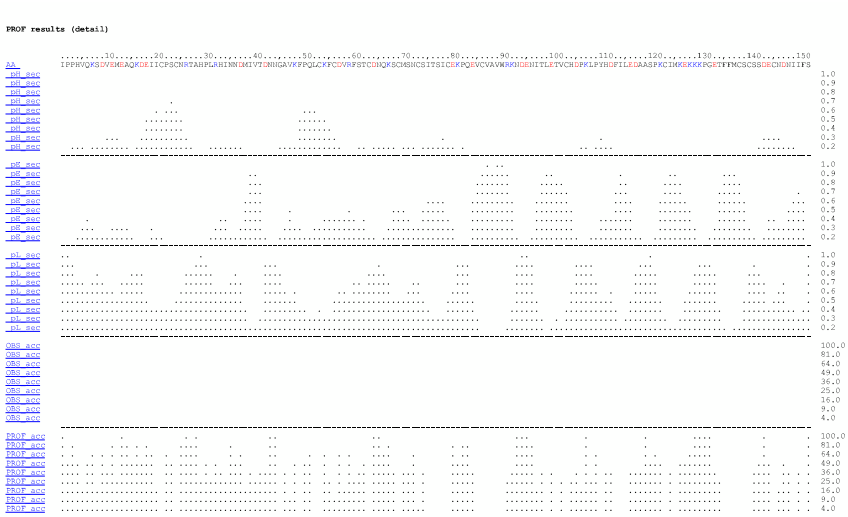

Top – Summary – Details – PredictProtein

GLOBE prediction of globularity

```
--
-- GLOBE: prediction of protein globularity
--
-- nexp =   104    (number of predicted expcsed residues)
-- nfit =    72    (number of expected exposed residues
-- diff =    32.00 (difference nexp-nfit)
-- =====> your protein appears not to be globular
--
--
-- GLOBE: further explanations preliminaryily in:
--        http://rostlab.org/papers/1999_globe/paper.html
--
-- END of GLOBE
```

Predicted protein-protein interaction sites from local sequence information.(Ofran Y, Rost B)

```
: strech=5 crowd_predictions=7 gap=8 itr=51
12345678901234567890123456789012345678901
IPPHVQKSDVEMEAQKDEIICPSCNRTAHPLRHINNDMIVT
PPP---------P------P---PPPPPPPP----P-P--PP

TSNNGAVKFPQLCKFCDVRFSTCDNQKSCMSNCSITSICE
--P-----------------PP-----PPPP-PP--------P

KPQEVCVAVWRKNDENITLETVCHDPKLPYHDFILEDAAS
------------PP-----------PPP-PP--------

PKCIMKEKKKPGETFFMCSCSSDECNDNIIFS
-------PPPPPP---P----P----------
```

Statement of authorship

Hiermit erkläre ich, daß ich die vorliegende Arbeit selbst angefertigt und keine anderen als die hier angegebenen Hilfsmittel verwendet habe. Ich versichere, daß ich diese Arbeit weder in dieser noch in anderer Form bei einer anderen Prüfungsbehörde eingereicht habe.

Berlin, 28. August 2010

Daniel Horbelt

Publications

Journal articles

Horbelt D., Guo G., Robinson P. N., and Knaus P. (2010). Quantitative Analysis of TGFBR2 Mutations in Marfan Syndrome Related Disorders Suggests Correlation between Phenotypic Severity and Smad Signaling Activity. *J Cell Sci*, accepted manuscript

Ott C.-E., Grünhagen J., Jäger M., **Horbelt D.**, Schwill S., Kallenbach K., Guo G., Manke T., Knaus P., Mundlos S., and Robinson P. N. (2010). MicroRNAs Differentially Expressed in Postnatal Aortic Development Downregulate Elastin via 3′ UTR and Coding-Sequence Binding Sites. submitted to *Nucleic Acids Res*

Chaikuad A., Alfano I., Thangaratnarajah C., **Horbelt D.**, Boergermann J. H., Kettenbach A.N., Filippakopoulos P., Fedorov O., Gerber S. A., Triffitt J. T., von Delft F., Knapp S., Knaus P., and Bullock A. N. (2010). Molecular basis for cytosolic assembly and activation of BMP receptors. submitted to *EMBOJ*

Obradovic-Wagner D., Becker J., **Horbelt D.**, Kasper G., Robinson P. N., Duda G., and Knaus P. (2010). BMP-2 signals predominantly through SMAD dependent pathway in human bone marrow-derived mesenchymal stem cells. *in preparation*

Rothe D., Werk D., Niedrig S., **Horbelt D.**, Grunert H., Zeichhardt H., Erdmann V.A., and Kurreck J. (2009). Antiviral activity of highly potent siRNAs against echovirus 30 and its receptor. *J Virol Methods*, 157(2):211-218.

Knaus P. and **Horbelt D.** (2004). Nobelpreis Chemie 2004. *Naturwissenschaftliche Rundschau* 12.

Posters and abstracts

Horbelt D., Schmidt S., Mauer M., Sickmann A., and Knaus P. *The TGF-beta Receptor Type II Interactome: Identification of a Novel Repressor of TGF-beta Signaling*. Endotrack. On the tracks of signalling. Il Ciocco, Italy, 2009

Heining E., Schwappacher R., **Horbelt D.**, Weigt M. E., Huber O., and Knaus P. *Crosstalk of cyclic GMP dependent kinase I and BMP signaling*. 1^{st} International BMP workshop. Modern trends in BMP signaling, Berlin, 2009

Heining E., Schwappacher R., **Horbelt D.**, Huber O., and Knaus P. *Crosstalk of cyclic GMP dependent kinase I and BMP signaling*. 4^{th} International Conference of cGMP, Regensburg, 2009

Horbelt D., Bengtsson L., Rechtman M. M., Henis Y.I., and Knaus P. *TGF-beta - Key Player in Tumorigenesis and Fibrotic Disease*. Tag der Chemie der Berliner Universitäten, Berlin, 2006

Horbelt D., Bauer M., and Knaus P. *Signaling via TGF-beta receptor type II splice variant TbetaRIIB*. German TGF-beta Workshop, Regensburg/Kehlheim, 2005

Horbelt D., Bauer M., and Knaus P. *TGF-beta receptor type II in cancer*. 13^{th} International AEK/AIO Congress of the German Cancer Society, Würzburg, 2005

Talks

Horbelt D., Knaus P. *Bildung, Heilung und Regeneration von Knochen.* Lange Nacht der Wissenschaften. Berlin, 2008.

Horbelt D. *Signaling by TGF-beta-Receptor II Mutants Associated with Marfan Syndrome Related Diseases* . 3^{rd} Graduate Students Workshop of PhD and Diploma Thesis Students of Biochemistry. Berlin, 2008 Mar.

Horbelt D. *Generation of Inhibitory Antibodies for Transforming Growth Factor beta Receptor Type II-B.* 2^{nd} Graduate Students Workshop of PhD and Diploma Thesis Students of Biochemistry. Berlin, 2006 Nov.

Horbelt D., Knaus P. *Bildung, Heilung und Regeneration von Knochen.* Lange Nacht der Wissenschaften. Berlin, 2006.

Horbelt D. *Signaling of TGF-beta Receptor Type II Alternatively Spliced Isoform TßRII-B.* 1^{st} Graduate Students Workshop of PhD and Diploma Thesis Students of Biochemistry. Berlin, 2006 Mar.

Danke! - Acknowledgements

Ich möchte diese Arbeit abschließen mit dem Dank alle die, die zu ihrer Entstehung beigetragen haben...

Prof. Petra Knaus danke ich für die Möglichkeit, in ihrer Arbeitsgruppe meine Doktorarbeit zu verfassen. Durch ihre wissenschaftlich inspirierende und menschlich beispielhafte Art, eine Arbeitsgruppe zu leiten habe ich viel lernen können. Danke für die stete Unterstützung mit Rat und Perspektiven.

PD Peter Nick Robinson danke ich für die Kooperation und die Unterstützung im TGFBR2-Marfan- und im miRNA-Projekt, die mir klinische Aspekte der TGF-β Forschung näher gebracht haben. Danke für die Übernahme der Zweitgutachterschaft meiner Dissertation.

I am grateful to Prof. Yoav Henis, Maya Mouler Rechtman (Tel Aviv University, Israel) and to Dr. Alex Bullock (University of Oxford, UK) for collaboration and for valuable discussions and correspondence which contributed a lot to this thesis. Ein großes Dankeschön an Prof. Jens Kurreck und Diana Rothe für die Kooperation im Echovirus Projekt und an Dr. Gao Guo für die Zusammenarbeit im TGFBR2-Marfan-Projekt.

Mein besonderer Dank geht an die Sonnenfeld Stiftung und Herrn Prof. Hansjürgen Freiherr von Villiez für die materielle und persönliche Untersützung mit einem Promotionsstipendium.

Danke an alle ehemaligen und gegenwärtigen Kollegen im KnausLab, die den Alltag und die Wissenschaft gut machen. Gerburg, Eva, Asja, Mohammad, Darja, Jessica B., Jessi, Chris, Sofia und Raghu, sowie aus der früheren Generation Sylke, Sammar, Martin, Tina, Peter, Raphaela, Luiza, Ricardo, und alle anderen. Mein besonderer Dank geht an Jan. Wenn es darum geht, zusammen Experimente zu diskutieren, Papers auseinanderzunehmen, Kits nachzubauen, Theorien zu entwerfen oder einfach nur Rücken an Rücken in Bay 2 zu arbeiten gibt's keinen besseren!

Danke an meine Diplomanden Manuel und Sandra, die in den wenigen Monaten ihrer Diplomarbeit viel gelernt und geleistet haben, und an meine studentischen Mitarbeiter/innen, insbesondere Pia, Maria, Robert und Tarek, die einen tollen Beitrag zu meinen Projekten geliefert haben.

Ich danke Sonja für ihre prima Unterstützung nicht nur mit FACS Experimenten, Gisela für klasse DNAs und Charlotte für ihren Einsatz bei der Etablierung der Realtime Pri-

merdatenbank, Neil und Wulf-Burkhard für IT-Unterstützung, Bini, Anna und Hermann fürs Abnehmen so vieler kleiner Dinge.

Für Katharinas grandiosen Einsatz an der Schnittstelle zur Bürokratie, bei Verträgen, Dienstreisen, Ausschreibungen, F-Praktika und vielem dergleichen mehr möchte ich mich besonders bedanken.

Ich danke Lisa für die tolle Teamarbeit bei der Organisation der PhD Students Workshops, Danke an Tobi und Anja und die anderen Kollegen aus der AG Multhaup und den anderen Arbeitsgruppen in der Biochemie.

Gott sei Dank gibt es auch ein Leben und Menschen die mir wichtig sind jenseits der ehrwürdigen Mauern des Otto-Hahn-Baus. Danke für die unerschütterliche Freundschaft, Angie und Patrick und Pia, und an die Berliner Christin, Andi, Christian, Arne, Hannah, Denise, Alia und Lara.

Ich bin unsagbar froh und dankbar, wie mich meine Familie zu Hause, meine Eltern, Eva, meine Omas und Anneliese durch die Jahre meines Studiums und meiner Doktorarbeit unterstützt haben. Danke für alles! Euch sei diese Arbeit gewidmet.

Zu guter Letzt möchte ich dem Menschen danken, der einen großen Teil meiner Doktorarbeit so intensiv wie sonst niemand mit*erlebt* hat... meiner liebsten Alice! Danke für's Anfeuern und für's Zur-Ruhe-bringen, und nebenbei auch für den einen oder anderen guten wissenschaftlichen Tipp!